Some aspects of the phenomenology of B mesons

By

Basudha Misra
The Institute of Mathematical Sciences, Chennai

A thesis submitted to the Board of Studies in Physical Sciences

In partial fulfillment of requirements For the Degree of

DOCTOR OF PHILOSOPHY

of

HOMI BHABHA NATIONAL INSTITUTE

Homi Bhabha National Institute

Recommendations of the Viva Voce Board

As members of the Viva Voce Board, we recommend that the dissertation prepared by Basudha Misra titled "Some aspects of the phenomenology of B mesons" may be accepted as fulfilling the dissertation requirement for the Degree of Doctor of Philosophy.

_____ **Date :**

Chairman - R. Jaganathan

_____ **Date :**

Convenor - Rahul Sinha

_____ **Date :**

Member 1 - D. Indumathi

_____ **Date :**

Member 2 - M. V. N. Murthy

_____ **Date :**

Member 3 -

_____ **Date :**

Dean - T. R. Govindarajan

Final approval and acceptance of this dissertation is contingent upon the candidate's submission of the final copies of the dissertation to HBNI.

I hereby certify that I have read this dissertation prepared under my direction and recommend that it may be accepted as fulfilling the dissertation

requirement.

_____ **Date :**

Supervisor - Rahul Sinha

_____ **Date :**

Co-supervisor - D. Indumathi

Declaration

I hereby certify that I have read this dissertation prepared under my direction and recommend that it may be accepted as fulfilling the dissertation requirement.

_____ **Date :**

Supervisor - Rahul Sinha

_____ **Date :**

Co-supervisor - D. Indumathi

Declaration

I, hereby declare that the investigation presented in this thesis has been carried out by me under the guidance of my supervisor Prof. Rahul Sinha and my co-supervisor Prof. D. Indumathi. The work is original and has not been submitted earlier as a whole or in part of a degree/diploma at this or any other Institution/University.

Basudha Misra

Dedicated to my parents

Abstract

The variation of the measured $B_d^0 - \overline{B_d^0}$ mixing phase β/ϕ_1 in $b \to c\bar{c}s$ and $b \to s\bar{q}q$ (where $q = u, d, s$) modes is regarded as a possible probe of New Physics. It has been speculated that this discrepancy is a signal of New Physics. Within the Standard Model the amplitude for modes involving $b \to s$ transitions, get contributions from two amplitudes with different weak phases. Unless the contribution from one of the amplitudes is negligible, one would expect some discrepancy between the various measurements. Estimates of this discrepancy using hadronic assumptions have indicated that the sign of the discrepancy within SM is opposite to the observed value.

We demonstrate using a model independent approach that the deviation in measured $B_d^0 - \overline{B_d^0}$ mixing phase caused by pollution from another amplitude, within the Standard Model, is always less in magnitude, and has the same sign as the weak phase of the polluting amplitude. The exception is to have large destructive interference between the two amplitudes. We show that any deviation larger than a few degrees is only possible if the observed decay rate results from fine tuned cancellations between significantly larger quark level amplitudes. These simple observations have very significant consequences for signals of New Physics.

One of the eligible New Physics candidate is the leptoquark model. Leptoquarks are hypothetical gauge particles which can be either scalar or vector. These particles allow having tree level transitions from a quark to lepton or vice versa which are not permitted in the standard model. In our work, upper bounds at the weak scale are obtained for all $\lambda_{ij}\lambda_{ik}$ type product couplings of leptoquark model which may affect $K^0 - \overline{K^0}$, $B_d^0 - \overline{B_d^0}$ and $B_s^0 - \overline{B_s^0}$ mixing. For $B_d^0 - \overline{B_d^0}$ we use both Δm_B and $\sin(2\beta)$ where as for $B_s^0 - \overline{B_s^0}$ we use Δm_{B_s}

and $\sin(2\beta_s)$ constraints. For $K^0 - \overline{K^0}$ we use the results on Δm_K and ε_K. Due to the presence of large theoretical uncertainties, ε'/ε is not considered in our analysis. The relevant mixing correlated leptonic and semileptonic decay channels are also presented in the analysis. We constrain all the possible product couplings in this sector, including some which were not considered earlier. The constraints obtained for the leptonic and semi-leptonic decay modes are much tighter than the bounds obtained from mixing for most of the cases. We also present the bounds on the real and imaginary parts of $\lambda\lambda$ which carry the information of the phase of new physics. This is a new observation, not considered in earlier literature.

Acknowledgements

I would like to thank my supervisor, Prof. R. Sinha, for teaching and helping me so much, both in Physics and in every day life. Each and every aspect of this thesis has taken its present shape under his constant guidance and supervision. I thank him for the way he led me towards the completion of this thesis. And more than anything else, I am extremely grateful to him for his patience and understanding towards me.

I would like to thank my co-supervisor Prof. D. Indumathi for teaching me different aspects of Quantum Chromodynamics. I specially like to thank her for her patience to teach me numerical programming. It is only because of her I have overcome my long-term fear in computer-programming and skills.

I am extremely grateful to my collaborator Dr. Jyoti Prasad Saha for his constant guidance in various aspects of phenomenology. As a senior he has helped me in clearing innumerable doubts in particle physics. I thank him for all the support.

I would like to thank my collaborators Prof. Anirban Kundu, Dr. Prasanta Kumar Das and Prof. Wei-shu Hou for their scintillating and lively discussions.

I thank Prof. M. V. N. Murthy, Prof. Rahul Basu, Prof. G. Rajasekaran and Prof. H. S. Mani for guiding me with their thoughtful suggestions at different stages of my work. I thank Prof. R. Jagannathan and Prof. T. R. Govindrajan for their encouraging role in the process of submission of the thesis to HBNI. I also thank all the Physics faculty at the Institute of Mathematical Sciences (IMSc) who have been responsible for imparting to me the knowledge of various aspects of Physics during my course work and through numerous seminars.

I thank all my teachers (right from high school through university) for their encouragement and for giving me the right flavour of Physics at different stages of my academic life, which was highly instrumental in motivating me to take up Physics at this level.

I thank my parents for their love, support and constant encouragement. I would like to dedicate all the success that I have achieved till date to my parents. Its because of their vision and perseverance during tough times that I have become what I am today.

The person without whose love and support I could not finish my thesis is my husband Swagnik. I thank him not only for constantly coping with my mood-swings, my late-hours but also for teaching me different numerical skills, helping me in proof-reading and always encouraging me to pursue my research career. He deserves special thanks.

I thank my sister, brother-in-law, Kutu and my father-in-law for supporting me to continue my research.

I am thankful to my hostel-mates. They have made my stay happy, comfortable and cozy. I will surely miss them when I will be away from IMSc. Thanks to Swagata, Nutan, Anisha, Gopal, Nilanjan, Annwesa, Soumyajit, Pooja for providing me the much needed non-academic breaks.

The work leading to this thesis was carried out completely at the Institute of Mathematical Sciences, Chennai. I would like to thank the institute for its financial support and providing the wonderful infrastructure and working environment. Last but not the least, I thank all the members of IMSc for making my stay at IMSc a memorable and enjoyable one.

Contents

List of Publications

- Rahul Sinha, Basudha Misra, Wei-shu Hou
  " Has new physics already been seen in B_d meson decays?", Phys. Rev. Lett. 97, 131802, 2006.

- Basudha Misra, Jyoti Prasad Saha, Prasanta Kumar Das
  " $\overline{B_s} \to \mu^+\mu^-$ decay in the Randall-Sundrum model", Phys. Rev. D74, 074011, 2006.

- D.Indumathi, Basudha Misra,
  "An extended model for nonet pseudoscalar meson fragmentation", arXiv:hep-ph/0901.0228, 2009.

- Jyoti Prasad Saha, Basudha Misra, Anirban Kundu
  " Constraining Scalar Leptoquarks from the K and B Sectors", arXiv:hep-ph/1003.1384, 2010 (accepted for publication in Physical Review D).

This thesis is based on the following two publications

- Rahul Sinha, Basudha Misra, Wei-shu Hou
  " Has new physics already been seen in B_d meson decays?", Phys. Rev. Lett. 97, 131802, 2006.

- Jyoti Prasad Saha, Basudha Misra, Anirban Kundu
  " Constraining Scalar Leptoquarks from the K and B Sectors", arXiv:hep-ph/1003.1384, 2010 (accepted for publication in Physical Review D).

List of Figures

List of Tables

Chapter 1

CP Violation in the Standard Model

1.1 Introduction

Discrete symmetries like C (charge conjugation), P (parity or space reflection) and T (time reversal) have played a very important role in the understanding of elementary particle interaction. C and P are conserved in strong and electromagnetic processes, but violated in weak decays. For several years it was believed that the product CP and T were conserved in all kinds of interactions. It was only in 1964, Christenson, Cronin, Fitch and Turlay [1] showed for the first time through their famous experiment in the neutral kaon decays that CP, like parity, was also not a good symmetry of nature. This surprising effect is a manifestation of *indirect* CP violation. The mass eigenstates $K_{L,S}$ of the neutral kaon system are the admixture of the flavour eigenstates K^0 and $\overline{K^0}$. The CP violation occurs due to the fact that $K_{L,S}$ are not eigenstates of the CP operator. In particular, the K_L state is governed by the CP-odd eigenstate, but also has a tiny admixture of the CP-even eigenstate, which may decay through CP-conserving interactions into the $\pi^+\pi^-$ final state. It was only in 1999 that the NA48 (CERN) [2] and KTeV (FNAL) [3] collaborations first time observed the *direct* CP violation which arises directly at the decay-amplitude level. A year later, in 2000 the CPLEAR experiment [4] reported the first direct evidence of T violation in the neutral-kaon system. However, CPT still remains conserved as expected from the Lorentz invariance of quantum field theories.

In 2001, CP violation was finally observed *outside the Kaon system*, in $B_d^0 \to J/\psi K_S$ mode by the BaBar [5] and Belle [6] collaborations. This is an example of mixing-induced CP violation. It is observed in the interference between $B_d^0 \to J/\psi K_S$ and $\overline{B_d^0} \to J/\psi K_S$ decay processes. Three years later, in 2004, *direct* CP violation was also detected in $B_d^0 \to \pi^{\pm} K^{\mp}$ decays [7].

In the Standard Model (SM), the phenomenon of CP violation can be accommodated in an efficient way through a complex phase. This phase enters in the coupling constants which describe the weak charge-changing transitions of quarks. These couplings are described by the unitary 3×3 Cabibbo-Kobayashi-Maskawa (CKM) [8], [9] matrix. Most of the CP-violating parameters observed at a level higher than 3σ are consistent with the CKM mechanism till date. That is why it is believed that probably CKM phase is the dominant source of CP violation in low-energy flavour-changing neutral current processes. But CKM mechanism fails to explain the *baryon asymmetry* observed in the universe. It cannot give any explanation to the *strong CP problem*. Moreover, the observation of the *neutrino masses* indicates that there should definitely be an origin of CP lying beyond the SM. It raises the question of having CP violation in the neutrino sector and its connection with the quark-flavour physics. All these problems suggest new sources of CP-violation, which may come from different new physics (NP) models like supersymmetry (SUSY), leftright-symmetric models, models with extra Z' bosons, extra dimensions, little Higgs or leptoquarks for example.

In this chapter, we first discuss about the CP violation scenario in the SM. It involves a discussion of the CKM mechanism and how CP violation is introduced in the quark sector through it. This is followed by a presentation of different parametrizations of the CKM matrix. Subsequently we have a brief discussion on the unitarity triangle (UT) and it's parameters. Next we discuss about the global fits to indicate why the CKM matrix is considered as the dominant source of CP violation in the SM. We finally conclude this chapter with a discussion of the fact that SM is not sufficient enough to explain nature completely and it is therefore necessary to continue with the search for NP. Part of this chapter has been reproduced from the standard references [10], [11] and [12].

1.2 CP violation in the standard model

In the framework of the SM, the quark Yukawa interaction is given by [10],

$$-\mathcal{L}^{q}_{\text{Yukawa}} = Y^{d}_{ij}\overline{Q^{I}_{Li}}\phi D^{I}_{Rj} + Y^{u}_{ij}\overline{Q^{I}_{Li}}\tilde{\phi}U^{I}_{Rj} + \text{h.c.} \tag{1.1}$$

where $Q^{I}_{L} = \binom{U^{I}_{L}}{D^{I}_{L}}$ is the left-handed quark doublet of $SU(2)_L$. U^{I}_{R}, D^{I}_{R} are the right-handed up and down type quark singlets respectively. ϕ is the scalar doublet and $\tilde{\phi} = -i\tau_2\phi^*$ where τ_2 is the standard Pauli matrix. The index I denotes interaction eigenstates and $i, j = 1, 2, 3$ are the flavor index. Y^u and Y^d are the Yukawa coupling matrices. it has been shown [13] that CP violation in SM can be incorporated if and only if

$$\mathcal{I}m(\det[Y^{d}Y^{d\dagger}, Y^{u}Y^{u\dagger}]) \neq 0. \tag{1.2}$$

It can be explained with a simple argument why CP violation is related to the complex Yukawa couplings. The hermiticity of the Lagrangian demands that $\mathcal{L}_{\text{Yukawa}}$ has its terms in pairs of the form

$$Y_{ij}\overline{\psi_{Li}}\phi\psi_{Rj} + Y^{*}_{ij}\overline{\psi_{Rj}}\phi^{\dagger}\psi_{Li},$$

whereas under CP transformation operator,

$$\overline{\psi_{Li}}\phi\psi_{Rj} \leftrightarrow \overline{\psi_{Rj}}\phi^{\dagger}\psi_{Li},$$

but the coefficients, Y_{ij} and Y^{*}_{ij}, remain unchanged. This means that $\mathcal{L}_{\text{Yukawa}}$ is symmetric under CP only if $Y_{ij} = Y^{*}_{ij}$.

After spontaneously broken symmetry from $SU(2)_L \times U(1)_Y \to U(1)_{\text{em}}$, the quarks acquire their mass terms from the Yukawa interactions in Eq. (1.1),

$$-\mathcal{L}^{q}_{M} = (M_d)_{ij}\overline{D^{I}_{Li}}D^{I}_{Rj} + (M_u)_{ij}\overline{U^{I}_{Li}}U^{I}_{Rj} + \text{h.c.}$$

where $M_q = \frac{v}{\sqrt{2}}Y^q$ and ϕ receives a vacuum expectation value (VEV), $\langle\phi\rangle = \binom{0}{\frac{v}{\sqrt{2}}}$. We can always find two unitary matrices V_{qL} and V_{qR} such that

$$V_{qL}M_qV^{\dagger}_{qR} = M^{\text{diag}}_{q} \quad (q = u, d),$$

with $M_q^{\rm diag}$ as a diagonal and real mass matrix. The quark mass eigenstates are then identified as

$$q_{Li} = (V_{qL})_{ij} q^I_{Lj}, \quad q_{Ri} = (V_{qR})_{ij} q^I_{Rj} \quad (q = u, d).$$

Following this formalism the charged current interactions for quark can be written in the mass basis as:

$$-\mathcal{L}^q_{W^\pm} = \frac{g}{\sqrt{2}} \overline{u_{Li}} \gamma^\mu (V_{uL} V^\dagger_{dL})_{ij} d_{Lj} W^+_\mu + \text{h.c.}$$

This 3×3 unitary matrix,

$$V = V_{uL} V^\dagger_{dL}, \quad (V V^\dagger = \mathbf{1}), \tag{1.3}$$

is the CKM mixing matrix for quarks [9], [8]. The elements of V are written as follows:

$$V = \begin{pmatrix} V_{ud} & V_{us} & V_{ub} \\ V_{cd} & V_{cs} & V_{cb} \\ V_{td} & V_{ts} & V_{tb} \end{pmatrix}. \tag{1.4}$$

In the SM, with 3 generations, the CKM matrix can be parametrized by 9 parameters, however, 5 of the phases can be absorbed or changed at will by rephasing the quarks fields. Therefore the number of physical parameters in V is only 4. An 3×3 orthogonal matrix is parametrized by 3 rotation angles. An unitary matrix is the complex extension of an orthogonal matrix. Therefore out of 4 parameters of V, 3 should be identified as the rotational angles. The remaining parameter is the physical Kobayashi-Maskawa phase δ which is the single source of CP violation in the quark sector of the Standard Model [9].

In order to determine the magnitudes $|V_{ij}|$ of the elements of the CKM matrix, the following tree-level processes may be used [11]:

- From nuclear beta decays and neutron decays $|V_{ud}|$ can be obtained.
- $K \to \pi l^- \nu$ decays can give the information about $|V_{us}|$.
- ν production of charm off valence d quarks give $|V_{cd}|$.

- $|V_{cs}|$ can be obtained from the charm-tagged W decays (as well as ν production and semileptonic D decays).
- Exclusive and inclusive $b \to cl^-\nu$ decays give $|V_{cb}|$.
- Exclusive and inclusive $b \to ul^-\nu$ decays constrain $|V_{ub}|$.
- $\bar{t} \to \bar{b}l^-\nu$ processes constrain $|V_{tb}|$.

If we use the corresponding experimental information, together with the CKM unitarity condition, and assume that there are only three generations, we arrive at the following 90% C.L. limits for the $|V_{ij}|$ [14], [15], [16], [17]:

$$V = \begin{pmatrix} 0.97419 \pm 0.00022 & 0.2257 \pm 0.0010 & 0.00359 \pm 0.00016 \\ 0.2256 \pm 0.0010 & 0.97334 \pm 0.00023 & 0.0415^{+0.0010}_{-0.0011} \\ 0.00874^{+0.00026}_{-0.00037} & 0.0407 \pm 0.0010 & 0.999133^{+0.000044}_{-0.000043} \end{pmatrix}. \tag{1.5}$$

1.3 Parametrizations of the CKM matrix

One has the freedom to rephase any of the five quark fields out of the six, leaving the physically observable quantities invariant under this rephasing. This gives us the opportunity to change the overall phase of any row or column of the CKM matrix without changing it's physics context. It gives us the freedom to constrain up to five matrix elements to be real or else to fix their phase in any desirable way. But one must be very careful not to implicitly fix the phase of any quartet while choosing any phase convention of the CKM matrix [12]. The quartet is defined as

$$Q_{\alpha i \beta j} \equiv V_{\alpha i} V_{\beta j} V^*_{\alpha j} V^*_{\beta i},$$

where $\alpha \neq \beta$ and $i \neq j$. As we have seen in last section that with 3 Euler angles and 1 complex phase, we can parametrize CKM matrix completely, but we still have the option to choose which axes to use for our rotations and in what order to perform them. This choice leads us to no less than 36 distinct but equivalent parametrizations for three generations [18]. However, the two most popular parametrization of CKM matrix, the standard parametrization [19] and the Wolfenstein parametrization [20] are discussed below.

1.3.1 Standard parametrization

The so called standard parametrization of CKM matrix was introduced by Chau and Keung [19]. This parametrization is followed by the particle data group. In this parametrization,

$$V = \begin{pmatrix} c_{12}c_{13} & s_{12}c_{13} & s_{13}e^{-i\delta} \\ -s_{12}c_{23} - c_{12}s_{23}s_{13}e^{i\delta} & c_{12}c_{23} - s_{12}s_{23}s_{13}e^{i\delta} & s_{23}c_{13} \\ s_{12}s_{23} - c_{12}c_{23}s_{13}e^{i\delta} & -c_{12}s_{23} - s_{12}c_{23}s_{13}e^{i\delta} & c_{23}c_{13} \end{pmatrix}, \quad (1.6)$$

where $c_{ij} \equiv \cos\theta_{ij}$ and $s_{ij} \equiv \sin\theta_{ij}$. In this parametrization only four matrix elements are chosen to be real and only one physical phase appears. The s_{ij} are related to directly measurable quantities,

$$\begin{aligned} s_{13} &= |V_{ub}| \\ s_{12} &\approx |V_{us}| \\ s_{23} &\approx |V_{cb}| \end{aligned}$$

1.3.2 Wolfenstein parametrization

In 1983 it was realized that bottom quark decays predominantly to the charm quark, i.e. $|V_{cb}| \gg |V_{ub}|$. Then it was noticed by Wolfenstein that $|V_{cb}| \sim |V_{us}|^2$. He introduced a parametrization which holds unitarity approximately. Since then it has become very popular. In this parametrization,

$$V = \begin{pmatrix} 1 - \frac{1}{2}\lambda^2 - \frac{1}{8}\lambda^4 & \lambda & A\lambda^3(\rho - i\eta) \\ -\lambda + \frac{1}{2}A^2\lambda^5[1 - 2(\rho + i\eta)] & 1 - \frac{1}{2}\lambda^2 - \frac{1}{8}\lambda^4(1 + 4A^2) & A\lambda^2 \\ A\lambda^3[1 - (1 - \frac{1}{2}\lambda^2)(\rho + i\eta)] & -A\lambda^2 + \frac{1}{2}A\lambda^4[1 - 2(\rho + i\eta)] & 1 - \frac{1}{2}A^2\lambda^4 \end{pmatrix} + \mathcal{O}(\lambda^6). \quad (1.7)$$

The parameter $\lambda \approx 0.22$ serves as an expansion parameter and $A \sim 1$ as $|V_{cb}| \sim |V_{us}|^2$. ρ and η should be smaller than one as $|V_{ub}|/|V_{cb}| \sim \lambda/2$. V may be further expanded to a higher power of λ in case one wants to obtain a better approximation to unitarity. Two more generalized Wolfenstein parameters can be introduced following [21] as,

$$\overline{\rho} \equiv \rho\left(1 - \frac{1}{2}\lambda^2\right), \quad \overline{\eta} \equiv \eta\left(1 - \frac{1}{2}\lambda^2\right). \quad (1.8)$$

This parametrization is very important as it gives insights to the experimental information like $|V_{us}| \ll 1, |V_{cb}| \sim |V_{us}|^2$ and $|V_{ub}| \ll |V_{cb}|$. The unitarity property of the CKM matrix can also be checked through this parametrization. The relation between standard parametrization and Wolfenstein parametrization can be depicted by the following relations [21]:

$$\begin{aligned} s_{12} &= \lambda, \\ s_{23} &= A\lambda^2, \\ s_{13}e^{-i\delta} &= A\lambda^3(\rho - i\eta). \end{aligned} \tag{1.9}$$

We can always define a CP violating quantity which is independent of different parametrizations of the CKM matrix V. The Jarlskog parameter, $J_{\rm CP}$ [13], can be interpreted as a measure of the strength of CP violation in the SM and is defined as,

$$J_{\rm CP} = |\mathcal{I}m(V_{i\alpha}V_{j\beta}V_{i\beta}V_{j\alpha})|, \quad (i \neq j, \alpha \neq \beta).$$

In terms of the explicit parametrizations given above, we have,

$$J_{\rm CP} = c_{12}c_{23}c_{13}^2 s_{12}s_{23}s_{13}\sin\delta \simeq \lambda^6 A^2 \eta.$$

If we translate Eq. (1.2) in the mass basis, we obtain the necessary and sufficient condition for CP violation in the quark sector of the SM (we define $\Delta m_{ij}^2 \equiv m_i^2 - m_j^2$):

$$\Delta m_{tc}^2 \Delta m_{tu}^2 \Delta m_{cu}^2 \Delta m_{bs}^2 \Delta m_{bd}^2 \Delta m_{sd}^2 J_{\rm CP} \neq 0. \tag{1.10}$$

Eq. (1.10) gives the following requirements on the SM in order that it violates CP:

1. Within each quark sector, there should be no mass degeneracy.
2. None of the three mixing angles should be zero or $\pi/2$.
3. The phase should be neither 0 nor π.

1.4 The unitarity triangles of the CKM matrix

We obtain a set of 12 equations, consisting of 6 normalization and 6 orthogonality relations using the unitarity property of the CKM matrix $V^\dagger V = \mathbf{1} = VV^\dagger$. These 6 different orthogonality relations can be depicted through

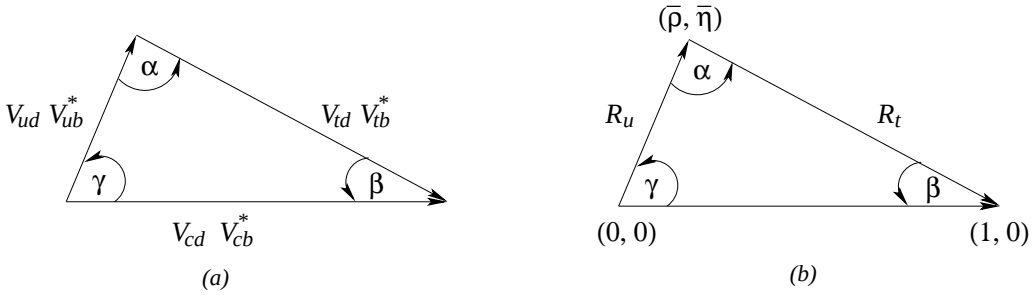

Figure 1.1: (a)Unitarity triangle depicted by Eq. (1.13), (b) Rescaled unitarity triangle.

6 different triangles in the complex plane [22]. Each of these triangles has the same area, $2A = J_{\rm CP}$ [23]. The orthogonality of different columns of the CKM matrix leads us to the following three relations:

$$V_{ud}V_{us}^* + V_{cd}V_{cs}^* + V_{td}V_{ts}^* = 0, \quad (1.11)$$
$$V_{us}V_{ub}^* + V_{cs}V_{cb}^* + V_{ts}V_{tb}^* = 0, \quad (1.12)$$
$$V_{ud}V_{ub}^* + V_{cd}V_{cb}^* + V_{td}V_{tb}^* = 0, \quad (1.13)$$

whereas orthogonality of different rows of the CKM matrix gives us the following relations:

$$V_{ud}V_{cd}^* + V_{us}V_{cs}^* + V_{ub}V_{cb}^* = 0, \quad (1.14)$$
$$V_{cd}V_{td}^* + V_{cs}V_{ts}^* + V_{cb}V_{tb}^* = 0, \quad (1.15)$$
$$V_{ud}V_{td}^* + V_{us}V_{ts}^* + V_{ub}V_{tb}^* = 0, \quad (1.16)$$

It can be noticed that among these six relations, only in Eq. (1.13) and Eq. (1.16), all three sides are of comparable magnitude of the $\mathcal{O}(\lambda^3)$, while in the remaining relations, one side is suppressed with respect to the others by factors of $\mathcal{O}(\lambda^2)$ or $\mathcal{O}(\lambda^4)$. It is the convention that the triangle described by Eq. (1.13) is called the "unitarity triangle" shown in fig. 1.1(a).

The unitarity triangle (UT) derived from Eq. (1.13) is rescaled further by choosing a phase convention such that $(V_{cd}V_{cb}^*)$ is real, and dividing the lengths of all sides by $|V_{cd}V_{cb}^*|$. This new phase convention helps to align

one side of the triangle on the real axis, while division of all the lengths by $|V_{cd}V_{cb}^*|$ makes the length of this side 1. It is shown in fig. 1.1(b). The form of the triangle remains unchanged. Two vertices of the rescaled unitarity triangle are thus fixed at (0,0) and (1,0). The coordinates of the remaining vertex correspond to the Wolfenstein parameters $(\overline{\rho}, \overline{\eta})$. Depicting the rescaled unitarity triangle in the $(\overline{\rho}, \overline{\eta})$ plane, the lengths of the two complex sides are

$$R_u \equiv \left|\frac{V_{ud}V_{ub}}{V_{cd}V_{cb}}\right| = \sqrt{\overline{\rho}^2 + \overline{\eta}^2}, \quad R_t \equiv \left|\frac{V_{td}V_{tb}}{V_{cd}V_{cb}}\right| = \sqrt{(1-\overline{\rho})^2 + \overline{\eta}^2}. \tag{1.17}$$

The three angles of the unitarity triangle are defined as follows [24]:

$$\alpha \equiv \arg\left[-\frac{V_{td}V_{tb}^*}{V_{ud}V_{ub}^*}\right], \quad \beta \equiv \arg\left[-\frac{V_{cd}V_{cb}^*}{V_{td}V_{tb}^*}\right], \quad \gamma \equiv \arg\left[-\frac{V_{ud}V_{ub}^*}{V_{cd}V_{cb}^*}\right]. \tag{1.18}$$

These three angles and sides of the rescaled unitary triangle are physical quantities and can be independently measured by different CP asymmetries in B decays. It is also useful to define the two small angles of triangles referred by Eq. (1.12) and Eq. (1.11):

$$\beta_s \equiv \arg\left[-\frac{V_{ts}V_{tb}^*}{V_{cs}V_{cb}^*}\right], \quad \beta_K \equiv \arg\left[-\frac{V_{cs}V_{cd}^*}{V_{us}V_{ud}^*}\right]. \tag{1.19}$$

It is important to notice that the angle β, γ and β_s are directly related to the complex weak-phases of the CKM matrix elements V_{td}, V_{ub} and V_{ts} respectively in the following fashion:

$$V_{td} = |V_{td}|e^{-i\beta}, \quad V_{ub} = |V_{ub}|e^{-i\gamma}, \quad V_{ts} = |V_{ts}|e^{-i\beta_s}. \tag{1.20}$$

It is important to measure all the UT parameters to understand SM better. Two groups CKM-fitter and UT-fit have performed a global analysis to convert experimental data into contours in the $\overline{\rho} - \overline{\eta}$ plane. Their main object is to over-constrain the UT as much as possible. They mainly use semi-leptonic $b \to ul^-\nu_l, cl^-\nu_l$ decays and $B_q^0 - \overline{B_q^0}$, $(q \to d, s)$ mixing to determine the UT sides R_u and R_t respectively by fixing two circles in the $\overline{\rho} - \overline{\eta}$ plane. They use the information of the indirect CP violation in the neutral kaon system described by ϵ_K and transform it into a hyperbola. They also use the direct measurement of $\sin 2\beta$ with the help of $B_d^0 \to J/\psi K_S$ modes. In Fig. (1.2),

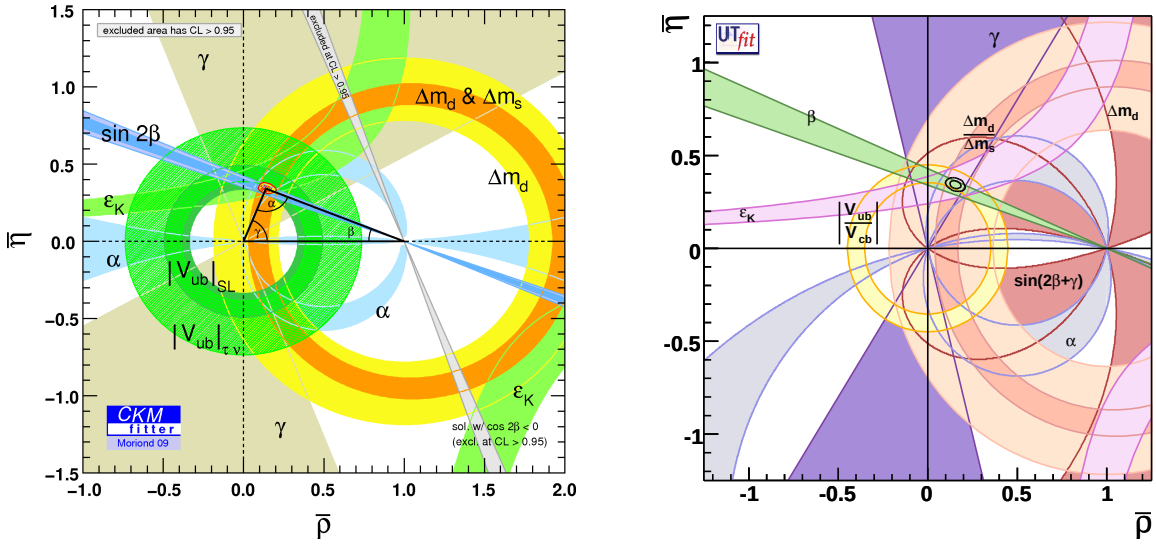

Figure 1.2: Analyses of the CKMfitter and UTfit collaborations [15, 17].

we show examples of the comprehensive analyses of the UT that are performed (and continuously updated) by the CKM Fitter Group [15] and the UTfit collaboration [17].

1.5 Beyond SM

The Standard Model however successful it might be, is not the end of the story. It is at best an effective theory, valid up to some high energy scale, which can at most be the Planck scale $M_{PL} \approx 10^{19}$GeV. There are enough reasons to suspect that some new physics will appear much before the Planck scale. The reasons are as follows.

- In SM, Higgs self energy correction from fermion loop, gauge boson loop or Higgs loop receives quadratic divergences which do not depend on the mass of the Higgs scalar m_S [25]. This indicates that m_S is an unnatural parameter of the SM and it is not protected by any symmetry of the SM. However, the requirement of perturbative unitarity in the amplitude $W^+W^- \to W^+W^-$ restricts $m_S < \mathcal{O}(1\text{TeV})$ [26]. These

quadratic divergences depend on the loop momenta $p^2 \sim \Lambda^2$ where Λ is the cut-off scale up to which SM is an adequate description of Nature. One could always renormalize such quadratic divergences away in the same way logarithmic divergences are disposed of. In that case, the residual correction to Higgs self energy due to fermion loop would be $\propto m_f^2 \lambda_f^2$, where λ_f is the coupling constant for the Yukawa interaction term of the Lagrangian. If it is believed that SM is a part of the more fundamental theory like Grand Unification Model (GUT) which unifies strong and electroweak forces in it at a energy scale $M_U \sim 10^{16}$ GeV, there will exist some fermions whose masses will be $\propto M_U$. The loop corrections to the scalar mass square δm_S^2 due to these fermion-antifermion pairs will be then $\propto M_U^2$. In this scenario, it requires an unnatural amount of fine tuning between the bare scalar mass squared $m_{S,0}^2$ and the renormalization δm_S^2 in order to keep the renormalized mass squared $m_S^2 = m_{S,0}^2 + \delta m_S^2$ less than a $(\text{TeV})^2$. There are many approaches to solve this fine-tuning problem: Supersymmetry (SUSY) is one of the possible candidate for it. SUSY has all the SM particles in it. In addition, for each SM fermion and vector boson SUSY has a corresponding new particle. SUSY requires at least two complex scalar doublets to give masses to its particles. The large radiative corrections due to these new particles cancel the corrections coming from the SM fields. The other NP candidates which shed some light on this problem are Technicolour, where the Higgs is assumed to be a composite of two fermions; Models with compactified extra dimensions, where the Planck scale is lowered to a few TeV by appealing to the fact that gravity is weak not because of a large Planck mass but due to a small intercept of higher dimensional gravitational wave function with our physical world; Little Higgs models, where the Higgs is constructed as a pseudo-Goldstone boson and hence has its mass is protected.

- There are 19 free parameters in the SM, which is a large number for any fundamental theory: the six quark masses, three lepton masses, three CKM mixing angles, one CKM CP-violating phase, three gauge couplings (U(1), SU(2), SU(3)), one QCD vacuum angle θ_{QCD}, 0ne Higgs quadratic coupling and one Higgs self coupling. It is hoped that a more fundamental theory might relate some of them.

- As in the SM the three gauge couplings do not unify, SM cannot lead

to a unified theory of strong and electroweak interactions. This is an aesthetic objection, but Supersymmetry provides a nice way to gauge coupling unification and hence a Grand Unified Theory (GUT). Leptoquark based models, where a lepton can directly transform into quark and vice-versa at tree level is one of the GUT inspired models, which can solve this problem.

- Experimental observation of neutrino mass and oscillations cannot be accounted for in the SM. One has to introduce the neutrino masses by hand.

We expect that any theory which tries to answer these fundamental problems should leave some low-energy signatures. In the 4th chapter we discuss one such NP model based on the leptoquarks.

Chapter 2

Parametrization Independent Studies of Neutral B Meson Decays

2.1 Introduction

The two B Factories PEP-II and KEK-B were designed to have peak luminosities $3 \times 10^{33}\text{cm}^{-2}\text{s}^{-1}$ and $1 \times 10^{34}\text{cm}^{-2}\text{s}^{-1}$ respectively. PEP-II, however, reached design luminosity in a remarkably short time, and before shutting down, it exceeded its design performance by a factor of three. KEK-B, with a more ambitious design objective, has also exceeded its design performance, and currently operates at even higher luminosity. The accumulation of all these events allow precision measurements of exclusive B meson decays. These measurements indicate subtle discrepancies between some experimental data and theoretical predictions within the standard model, though at present error bars are still large to come to any concrete conclusion. These discripencies are quite puzzling and it is difficult to ignore them.

One of such puzzles involve the weak phase $\beta \equiv \arg\left(-V_{cd}V_{cb}^*/V_{td}V_{tb}^*\right)$ which is defined via the CKM matrix element $V_{td} = |V_{td}|e^{i\beta}$. This phase can be extracted either from the tree-dominated $b \to c\bar{c}s$, e.g. $B \to J/\psi K_S$ or penguin-dominated $b \to sq\bar{q}$, e.g. $B \to \phi K_S$ modes. The two determinations should be same in the SM, but would differ, if new physics contributions modify the penguin dominated decay amplitudes. For several years a large deviation $\Delta S \equiv S_{sq\bar{q}} - S_{c\bar{c}s}$ has been measured where S_i has been defined in

Eq. (2.24) in Section (2.3.1). Several studies have been done to estimate the penguin pollution in the $b \to c\bar{c}s$ trees and the tree pollution in the $b \to sq\overline{q}$ penguins using various QCD based models and SU(3) based models. However, these studies [27], [28], [29], [30] are unable to produce the observed effect. For most of the cases, these studies indicate that the sign of the discrepancy within SM is opposite to the observed value. It has become one of the most challenging puzzle in B-physics to provide convincing arguments regarding the nature of this discrepancy and whether it can be regarded as an unambiguous signal of NP. In this chapter we have tried to answer these questions.

First we discuss about the parametrization of the most general amplitude for $\overline{b} \to \overline{q}$ transition modes where q is either d or s quark, then we present a quick review about the progress of the SM estimation of these modes. Finally we discuss in details about our own method to try to solve this puzzle.

2.2 Parametrizing the amplitude

The most general amplitude for $\overline{b} \to \overline{q}$ transition modes where q is either d or s quark may be written as [31],

$$A^{\overline{b}\to\overline{q}} = \mathcal{A}_{uq} e^{i\delta_{uq}} v_{uq} + \mathcal{A}_{cq} e^{i\delta_{cq}} v_{cq} + \mathcal{A}_{tq} e^{i\delta_{tq}} v_{tq}, \tag{2.1}$$

where $v_{jq} = V_{jb}^* V_{jq}$ with $j = u, c$ or t are the product of CKM matrix elements and $\mathcal{A}_{jq}$ and δ_{jq} are the amplitudes and strong phases associated with the CKM factor v_{jq}. The unitarity property of CKM matrix gives us a relation $v_{uq} + v_{cq} + v_{tq} = 0$. Using this property we can eliminate any one of the v_{jq} from Eq. (2.1) and express it in terms of only two independent contributions having different weak phases.

In SM, within the framework of Wolfenstein parametrization [20] the various v_{jq} are expressed up to order $\mathcal{O}(\lambda^6)$ as follows:

$$\begin{aligned} v_{cs} &= A\lambda^2\Big(1 - \frac{1}{2}\lambda^2\Big), \\ v_{cd} &= -A\lambda^3, \\ v_{us} &= A\lambda^4(\rho + i\eta), \end{aligned} \tag{2.2}$$

$$\begin{aligned} v_{ud} &= A\lambda^3(\rho+i\eta)\Big(1-\frac{\lambda^2}{2}\Big), \\ v_{ts} &= -A\lambda^2\Big(1-(\frac{1}{2}-\rho-i\eta)\lambda^2\Big), \\ v_{td} &= A\lambda^3\Big(1-\Big(1-\frac{\lambda^2}{2}\Big)(\rho+i\eta)\Big). \end{aligned} \tag{2.3}$$

In the above parametrization it is clear that v_{cs} and v_{cd} are real at least to order $\mathcal{O}(\lambda^6)$. The weak phase arising from v_{us} and v_{ud} are represented by the familiar unitary triangle angle γ, where

$$\gamma \equiv \arg\left[-\frac{V_{ud}V_{ub}^*}{V_{cd}V_{cb}^*}\right] \approx 60^o \ . \tag{2.4}$$

The weak phase of v_{td} is the well known phase β, where [32]

$$\beta \equiv \arg\left[-\frac{V_{cd}V_{cb}^*}{V_{td}V_{tb}^*}\right] = (21.1 \pm 0.9)^o. \tag{2.5}$$

The weak phase of v_{ts} is represented by β_s, where

$$\beta_s \equiv \arg\left[-\frac{V_{ts}V_{tb}^*}{V_{cs}V_{cb}^*}\right] = 1.045^{o\,+0.061^o}_{\,-0.057^o} \ . \tag{2.6}$$

Since v_{cq} is almost real, the amplitude $A^{\bar{b}\to\bar{q}}$ may be rewritten in terms of only one non-zero weak phase, by eliminating either v_{uq} or v_{tq} using the unitarity condition. This results in a choice of two different ways to parametrize the $\bar{b}\to\bar{q}$ amplitude.

The elimination of v_{tq} leads to the amplitude being expressed in terms of the weak phase γ independent of q, since v_{us} and v_{ud} have the same weak phase. We can write,

$$A^{\bar{b}\to\bar{q}} = (\mathcal{A}_{cq}e^{i\delta_{cq}} - \mathcal{A}_{tq}e^{i\delta_{tq}})v_{cq} + (\mathcal{A}_{uq}e^{i\delta_{uq}} - \mathcal{A}_{tq}e^{i\delta_{tq}})v_{uq}. \tag{2.7}$$

The amplitude may then be re-expressed as follows:

$$A^{\bar{b}\to\bar{q}} = e^{i\Theta'_q}\big[a'_q + b'_q e^{i\delta'_q}e^{i\gamma}\big], \tag{2.8}$$

$$a'_q = |v_{cq}|\,\hat{a}'_q = |v_{cq}|\left|\mathcal{A}_{cq}e^{i\delta_{cq}} - \mathcal{A}_{tq}e^{i\delta_{tq}}\right|, \tag{2.9}$$

$$b'_q = |v_{uq}|\,\hat{b}'_q = |v_{uq}|\left|\mathcal{A}_{uq}e^{i\delta_{uq}} - \mathcal{A}_{tq}e^{i\delta_{tq}}\right|. \tag{2.10}$$

Here, Θ'_q is an overall strong phase which cannot be detected experimentally; we hence set it to be zero. This fact will become clear once we write down the observables in the next section (Sec. 2.3) and find that no observable depends on Θ'_q. δ'_q is the relative strong phase difference between a'_q and b'_q. At this stage we emphasize an essential difference between our parametrization for $q = s$ or $q = d$: *the negative sign of v_{cd} is absorbed into the definition of δ'_d for convenience.*

Similarly the elimination of v_{uq} leads us to parametrization, the details of which depend on whether $q = s$ or $q = d$. We first consider $q = s$, this results in the β_s parametrization. Here we can write,

$$A^{\bar{b}\to\bar{s}} = (\mathcal{A}_{cs}e^{i\delta_{cs}} - \mathcal{A}_{us}e^{i\delta_{us}})v_{cs} + (\mathcal{A}_{ts}e^{i\delta_{ts}} - \mathcal{A}_{us}e^{i\delta_{us}})v_{ts}. \tag{2.11}$$

This amplitude may also be re-expressed as follows:

$$A^{\bar{b}\to\bar{s}} = e^{i\Theta''_s}\left[a''_s + b''_s e^{i\delta''_s}e^{i\beta_s}\right], \tag{2.12}$$

$$a''_s = |v_{cs}|\,\hat{a}''_s = |v_{cs}|\left|\mathcal{A}_{cs}e^{i\delta_{cs}} - \mathcal{A}_{us}e^{i\delta_{us}}\right|, \tag{2.13}$$

$$b''_s = |v_{ts}|\,\hat{b}''_s = |v_{ts}|\left|\mathcal{A}_{ts}e^{i\delta_{ts}} - \mathcal{A}_{us}e^{i\delta_{us}}\right|. \tag{2.14}$$

We will set $\Theta''_s = 0$ for the same reasons we set $\Theta'_q = 0$ above. δ''_s is the relative strong phase difference between a''_s and b''_s. Note that a negative sign originating from v_{ts} has been absorbed in the definition of δ''_s for convenience. Interestingly, one may also note that the magnitudes of $\hat{b}'_s$ and $\hat{b}''_s$ are same. The elimination of v_{uq} for $q = d$ results in the amplitude:

$$A^{\bar{b}\to\bar{d}} = (\mathcal{A}_{cd}e^{i\delta_{cd}} - \mathcal{A}_{ud}e^{i\delta_{ud}})v_{cd} + (\mathcal{A}_{td}e^{i\delta_{td}} - \mathcal{A}_{ud}e^{i\delta_{ud}})v_{td}, \tag{2.15}$$

which is re-expressed as,

$$A^{\bar{b}\to\bar{d}} = e^{i\Theta''_d}\left[a''_d + b''_d e^{i\delta''_d}e^{i\beta}\right], \tag{2.16}$$

$$a''_d = |v_{cd}|\,\hat{a}''_d = |v_{cd}|\left|\mathcal{A}_{cd}e^{i\delta_{cd}} - \mathcal{A}_{ud}e^{i\delta_{ud}}\right|, \tag{2.17}$$

$$b''_d = |v_{td}|\,\hat{b}''_d = |v_{td}|\left|\mathcal{A}_{td}e^{i\delta_{td}} - \mathcal{A}_{ud}e^{i\delta_{ud}}\right|. \tag{2.18}$$

We have thus demonstrated how the amplitudes for $\overline{b} \to \overline{s}$ or $\overline{b} \to \overline{d}$ may be expressed as a sum of two contributions, one with zero weak phase and the other with a chosen weak phase that is either β_s or γ for $\overline{b} \to \overline{s}$, and β or γ for $\overline{b} \to \overline{d}$.

We consider the decay $B_d^0 \to f_q$, which results from an underlying $\overline{b} \to \overline{q}$ quark level process, where q could be either s quark or d quark. From the above arguments it is easy to conclude that the amplitude A_q for such a decay, can be expressed in a parametrization independent way, in terms of two contributing amplitudes as follows:

$$A_q = a_q + b_q e^{i\delta_q} e^{i\phi_q}, \tag{2.19}$$

where a_q and b_q are the magnitudes of the two contributions, δ_q is the corresponding strong phase difference, and ϕ_q is the weak phase. The weak phase ϕ_q can be chosen from two different values, which define the choice of parametrization. Once the parametrization is chosen, ϕ_q has the same value for all possible final states which result from the same underlying quark level process $\overline{b} \to \overline{s}$ or $\overline{b} \to \overline{d}$. The values of a_q, b_q and δ_q, however, depend on the decay mode.

a_q can be either a'_q or a''_q; b_q can be either b'_q or b''_q depending on the two parametrization and ϕ_q can be γ or β_s. Assuming the CPT invariance, the amplitude for the CP conjugate mode can be written as:

$$\overline{A_q} = a_q + b_q e^{i\delta_q} e^{-i\phi_q}. \tag{2.20}$$

For simplification of notation we assume that A_q, $\overline{A_q}$, a_q and b_q are normalized by the total decay width of B_d^0. This will not change the Physics.

2.3 Observables and Variables

2.3.1 Observables

The time dependent decay rate of B_d^0 to a mode f_i(or f_q) can be written as

$$\Gamma(B_d^0(t) \to f_i) \propto B_i(1 + C_i \cos(\Delta M t) - S_i \sin(\Delta M t)), \tag{2.21}$$

where B_i is the branching ratio, C_i is the direct CP asymmetry arising from the fact that $|A_i| \neq |\overline{A_i}|$ and S_i is the time dependent CP asymmetry which arises from the interference between the decay. This three quantities are observables and can be expressed as

$$B_i = \frac{|A_i|^2 + |\overline{A_i}|^2}{2} = a_i^2 + b_i^2 + 2a_i b_i \cos\phi \cos\delta_i, \tag{2.22}$$

$$C_i = \frac{|A_i|^2 - |\overline{A_i}|^2}{|A_i|^2 + |\overline{A_i}|^2} = \frac{-2a_i b_i \sin\phi \sin\delta_i}{B_i}, \tag{2.23}$$

$$S_i = \sqrt{1 - C_i^2} \sin 2\beta_i^{\text{meas}}. \tag{2.24}$$

with

$$\sin 2\beta_i^{\text{meas}} = -\frac{\text{Im}(e^{-2i\beta} A_i^* \overline{A_i})}{|A_i||\overline{A_i}|}, \tag{2.25}$$

The phase β in S_i comes from $B_d^0 - \overline{B_d^0}$ mixing box diagrams.

2.3.2 Extraction of $2\beta^{\text{meas}}$

Within the SM, β can not be extracted experimentally due to the pollution through the phase difference between A_i and $\overline{A_i}$. As a result, S_i provides a measurement of $\sin 2\beta_i^{\text{meas}}$. Further extraction of $2\beta_i^{\text{meas}}$ gives a two fold ambiguity $(2\beta_i^{\text{meas}}, \pi - 2\beta_i^{\text{meas}})$. Therefore we get a four fold ambiguity in the difference between the two values of $2\beta^{\text{meas}}$ as $\Big(\pm(2\beta_1^{\text{meas}} - 2\beta_2^{\text{meas}}), \pm\pi \mp (2\beta_1^{\text{meas}} + 2\beta_2^{\text{meas}}) \Big)$ which can be measured using two different modes f_1 and f_2. However, we will only be interested in the principal value $2\beta_i^{\text{meas}}$, obtained from $\sin 2\beta_i^{\text{meas}}$, so as to have a well defined value of the difference. This value of the difference is denoted by 2ω and is defined as

$$2\omega = 2\beta_1^{\text{meas}} - 2\beta_2^{\text{meas}}. \tag{2.26}$$

The two modes f_1 and f_2 are chosen such that $\beta_1^{meas} > \beta_2^{meas}$. This choice results in 2ω always being positive.

2.3.3 Variables

The phase difference between A_i and $\overline{A_i}$ is defined as η_i, i.e.,

$$\eta_i = \arg A_i - \arg \overline{A_i}. \tag{2.27}$$

Hence, $A_i^* \overline{A_i} = |A_i||\overline{A_i}|e^{-i\eta_i}$ and the expression for $\sin 2\beta_i^{\rm meas}$ from Eq. (2.25) implies that $\eta_i = 2\beta_i^{\rm meas} - 2\beta$. η_i is thus the deviation of $2\beta_i^{\rm meas}$ from 2β. ω can now be expressed in terms of $\eta_{1,2}$ as

$$2\omega = \eta_1 - \eta_2. \tag{2.28}$$

We have three observables B_i, C_i, S_i and five variables $a_i, b_i, \delta_i, \eta_i$ and ϕ. It implies the number of independent variables is only two. The choice of these two independent variables is completely in our hand. From Eqs. (2.19) - (2.20) and Eqs. (2.22) - (2.24), a_i, b_i and δ_i can be expressed in terms of B_i, C_i, S_i and η_i, ϕ as

$$a_i^2 = \frac{B_i}{2\sin^2\phi}\Big(1 - \sqrt{1-C_i^2}\cos(\eta_i - 2\phi)\Big), \tag{2.29}$$

$$b_i^2 = \frac{B_i}{2\sin^2\phi}\Big(1 - \sqrt{1-C_i^2}\cos(\eta_i)\Big), \tag{2.30}$$

$$\tan\delta_i = \frac{C_i \sin\phi}{\cos\phi - \sqrt{1-C_i^2}\cos(\eta_i - \phi)}. \tag{2.31}$$

Before we discuss about our analysis in Sec. (2.5), we present a brief summary of the bounds obtained from SM analysis in the tree and penguin sector in the next section.

2.4 Standard Model analysis

The decay mode $b \to c\bar{c}s$ e.g. $B_d^0 \to J/\psi K_S$ has been regarded as the golden mode for extracting the standard-model parameter $\sin 2\beta$ [33]. The penguin pollution in this mode is only of the order of 5% and hence almost negligible. On the other hand, the $b \to sq\overline{q}$ e.g. $B_d^0 \to \phi K_S$ is penguin dominated and hence there is a large possibility that it can receive a contribution from beyond SM physics. The theoretical estimation of these penguin dominated modes have been progressed mainly in two different directions. Firstly, sev-

eral studies have been done to include QCD corrections based on different hadronic assumptions e.g QCD factorization(QCDF), Soft Collinear Effective Theory(SCET) and Perturbative QCD(PQCD). Secondly SU(3) flavour symmetry between s and d quarks has been used to constrain the penguin dominated modes. Here we present a very brief summary of all these constraints.

Mode	**QCDF bound**	**SCET bound**	**PQCD bound**
ϕK_S	0.02 ± 0.01 [35]	-	0.02 ± 0.01 [36]
$\eta' K_S$	0.01 ± 0.01 [37]	-0.019 ± 0.008, Sol-I -0.010 ± 0.010, Sol-II [28]	-
$\pi^0 K_S$	$0.07^{+0.05}_{-0.04}$ [29]	0.077 ± 0.030 [28]	$0.053^{+0.02}_{-0.03}$ [38], [39]
$\rho^0 K_S$	$-0.08^{+0.08}_{-0.12}$ [29]	-	$0.187^{+0.10}_{-0.06}$ [38], [39]
ωK_S	0.13 ± 0.08 [29]	-	$0.153^{+0.03}_{-0.07}$ [38], [39]

Table 2.1: Constraints on ΔS_i from QCDF, SCET, PQCD.

For $B_d^0 \to f_i$ decay, a parameter r_i can be defined from Eq. (2.7) as [34],

$$r_i e^{i\delta_i} = \left|\frac{v_{uq}}{v_{cq}}\right| \frac{(\mathcal{A}_{uq} e^{i\delta_{uq}} - \mathcal{A}_{tq} e^{i\delta_{tq}})}{(\mathcal{A}_{cq} e^{i\delta_{cq}} - \mathcal{A}_{tq} e^{i\delta_{tq}})} \approx 0.02 \frac{A_i^u}{A_i^c}, \tag{2.32}$$

where δ_i is the strong phase. Expanding Eq. (2.25) in terms of the small

ratio r_i,

$$\sin 2\beta^{\rm meas} = \sin 2\beta + 2r_i \cos\delta_i \cos 2\beta \sin\gamma, \quad (2.33)$$

$$C_i = -2r_i \sin\delta_i \sin\gamma. \quad (2.34)$$

In the limit of negligible r_i, $\sin 2\beta^{\rm meas} = \sin 2\beta$ and $C_i = 0$. If the direct CP asymmetry C_i is found to be non-zero experimentally, it would establish the fact that r_i dependent terms are important. The quantity $\Delta S_i \equiv S_{sq\bar{q}} - S_{c\bar{c}s}$ can be written as

$$\Delta S_i = \sin 2\beta^{\rm meas}_{sq\bar{q}} - \sin 2\beta^{\rm meas}_{c\bar{c}s}. \quad (2.35)$$

Without going into the detail discussion of different hadronic assumptions, we present a summary of the predicted ΔS_i by different QCD based models like QCDF, SCET and PQCD for different penguin dominated modes in Table. (2.1).

$\Delta S = 0$ modes are related to $\Delta S = 1$ modes by SU(3) flavour symmetry, and using this symmetry the bounds on r_i can be obtained as [40],

$$r_i \leq \frac{\mathcal{R} + \overline{\lambda}^2}{1 - \mathcal{R}}, \quad \mathcal{R} \leq \overline{\lambda} \sum_{f'} |n_{f'}| \sqrt{\frac{\overline{\mathcal{B}_{f'}}(\Delta S = 0)}{\overline{\mathcal{B}_f}(\Delta S = 1)}}, \quad (2.36)$$

where $n_{f'}$ are numerical coefficients,

$$\mathcal{R}^2 \equiv \frac{\overline{\lambda^2}\left(|\sum_f n_f A(f)|^2 + |\sum_f n_f \overline{A}(f)|^2\right)}{\left(|A(B^0 \to \eta' K^0)|^2 + |A(\overline{B^0} \to \eta' \overline{K^0})|^2\right)} \quad (2.37)$$

and

$$\overline{\lambda} = -\frac{V^*_{cb} V_{cd}}{V^*_{cb} V_{cs}} \approx 0.225. \quad (2.38)$$

The sum over f in Eq. (2.37) is a sum over all the amplitudes of $\pi^0\pi^0, \pi^0\eta, \pi^0\eta', \eta\eta, \eta'\eta', \eta\eta'$ modes. In the limit in which small amplitudes involving the spectator quarks may be neglected, $\pi^0\eta, \pi^0\eta'$ and $\eta\eta'$ amplitudes can be ignored . The bound on $\mathcal{R}$ is thus in general better, if the sum is over a smaller set of modes f'. Furthermore, all the branching ratios f' in the bound need to be measured to have the best bound. Using branching ratios of $\pi^0\eta, \eta'\eta', \pi^0\pi^0, \pi^0\eta', \eta\eta, \eta\eta'$, $\mathcal{R}_{\eta' K_s} < 0.116$ [40]. Using QCDF predicted

branching ratios, $\mathcal{R}_{\eta' K_s} < 0.045$ [37]. The bound on $\mathcal{R}_{\eta' K_s} < 0.088$ using SCET predicted branching ratios [28]. Bounds on $\phi K_S, KKK$ modes are not good [41], [42], [43]. The bounds on $r_{K^+K^-K^0} < 1.02, r_{K_sK_sK_s} < 0.31$ [42], [43]. Performing a global fit to experimental data, SU(3) prediction for $\sin 2\beta^{\rm meas}_{\pi^0 K_s} = -0.81 \pm 0.03$ which is far away from the measured experimental value [42], [44].

The experimental values of ΔS_i are found negative in most of the cases as can be seen from Fig. (2.1). These values are less than the theoretically predicted values also. Presently the error in these experimental values are in such a regime that the tree pollutions in different $b \to sq\overline{q}$ modes with $q \to d, s$ can not be neglected any more. Even with the SU(3) approach, at present, only upper limits are available for many of the branching ratios that enter into Eq. (2.36). That is why these bounds obtained from the SU(3) analysis are probably a significant overestimate and will improve with further data. Hence, in both approaches, the theoretical bounds will be more robust with further availability of the experimental data.

In the next section we present a completely different approach based on geometrical interpretation to argue whether the discrepancies in the measured values of ΔS_i can be an indication of NP or not.

2.5 Relation between ω and ϕ

We want to find a relation between ω and ϕ. Eq. (2.28) depicts that ω and η's are related to each other. Using this fact we first try to obtain a relation between η and ϕ which finally leads to a relation between ω and ϕ. The first thing which can be noticed is how sign of η depends on sign of ϕ and then how amplitude of η depends on amplitude of ϕ. In this section we present a geometric approach, though we have verified all the results numerically. The simplicity of the arguments is the real beauty of this approach.

2.5.1 Relation between sign of η and ϕ

A_i and $\overline{A_i}$ are represented geometrically. Given values of a_i, b_i, δ_i and ϕ, $|A_i|$ and $|\overline{A_i}|$ are as shown in the Fig. 2.2. For the purpose of illustration first we choose $\delta_i > 0$ and $\phi > 0$. $\vec{a_i}$ is represented by QV, and $\vec{b_i}$ is represented by SV or PV depending on the phase $\delta_i + \phi$ or $\delta_i - \phi$, resulting into the

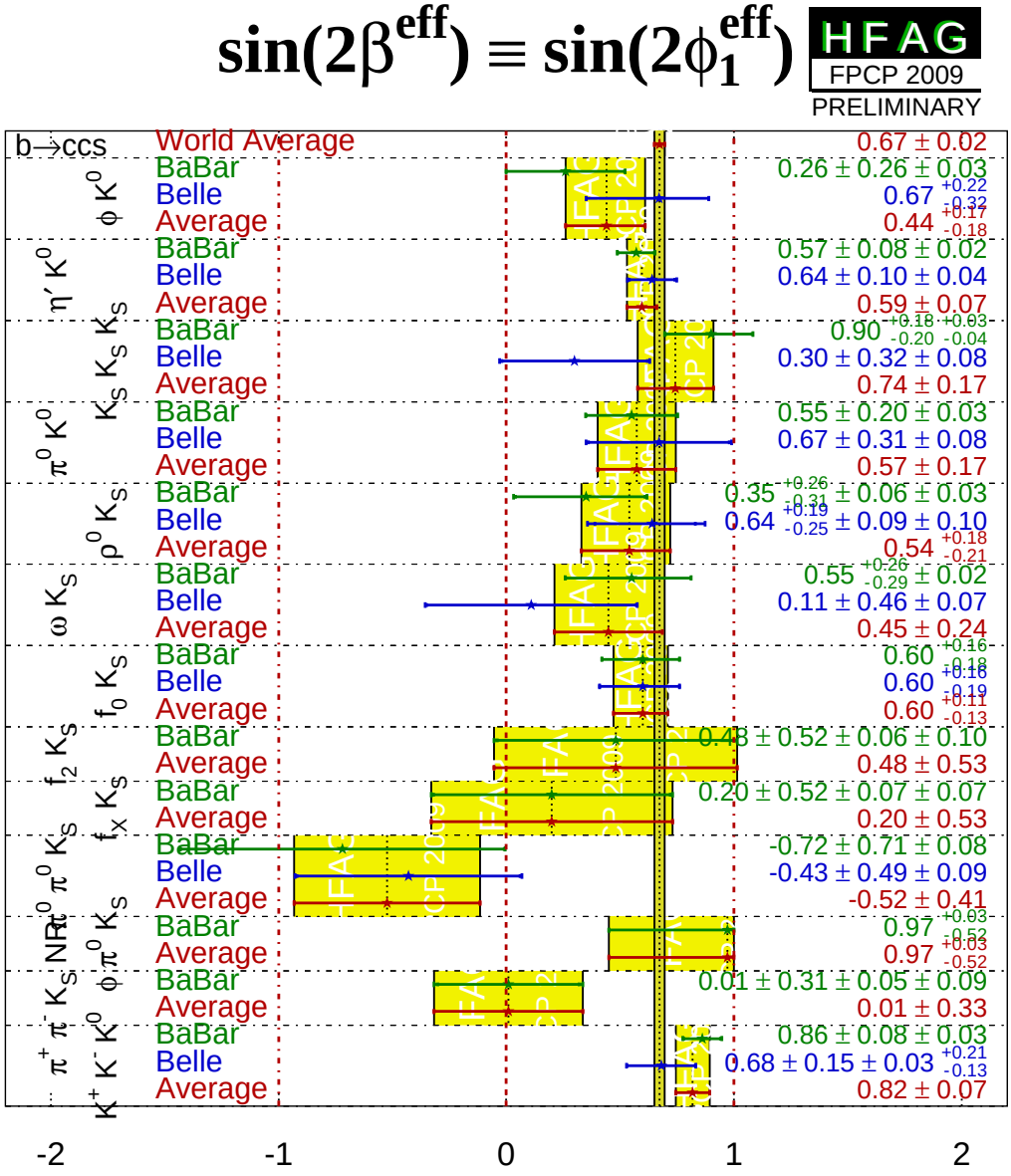

Figure 2.1: $\sin 2\beta^{\rm eff} \equiv \sin 2\beta^{\rm meas}$ from the HFAG collaboration [32].

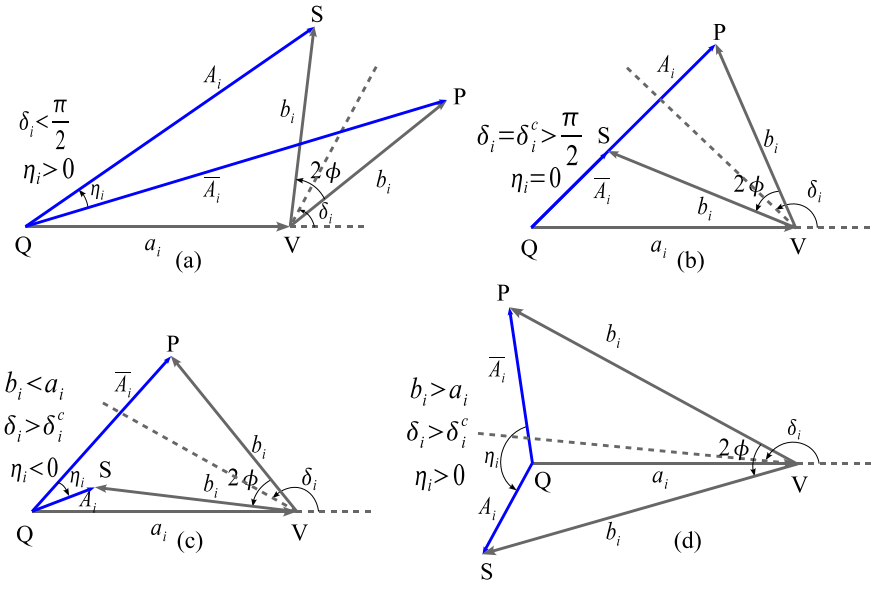

Figure 2.2: The amplitudes A_i and $\overline{A}_i$ in terms of a_i and b_i for the case $\phi > 0$ and $\delta_i > 0$.

amplitude A_i and $\overline{A_i}$ respectively. It may be noted that the same values of $|A_i|$, $|\overline{A_i}|$ and η_i can be obtained using different values of a_i, b_i, δ_i and ϕ. The set of points for which this is possible is obtained by moving the point V along the bisector to SP, since SV and PV are both b_i, they must always be equal. It is hence essential to express all quantities in terms of irreducible variables.

In Fig. 2.2(a) we choose δ_i to lie in the range between 0 and $\pi/2$. Clearly η_i is always positive (if $\phi > 0$) irrespective of the values of the amplitudes a_i and b_i. If δ_i is increased beyond $\pi/2$, at some critical value of $\delta_i = \delta_i^c$, η_i becomes 0. This is expressed in Fig. 2.2(b). This critical value δ_i^c can be easily derived from Eq. (2.31) substituting $\eta_i = 0$ and the expression for it is

$$\tan\delta_i^c = \frac{C_i \sin\phi}{\cos\phi\left(1 - \sqrt{1 - C_i^2}\right)}. \tag{2.39}$$

If δ_i is increased further beyond δ_i^c the sign of η_i depends on the relative

magnitudes of a_i and b_i; $\eta_i < 0$ if $b_i < a_i$ (Fig. 2.2(c)) and $\eta_i > 0$ if $b_i > a_i$ (Fig. 2.2(d)). It is easy to generalize to the cases where both δ_i and ϕ can be positive or negative. Note that from Eq. (2.23), if δ_i and ϕ have the same sign then $C_i < 0$, else $C_i > 0$.
δ_i^c lies in the range $\pi/2$ to π for $C_i < 0$ and $-\pi$ to $-\pi/2$ for $C_i > 0$. Here we want to mention that δ_i^c is strictly not defined for $C_i = 0$, but may be taken to have any value between $\pi/2$ and π. And Fig. 2.2(b) and Fig. 2.2(c) do not apply to the case where $C_i = 0$, as only two values of δ_i are allowed, it can be either 0 or π. Hence, we conclude that η_i always has the same sign as ϕ if $|\delta_i| \leq |\delta_i^c|$. The weak phase ϕ is fixed by the parametrization chosen within SM and is same for all modes. Hence as long as $|\delta_i| \leq |\delta_i^c|$ for each mode f_i, the sign of ϕ and η_i must be same for all modes.

2.5.2 Relation between magnitude of η and ϕ

Next, we want to see how the magnitude of η_i depends on magnitude of ϕ, when the magnitude of the strong phase is constrained to be less than δ_i^c, i.e. $|\delta_i| < \delta_i^c$.

Cases for $\phi > 0$: To start with, let us consider $\phi > 0$. The magnitude of η depends on both δ_i and ϕ. $|\delta_i|$ itself can be either less than ϕ or larger than ϕ. Further, δ_i can be both positive and negative. We thus require a case by case study depending on the value of δ_i. The three possible cases that need individual consideration are shown in Fig 2.3.

Fig. 2.3(a) represents the case with positive δ_i greater than ϕ, i.e. $0 \leq \phi \leq \delta_i \leq \delta_i^c$. Using simple geometry it is easy to deduce that

$$2\phi = \eta_i + \zeta_i - \overline{\zeta_i}. \tag{2.40}$$

In Eq. (2.23), since the amplitudes a_i, b_i and the branching ratio B_i are all positive quantities, it is clear that for this case ($0 \leq \phi \leq \delta_i \leq \delta_i^c$), $C_i < 0$. Eq. (2.23) also in turn implies that $|A_i| < |\overline{A_i}|$, if $C_i < 0$. It is then easy to prove that if $|A_i| < |\overline{A_i}|$, $|\overline{\zeta_i}| < |\zeta_i|$ must hold. Before we present the proof we focus on Fig. 2.4(a) and 2.4(b). Fig. 2.4(a) is a repetition of Fig. 2.3(a) with only the essential labels retained. In Fig. 2.4(b) the triangle $\triangle QVP$ of Fig. 2.4(a) is flipped to triangle $\triangle QVP'$. In $\triangle QSP'$,

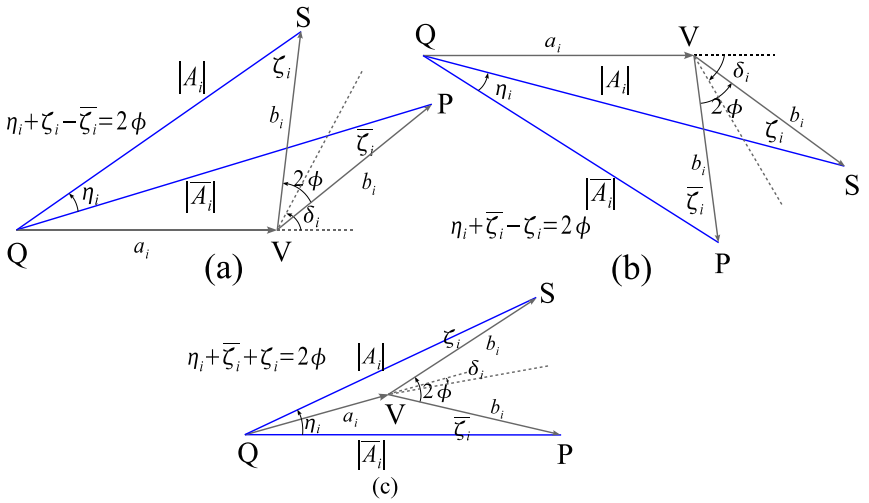

Figure 2.3: Case $\phi > 0$ and $-\delta_i^c < \delta_i < \delta_i^c$. The amplitudes A_i and $\overline{A}_i$ in terms of a_i and b_i. The three possible cases need individual consideration. In cases (a) and (b) we consider $\phi \leq |\delta|$ where as in case (c) we consider $|\delta| < \phi$. The two cases requiring different treatment for $\phi \leq |\delta|$, i.e. $0 \leq \delta_i \leq \delta_i^c$ and $0 \leq \delta_i \leq \delta_i^c$ are considered in (a) and (b) respectively.

$$
\begin{aligned}
& |A_i| < |\overline{A_i}| \quad \Rightarrow \quad \angle QP'S < \angle QSP'. \\
\therefore \quad & (\angle QP'V + \angle VSP) \; < \; \angle QSV + \angle VSP'). \\
\text{Further,} \quad & VS = VP' = b_i \quad \Rightarrow \quad \angle VSP' = \angle VP'S. \\
\text{Hence,} \quad & \angle QP'V < \angle QSV \text{ or } |\overline{\zeta_i}| < |\zeta_i|.
\end{aligned}
$$

It is proved that $|\overline{\zeta_i}| < |\zeta_i|$ for $0 \leq \phi \leq \delta_i \leq \delta_i^c$. From Eq. (2.40), hence it can be concluded that for the case under consideration $\eta_i \leq 2\phi$.

The next case, $-\delta_i^c \leq \delta_i \leq 0$ is depicted in Fig. 2.3(b). For this case η_i and ϕ are related by

$$2\phi = \eta_i - \zeta_i + \overline{\zeta_i}. \tag{2.41}$$

Using Eq. (2.23) and logic similar to the case above, it is easy to see that $0 < C_i$ is implying that $|\overline{A_i}| < |A_i|$. Thus, $|\zeta_i| < |\overline{\zeta_i}|$ must hold, as can be seen by a proof analogous to the above. Hence, it can be deduced that

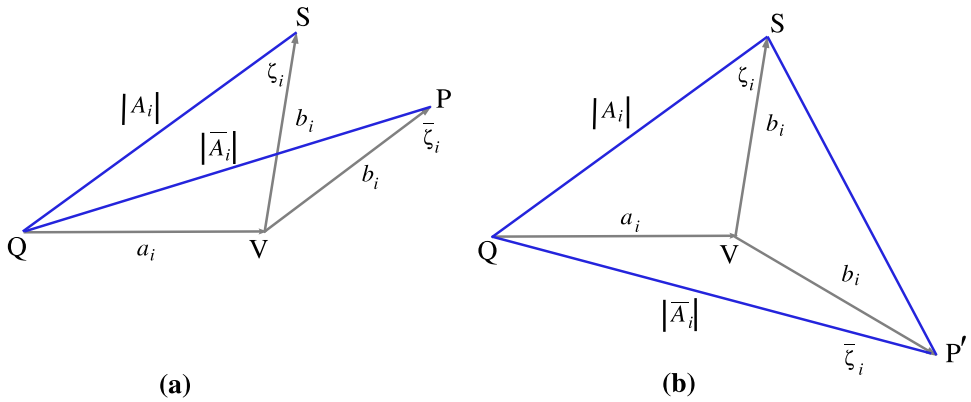

Figure 2.4: For $|\overline{A_i}| > |A_i|$, (a) before flipping ΔQVP, (b) after flipping ΔQVP to ΔQVP$'$.

$\eta_i \leq 2\phi$ even when $-\delta_i^c \leq \delta_i \leq 0$ as long as ϕ is positive.

The case of Fig. 2.3(c), when $|\delta_i| < \phi$ is simpler to deal with as it does not depend on the sign of δ_i. It is easy to see that for this case

$$2\phi = \eta_i + \zeta_i + \overline{\zeta_i}. \tag{2.42}$$

Hence, $\eta_i \leq 2\phi$ for this case as well. Having considered all the three possible cases *for* $0 < \phi$ *and* $|\delta_i| \leq \delta_i^c$ *we can conclude that* $0 \leq \eta_i \leq 2\phi$.

Cases for $\phi < 0$:
The different cases for $\phi < 0$ can be treated in a way that is essentially similar to those for $0 < \phi$. However, we discuss these cases in some detail for establishing the completeness of our conclusion. Moreover, due to the negative value of ϕ complications arise, that warrant a detailed consideration. To begin with, since ϕ is negative, it is easy to see from Fig. 2.5 that $\eta_i < 0$ as well. Hence we need to consider $|\phi|$ and $|\eta_i|$ to follow an approach that is analogous to the one used for $0 < \phi$. Further, the direct CP-asymmetry C_i has opposite sign when compared to the corresponding cases for $0 < \phi$. Also, Eqs. (2.19) and (2.20) imply that $|A_i|$ and $\left|\overline{A_i}\right|$ switch. The flip in the positions of $|A_i|$ and $\left|\overline{A_i}\right|$ can be seen when comparing Fig. 2.5 with Fig. 2.3.

Fig. 2.5(a) represents the case $\phi \leq 0 \leq \delta_i \leq \delta_i^c$. It is easy to conclude that for

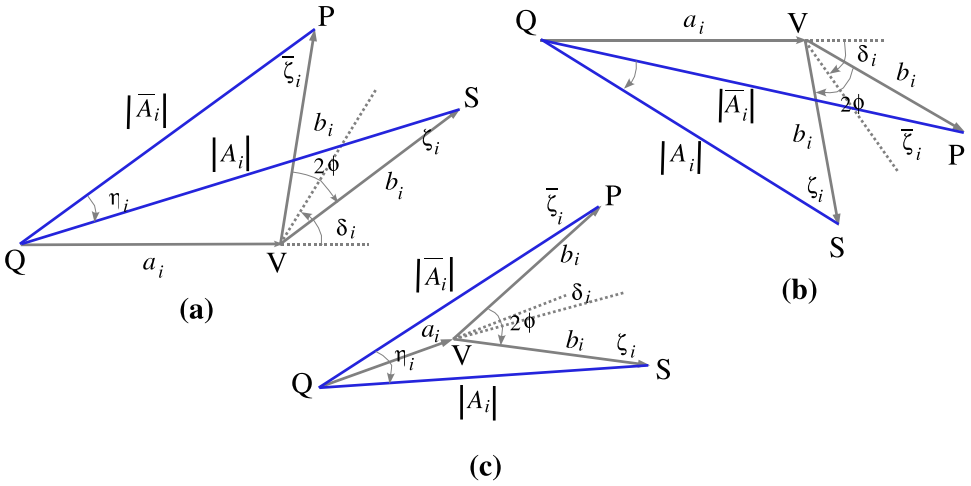

Figure 2.5: Case $\phi < 0$ and $-\delta_i^c < \delta_i < \delta_i^c$. The amplitudes A_i and $\overline{A}_i$ in terms of a_i and b_i.

this case, $2|\phi| = |\eta_i| + \overline{\zeta}_i - \zeta_i$. Since, $\phi < 0$ and $0 < \delta_i$, C_i must be positive, i.e. $0 < C_i$, implying that $|\overline{A}_i| < |A_i|$. Following an approach identical to the one introduced for the case of Fig. 2.3(a) in Fig. 2.4, we conclude that $|\zeta_i| < |\overline{\zeta}_i|$. Hence, $|\eta_i| \leq 2|\phi|$ for $\phi \leq 0 \leq \delta_i \leq \delta_i^c$. We next consider Fig. 2.5(b), where $\delta_i^c \leq \delta_i \leq \phi \leq 0$. For this case, $2|\phi| = |\eta_i| + \zeta_i - \overline{\zeta}_i$. Here, $C_i < 0$, as both $\phi < 0$ and $\delta_i < 0$ imply that $|A_i| \leq |\overline{A}_i|$ and $|\overline{\zeta}_i| < |\zeta_i|$. We hence conclude that $|\eta_i| \leq |\phi|$. We finally consider the case when $|\delta_i| \leq |\phi|$ but ϕ itself is negative. This case is straightforward; since, $2|\phi| = |\eta_i| + \zeta_i + \overline{\zeta}_i$, we easily conclude that $|\eta_i| \leq 2|\phi|$. It can be concluded that even for each of the $\phi < 0$ sub-cases, $|\eta_i| \leq 2|\phi|$, though within the SM, the weak phase ϕ is always positive as mentioned earlier.

2.5.3 Conclusion of this section

As a conclusion of this section it can be stated that,

1. *η_i always has the same sign as of ϕ if $|\delta_i| \leq |\delta_i^c|$.*

2. $|\eta_i| \leq 2|\phi|$.

Combining these two solutions, the constraints are

$$|\delta_i| < |\delta_i^c| \Rightarrow 0 \leq \eta_i \leq 2\phi, \tag{2.43}$$
$$|\delta_i| > |\delta_i^c| \Rightarrow \eta_i < 0 \text{ or } \eta_i > 2\phi. \tag{2.44}$$

2.6 Constraints on η_i and 2β

The present world average value of $\sin 2\beta^{\rm meas}(b \to c\bar{c}s) = 0.67 \pm 0.02$, The measured values of $\sin 2\beta^{\rm meas}(b \to s\bar{q}q)$ are given in fig. (2.1). The modes f_1 and f_2 are chosen in such a way that the estimated values of 2ω's are always positive. These values are listed in Table. (2.2).

β can be chosen in three possible ways, it can be either greater than both of $\beta_1^{\rm meas}, \beta_2^{\rm meas}$ or in between them or less than both of them. In Table. (2.3) we consider these three cases with the possible sub cases depending on the value of $\phi = \gamma$ parametrization to obtain bounds on η_1, η_2 and 2β. In Table. (2.4) the bounds are given for $\phi = \beta_s$ parametrization.

2.7 $\mathcal{A}_j$s as a function of η_i

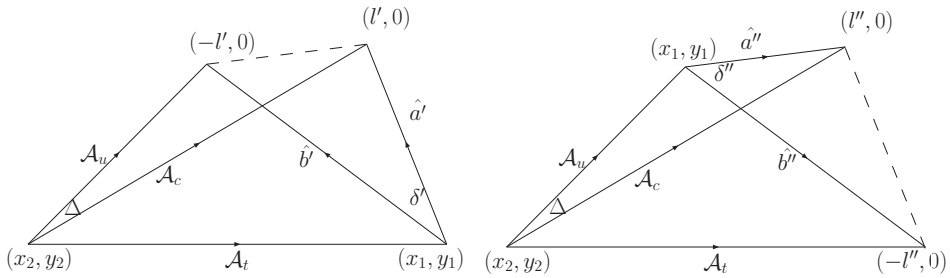

Figure 2.6: In (a) geometric representation of Eq. (2.8) with $\phi = \gamma$ parametrization and in (b) geometric representation of Eq. (2.12) with $\phi = \beta_s$ parametrization.

Fig. 2.6(a) and Fig. 2.6(b) are the geometrical representation of Eq. (2.8) with $\phi = \gamma$ parametrization and Eq. (2.12) with $\phi = \beta_s$ parametrization

f_1	f_2	2ω	$\Delta 2\omega$
$b \to c\bar{c}s$	ϕK^0	15.96^o	$+11.02^o$ -11.67^o
$b \to c\bar{c}s$	$\eta' K^0$	5.91^o	$\pm 5.21^o$
$K_S K_S K_S$	$b \to c\bar{c}s$	5.66^o	$\pm 14.75^o$
$b \to c\bar{c}s$	$\pi^0 K^0$	7.32^o	$\pm 12.04^o$
$b \to c\bar{c}s$	$\rho^0 K_S$	9.38^o	$+12.45^o$ -24.53^o
$b \to c\bar{c}s$	ωK_S	15.32^o	$\pm 15.67^o$
$b \to c\bar{c}s$	$f^0 K_S$	5.20^o	$+8.05^o$ -9.48^o
$b \to c\bar{c}s$	$f_2 K_S$	13.38^o	$\pm 37.21^o$
$b \to c\bar{c}s$	$f_X K_S$	30.53^o	$\pm 32.79^o$
$b \to c\bar{c}s$	$\pi^0\pi^0 K_S$	73.40^o	$\pm 28.74^o$
$b \to c\bar{c}s$	$\pi^+\pi^- K_S$	41.49^o	$\pm 19.34^o$
$K^+K^-K^0$	$b \to c\bar{c}s$	13.02^o	$\pm 7.19^o$
$K^+K^-K^0$	$\pi^+\pi^- K_S$	54.51^o	$\pm 20.61^o$
$K_S K_S K_S$	$\pi^+\pi^- K_S$	47.16^o	$\pm 24.56^o$
$K^+K^-K^0$	$\eta' K^0$	18.93^o	$\pm 8.62^o$

Table 2.2: Estimated 2ω and its error $\Delta 2\omega$ values from Fig. (2.1)

respectively. The co-ordinates (x'_1, y'_1) and (x'_2, y'_2) and l' can be solvable as a function of $\mathcal{A}_j$s and a'_i, b'_i and δ'_i. Similarly we can solve for the co-ordinates (x''_1, y''_1), (x''_2, y''_2) and l'' as a function of $\mathcal{A}_j$s and a''_i, b''_i and δ''_i. Following Eqs. (2.29) - (2.31), a'^2_i, b'^2_i, $\tan\delta'_i$ and a''^2_i, b''^2_i, $\tan\delta''_i$ can be expressed as a function of only η_i, as B_i and C_i are observables and ϕ is known experimentally. This straight-forwardly leads to express $\mathcal{A}_t$ and $\Delta \equiv |\delta_c - \delta_u|$ in terms of $\mathcal{A}_c$, $\mathcal{A}_u$ and η_i.

		$0 < 2\gamma$	η_2 bound	η_1 bound	β bound
$\beta_2^{meas} \leq \beta_1^{meas} \leq \beta$	I	$\eta_2 \leq \eta_1 \leq 0 \leq 2\gamma$	$\eta_2 \leq -2\omega$;	$\eta_1 \leq 0$	$2\beta_1^{meas} \leq 2\beta$;
$\beta_2^{meas} \leq \beta \leq \beta_1^{meas}$	II	$\eta_2 \leq 0 \leq \eta_1 \leq 2\gamma$	$\eta_2 \leq 0$	$0 \leq \eta_1 \leq 2\omega$;	$2\beta_2^{meas} \leq 2\beta \leq 2\beta_1^{meas}$;
$\beta \leq \beta_2^{meas} \leq \beta_1^{meas}$	III(a)	$0 \leq \eta_2 \leq \eta_1 \leq 2\gamma$	$0 \leq \eta_2 \leq 2\gamma - 2\omega$;	$2\omega \leq \eta_1 \leq 2\gamma$;	$2\beta_1^{meas} - 2\gamma \leq 2\beta \leq 2\beta_2^{meas}$;
	III(b)	$0 \leq \eta_2 \leq 2\gamma \leq \eta_1$	$2\gamma - 2\omega \leq \eta_2 \leq 2\gamma$;	$2\gamma \leq \eta_1 \leq 2\gamma + 2\omega$;	$2\beta_1^{meas} - 2\gamma - 2\omega \leq 2\beta \leq 2\beta_1^{meas} - 2\gamma$;
	III(c)	$0 \leq 2\gamma \leq \eta_2 \leq \eta_1$	$2\gamma \leq \eta_2$;	$2\omega + 2\gamma \leq \eta_1$;	$2\beta \leq 2\beta_2^{meas} - 2\gamma$;

Table 2.3: Constraints on η_i and 2β for the γ parametrization.

2.7.1 Solution of $\mathcal{A}_t$ and Δ in γ parametrization

From Fig. 2.6(a),

$$\begin{aligned} \mathcal{A}_c^2 &= (x'_2 - l')^2 + y'^2_2, \\ \mathcal{A}_u^2 &= (x'_2 + l')^2 + y'^2_2, \\ \mathcal{A}_t^2 &= (x'_2 - x'_1)^2 + (y'_2 - y'_1)^2, \\ \hat{a}'^2 &= (x'_1 - l')^2 + y'^2_1, \\ \hat{b}'^2 &= (x'_1 + l')^2 + y'^2_1, \end{aligned} \tag{2.45}$$

$$4l'^2 = \hat{a}'^2 + \hat{b}'^2 - 2\hat{a}'\hat{b}'\cos\delta'. \tag{2.46}$$

		$0 < 2\beta_s$	η_2 bound	η_1 bound	β bound
$\beta_2^{meas} \leq \beta_1^{meas} \leq \beta$	I	$\eta_2 \leq \eta_1 \leq 0 \leq 2\beta_s$	$\eta_2 \leq -2\omega$	$\eta_1 \leq 0$	$2\beta_1^{meas} \leq 2\beta$
$\beta_2^{meas} \leq \beta \leq \beta_1^{meas}$	II(a)	$\eta_2 \leq 0 \leq \eta_1 \leq 2\beta_s$	$\eta_2 \leq 2\beta_s - 2\omega$	$0 \leq \eta_1 \leq 2\beta_s$	$2\beta_1^{meas} - 2\beta_s \leq 2\beta$
	II(b)	$\eta_2 \leq 0 \leq 2\beta_s \leq \eta_1$	$2\beta_s - 2\omega \leq \eta_2$	$2\beta_s \leq \eta_1 \leq 2\omega$	$2\beta_2^{meas} \leq 2\beta \leq 2\beta_1^{meas} - 2\beta_s$
$\beta \leq \beta_2^{meas} \leq \beta_1^{meas}$	III(a)	$0 \leq \eta_2 \leq 2\beta_s \leq \eta_1$	$0 \leq \eta_2 \leq 2\beta_s$	$2\omega \leq \eta_1$	$2\beta_2^{meas} - 2\beta_s \leq 2\beta \leq 2\beta_2^{meas}$
	III(b)	$0 \leq 2\beta_s \leq \eta_2 \leq \eta_1$	$2\beta_s \leq \eta_2$	$2\omega + 2\beta_s \leq \eta_1$	$2\beta \leq 2\beta_2^{meas} - 2\beta_s$

Table 2.4: Constraints on η_i and 2β for β_s parametrization.

Considering the present experimental data, it is a valid assumption to assume the direct CP asymmetry $C_i = 0$ which is used to plot Fig. 2.7. $C_i = 0$ implies either $\delta_i' = 0$ or $\delta_i' = \pi$. Eq. (2.46) follows $\delta_i' = 0$ has two sub-cases $l' = \pm\frac{(\hat{a}'-\hat{b}')}{2}$. These cases are discussed in details in this subsection.

Case-I (a):- $\delta_i' = 0$ **and** $l' = \frac{(\hat{a}'-\hat{b}')}{2}$
Eqns. (2.45) - (2.46)leads to

$$\begin{aligned}
x_1' &= -\frac{(\hat{a}'+\hat{b}')}{2}, \\
y_1' &= 0, \\
x_2' &= \frac{\mathcal{A}_u^2 - \mathcal{A}_c^2}{2(\hat{a}'-\hat{b}')}, \\
y_2' &= \pm\Big[\mathcal{A}_c^2 - \Big(\frac{\mathcal{A}_u^2 - \mathcal{A}_c^2 - (\hat{a}'-\hat{b}')^2}{2(\hat{a}'-\hat{b}')}\Big)^2\Big]^{\frac{1}{2}}, \\
\mathcal{A}_t &= \pm\Big[2\hat{a}'\hat{b}' + \frac{(\hat{a}'\mathcal{A}_u^2 - \hat{b}'\mathcal{A}_c^2)}{(\hat{a}'-\hat{b}')}\Big]^{\frac{1}{2}}, \\
\Delta &= \cos^{-1}\Big[\frac{\mathcal{A}_u^2 + \mathcal{A}_c^2 - 4l'^2}{2\mathcal{A}_u\mathcal{A}_c}\Big].
\end{aligned} \tag{2.47}$$

Case-I (b):- $\delta_i' = 0$ **and** $l' = \frac{(\hat{b}'-\hat{a}')}{2}$

In this case,

$$\begin{aligned} x_1' &= \frac{(\hat{a}' + \hat{b}')}{2}, \\ y_1' &= 0, \\ x_2' &= \frac{\mathcal{A}_u^2 - \mathcal{A}_c^2}{2(\hat{b}' - \hat{a}')}, \\ y_2' &= \pm\Big[\mathcal{A}_c^2 - \Big(\frac{\mathcal{A}_u^2 - \mathcal{A}_c^2 - (\hat{b}' - \hat{a}')^2}{2(\hat{b}' - \hat{a}')}\Big)^2\Big]^{\frac{1}{2}}, \\ \mathcal{A}_t &= \pm\Big[2\hat{a}'\hat{b}' + \frac{(\hat{a}'\mathcal{A}_u^2 - \hat{b}'\mathcal{A}_c^2)}{(\hat{a}' - \hat{b}')}\Big]^{\frac{1}{2}}, \\ \Delta &= \cos^{-1}\Big[\frac{\mathcal{A}_u^2 + \mathcal{A}_c^2 - 4l'^2}{2\mathcal{A}_u\mathcal{A}_c}\Big]. \end{aligned} \tag{2.48}$$

Finally in both of the sub-cases for $\delta_i' = 0$, the values of $\mathcal{A}_t$ and Δ remain same.

Case-II :- $\delta_i' = \pi$ **and** $l' = \frac{(\hat{a}' + \hat{b}')}{2}$
In this case,

$$\begin{aligned} x_1' &= \frac{(\hat{b}' - \hat{a}')}{2}, \\ y_1' &= 0, \\ x_2' &= \frac{\mathcal{A}_u^2 - \mathcal{A}_c^2}{2(\hat{a}' + \hat{b}')}, \\ y_2' &= \pm\Big[\mathcal{A}_c^2 - \Big(\frac{\mathcal{A}_u^2 - \mathcal{A}_c^2 - (\hat{a}' + \hat{b}')^2}{2(\hat{a}' + \hat{b}')}\Big)^2\Big]^{\frac{1}{2}}, \\ \mathcal{A}_t &= \pm\Big[-2\hat{a}'\hat{b}' + \frac{(\hat{a}'\mathcal{A}_u^2 + \hat{b}'\mathcal{A}_c^2)}{(\hat{a}' + \hat{b}')}\Big]^{\frac{1}{2}}, \\ \Delta &= \cos^{-1}\Big[\frac{\mathcal{A}_u^2 + \mathcal{A}_c^2 - 4l'^2}{2\mathcal{A}_u\mathcal{A}_c}\Big]. \end{aligned} \tag{2.49}$$

These are the possible cases for γ parametrization. The cases for β_s parametriza-

tion are discussed in the next subsection.

2.7.2 Solution of $\mathcal{A}_t$ and Δ in β_s parametrization

Fig. 2.6(b)follows:

$$\begin{aligned}
\mathcal{A}_c^2 &= (x_2'' - l'')^2 + y_2''^2, \\
\mathcal{A}_u^2 &= (x_2'' - x_1'')^2 + (y_2'' - y_1'')^2, \\
\mathcal{A}_t^2 &= (x_2'' + l'')^2 + y_2''^2, \\
\hat{a}''^2 &= (x_1'' - l'')^2 + y_1''^2, \\
\hat{b}''^2 &= (x_1'' + l'')^2 + y_1''^2,
\end{aligned} \tag{2.50}$$

$$4l''^2 = \hat{a}''^2 + \hat{b}''^2 - 2\hat{a}''\hat{b}''\cos\delta''. \tag{2.51}$$

The $C_i = 0$ cases are discussed below.

Case-IV (a):- $\delta_i'' = 0$ and $l'' = \frac{(\hat{a}'' - \hat{b}'')}{2}$.

From Eqs.(2.50)-(2.51),

$$\begin{aligned}
x_1'' &= -\frac{(\hat{a}'' + \hat{b}'')}{2}, \\
y_1'' &= 0, \\
x_2'' &= \frac{\mathcal{A}_u^2 - \mathcal{A}_c^2 - \hat{a}''\hat{b}''}{2\hat{a}''}, \\
y_2'' &= \pm\Big[\mathcal{A}_u^2 - \Big(\frac{\mathcal{A}_u^2 - \mathcal{A}_c^2 + \hat{a}''^2}{2\hat{a}''}\Big)^2\Big]^{\frac{1}{2}}, \\
\mathcal{A}_t &= \pm\Big[\mathcal{A}_u^2 + \hat{b}''^2 - \frac{\hat{b}''}{\hat{a}''}(\mathcal{A}_u^2 - \mathcal{A}_c^2 + \hat{a}''^2)\Big]^{\frac{1}{2}}, \\
\Delta &= \cos^{-1}\Big[\frac{\mathcal{A}_u^2 + \mathcal{A}_c^2 - \hat{a}''^2}{2\mathcal{A}_u\mathcal{A}_c}\Big].
\end{aligned} \tag{2.52}$$

Case-IV (b):- $\delta_i'' = 0$ and $l'' = \frac{(\hat{b}'' - \hat{a}'')}{2}$.

In this case,

$$\begin{aligned}
x_1'' &= \frac{(\hat{a}'' + \hat{b}'')}{2}, \\
y_1'' &= 0, \\
x_2'' &= -\frac{\mathcal{A}_u^2 - \mathcal{A}_c^2 - \hat{a}''\hat{b}''}{2\hat{a}''}, \\
y_2'' &= \pm\Big[\mathcal{A}_u^2 - \Big(\frac{\mathcal{A}_u^2 - \mathcal{A}_c^2 + \hat{a}''^2}{2\hat{a}''}\Big)^2\Big]^{\frac{1}{2}}, \\
\mathcal{A}_t &= \pm\Big[\mathcal{A}_u^2 + \hat{b}''^2 - \frac{\hat{b}''}{\hat{a}''}(\mathcal{A}_u^2 - \mathcal{A}_c^2 + \hat{a}''^2)\Big]^{\frac{1}{2}}, \\
\Delta &= \cos^{-1}\Big[\frac{\mathcal{A}_u^2 + \mathcal{A}_c^2 - \hat{a}''^2}{2\mathcal{A}_u\mathcal{A}_c}\Big].
\end{aligned} \tag{2.53}$$

Finally in both of the sub-cases for $\delta_i'' = 0$, the value of $\mathcal{A}_t$ and Δ remain same.

Case-V :- $\delta_i'' = \pi$

For this case,

$$\begin{aligned}
l'' &= \frac{(\hat{a}'' + \hat{b}'')}{2}, \\
x_1'' &= \frac{(\hat{b}'' - \hat{a}'')}{2}, \\
y_1'' &= 0, \\
x_2'' &= -\frac{\mathcal{A}_u^2 - \mathcal{A}_c^2 + \hat{a}''\hat{b}''}{2\hat{a}''}, \\
y_2'' &= \pm\Big[\mathcal{A}_u^2 - \Big(\frac{\mathcal{A}_u^2 - \mathcal{A}_c^2 + \hat{a}''^2}{2\hat{a}''}\Big)^2\Big]^{\frac{1}{2}}, \\
\mathcal{A}_t &= \pm\Big[\mathcal{A}_u^2 + \hat{b}''^2 + \frac{\hat{b}''}{\hat{a}''}(\mathcal{A}_u^2 - \mathcal{A}_c^2 + \hat{a}''^2)\Big]^{\frac{1}{2}}, \\
\Delta &= \cos^{-1}\Big[\frac{\mathcal{A}_u^2 + \mathcal{A}_c^2 - \hat{a}''^2}{2\mathcal{A}_u\mathcal{A}_c}\Big].
\end{aligned} \tag{2.54}$$

In Fig. 2.7, the values of $\mathcal{A}_t$ are plotted as a function of $\mathcal{A}_c$ and $\mathcal{A}_u$ for six

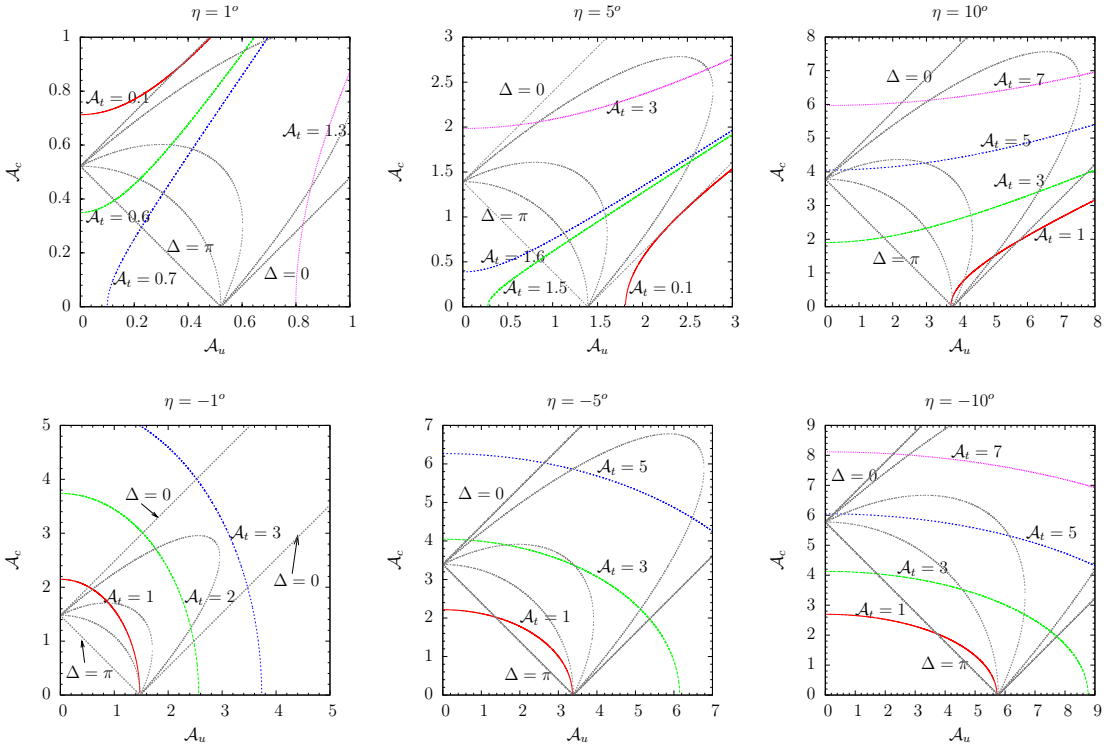

Figure 2.7: Values of $\mathcal{A}_t$ and $\Delta \equiv |\delta_u - \delta_c|$ as a function of $\mathcal{A}_u$ and $\mathcal{A}_c$ for $C_i = 0$. $\mathcal{A}_j$ are normalized such that, if $\mathcal{A}_u = 0$ and $\mathcal{A}_t = 0$, $\mathcal{A}_c$ would be unity. The allowed values are bounded by the curves for $\Delta = 0, \pi$. The unlabelled parabolic curves represent $\Delta = \frac{\pi}{2}$, $\frac{\pi}{3}$ and $\frac{\pi}{6}$.

fixed values of η_i for $C_i = 0$.

2.8 Analysis of the bounds

2.8.1 $f_1 \to (\overline{b} \to c\overline{c}\overline{s}), f_2 \to (\overline{b} \to \overline{s}q\overline{q})$

In $\overline{b} \to c\overline{c}\overline{s}$ channel, tree contributions dominate over the penguin, which leads to the constraint $\mathcal{A}_c > \mathcal{A}_{u,t}$. In $\overline{b} \to \overline{s}s\overline{s}$ channel only penguin diagram contributes, it does not lead to any such constraint. From Fig. 2.7, it is clear that large $\eta > 0$ (of the order of 5^o) is easily obtained by having only $\mathcal{A}_u$ sizeable but $\mathcal{A}_c > \mathcal{A}_{u,t}$ only for negative η_1 cases. This immediately rules out all the cases except Case I of Table. (2.3) and Table. (2.4). In

these cases, η_1 is negative, but $\eta_2 \leq -2\omega$. The estimated values of 2ω's are given in Table. (2.2), though $\Delta 2\omega$'s are very large, still for most of the cases, the central value of $2\omega > 5^o$. Following Fig. 2.7, it can be seen that for Case I, this large negative value of η_2 requires the square of quark level amplitudes $|\mathcal{A}_c|^2$ ($|\mathcal{A}_u|^2$) and $|\mathcal{A}_t|^2$ which are at least 10 times larger than the observed branching ratio. Eq. (2.7) or Eq. (2.11) implies that these large quark level amplitudes have to be fine tuned such a way that they produce $A^{\bar{b}\to\bar{s}}$ of the order one. It becomes extremely difficult to fine tune in such a fashion to explain all the channels within SM. Hence, none of the cases can be accommodated within the SM, unless one requires that the observed branching ratios result from considerable fine tuned cancellations of quark level amplitudes.

2.8.2 $f_1 \to (\bar{b} \to \bar{s}q\bar{q}), f_2 \to (\bar{b} \to c\bar{c}\bar{s})$

According to the previous logic, in this case $\mathcal{A}_c > \mathcal{A}_{u,t}$ demands negative η_2. This automatically rules out the Case III of Table. (2.3) and Table. (2.4). Case I is also not relevant as $\eta_2 \leq -2\omega$. Hence, this case is also ruled out according to the same logic discussed in the previous case. Case II of Table. (2.3) and Case II(a) and II(b) of Table. (2.4) are allowed. The constraints obtained from Case II(a) and II(b) of Table. (2.4) are tighter than their counterparts of Table. (2.3).

2.8.3 $f_1 \to (\bar{b} \to \bar{s}q_1\overline{q_1}), f_2 \to (\bar{b} \to \bar{s}q_2\overline{q_2})$

In this case none of the η belongs to $\bar{b} \to c\bar{c}\bar{s}$. q_1 and q_2 can be either same quarks or different quarks. Case III(b) and III(c) of Table. (2.3) are naturally ruled out as it is expected that $\gamma \sim 60^o$. Case I of both Table. (2.3) and Table. (2.4) and Case III(a) and III(b) of Table. (2.4) are ruled out due to $\eta_2 \leq -2\omega$, $2\omega \leq \eta_1$ and $2\omega + 2\beta_s \leq \eta_1$ constraints respectively. Case II, III(a) of Table. (2.3) and Case II(a), II(b) of Table. (2.4) are allowed by the present experimental data. In this case also, constraints obtained from β_s parametrization is better than the ones from γ parametrization.

The above discussion clearly indicates that in all cases a large value of 2ω must correspond to a large η for at least one of the modes being compared. The values of the amplitudes $\mathcal{A}_u$, $\mathcal{A}_c$ and $\mathcal{A}_t$ and their relative strong phases are depicted in Fig. 2.7. It is easy to conclude from Fig. 2.7 that in all cases,

the amplitudes $\mathcal{A}_u$, $\mathcal{A}_c$ and $\mathcal{A}_t$ must be large and destructively interfere in order to obtain negative η larger than a few degrees. A scenario of large destructive interferences among the different contributions seems unnatural. It may be noted that within the same mode it is not possible to change the relative strengths of the amplitudes $\mathcal{A}_u$, $\mathcal{A}_c$ and $\mathcal{A}_t$ by rescattering, since by definition they are distinct amplitudes corresponding to v_u, v_c and v_t respectively. Given our relatively successful understanding of B_d decay amplitudes, it seems unlikely that our estimates for the contributing amplitudes of an individual mode (excluding coupled channel final state interactions) are incorrect by a factor of 3 or more; it is even more unlikely that large enough strong phases are generated so as to result in fine tuned cancellations of these large amplitudes. One may finally, consider the possibility of large coupled channel rescattering effects. In such a case, one can fine tune the individual contributions for each mode. However, note that large η necessities a large contribution from $\mathcal{A}_t$ and at least one of $\mathcal{A}_u$ or $\mathcal{A}_c$. In modes that can be coupled by rescattering, a large deviation η must be compensated by a mode that has reduced contribution from $\mathcal{A}_t$ and an enhanced contribution to $\mathcal{A}_u$ and $\mathcal{A}_c$. Significantly larger data samples would shed light on whether such a scenario is plausible. Large coupled channel effects would require unnatural fine-tuning of amplitudes, and large coupled channel effects are not expected theoretically.

To conclude, without making any hadronic model assumptions, we have shown that it would be impossible to explain within SM a large discrepancy in the $B_d^0 - \overline{B_d^0}$ mixing phase measured using various modes. The only possibility to forgo this conclusion is to accept that the observed branching ratios result from rather fine-tuned cancellations of significantly larger amplitudes.

Chapter 3

Standard Model Scenario of Mixing and Rare Processes

3.1 Introduction

The neutral meson mixing, such as $K^0 - \overline{K^0}$, $B_d^0 - \overline{B_d^0}$, $B_s^0 - \overline{B_s^0}$ and $D^0 - \overline{D^0}$ play a very crucial role to test the SM. In 1955 Gell-Mann and Pais proposed the neutral kaon mixing for the first time [45]. Later in 1964, CP violation, one of the most pioneering discovery in particle physics was observed for the first time in the neutral kaon system [1]. This triumph continued through the observation of the $B_d^0 - \overline{B_d^0}$ mixing in 1986 [46], $B_s^0 - \overline{B_s^0}$ mixing in 2006 [47] and $D^0 - \overline{D^0}$ mixing in 2007 [48]. Thanks to the two B factories and CDF, D0 collaborations, many important constraints on the CKM parameters are now known.

On the other hand, the neutral meson mixing provides an ideal place to explore new physics beyond the SM. The mixing is caused by flavor-changing neutral current (FCNC) transitions and only occurs via loops in the framework of the SM. The dominant contribution to the mixing comes from the box diagrams. That is why these box diagrams can be very sensitive to the new physics effects.

In the next chapter, we discuss a NP model related to leptoquarks. In that chapter, an analysis of the neutral K and B mesons mixing is done in the presence of this NP model. In chapter 4 constraints on the NP are given for the mixing correlated leptonic and semileptonic decays of neutral K and B

mesons. Before presenting the NP model scenario, in this chapter we briefly summarize the status of the these neutral mesons mixing and their leptonic and semileptonic decays within the SM. The standard reference for these analysis is [49]. For ready references, in this chapter we have reproduced the SM scenario of the relevant mixing and decay analysis mainly from [49].

3.2 Neutral-Meson Mixing

We denote the neutral meson by P^0 and its anti-meson by $\overline{P^0}$. P^0 represents any one of the K^0, D^0, B_d^0, B_s^0. P^0 and $\overline{P^0}$ can oscillate between themselves before decaying. In the Wigner-Weisskopf approximation, the two component wave function of an oscillating and decaying beam, in its rest frame can be written as

$$|\psi(t)\rangle = \psi_1(t)|P^0\rangle + \psi_2(t)|\overline{P^0}\rangle, \tag{3.1}$$

where t is the proper time. The Schrodinger equation for this wave function can be written as

$$i\frac{d}{dt}\begin{pmatrix}\psi_1\\ \psi_2\end{pmatrix} = \begin{pmatrix} R_{11} & R_{12}\\ R_{21} & R_{22}\end{pmatrix}\begin{pmatrix}\psi_1\\ \psi_2\end{pmatrix} \tag{3.2}$$

As the neutral-mesons both oscillate and decay, the matrix $\mathbf{R}$ is not Hermitian. It can be written as

$$\mathbf{R} = \mathbf{M} - \frac{i}{2}\mathbf{\Gamma}, \tag{3.3}$$

with

$$\mathbf{M} = \mathbf{M}^\dagger, \tag{3.4}$$
$$\mathbf{\Gamma} = \mathbf{\Gamma}^\dagger, \tag{3.5}$$

$\mathbf{M}$ and $\mathbf{\Gamma}$ are associated with $(P^0, \overline{P^0}) \leftrightarrow (\overline{P^0}, P^0)$ transitions via off-shell (dispersive), and on-shell (absorptive) intermediate states, respectively. Diagonal elements of $\mathbf{M}$ and $\mathbf{\Gamma}$ are associated with the flavor-conserving transitions $P^0 \to P^0$ and $\overline{P^0} \to \overline{P^0}$, while off-diagonal elements are associated with the flavor-changing transitions $P^0 \to \overline{P^0}$. If the two eigenstates of $\mathbf{R}$ are denoted be P_H and P_L, the mixing parameters can be defined as,

$$\Delta m \equiv m_H - m_L, \tag{3.6}$$
$$\Delta\Gamma \equiv \Gamma_H - \Gamma_L, \tag{3.7}$$

where m_H and m_L correspond to the masses of P_H and P_L respectively. Γ_H, Γ_L correspond to the decay widths of P_H and P_L respectively. The convention is that the mass difference Δm is always positive. The sign of $\Delta\Gamma$ is fixed through experiments. The mixing in the K^0 - $\overline{K^0}$, B_d^0 - $\overline{B_d^0}$ and B_s^0 - $\overline{B_s^0}$ sectors is discussed below.

3.2.1 Mixing in Neutral Kaon system

K^0 and $\overline{K}^0$ are the flavour eigenstates in the SM. Following the convention $(CP|K^0\rangle = |\overline{K}^0\rangle)$, the CP eigenstates K_1 and K_2 are defined as [49]

$$K_1 = \frac{1}{\sqrt{2}}(K^0 + \overline{K}^0), \qquad CP|K_1\rangle = |K_1\rangle, \tag{3.8}$$

$$K_2 = \frac{1}{\sqrt{2}}(K^0 - \overline{K}^0), \qquad CP|K_2\rangle = -|K_2\rangle. \tag{3.9}$$

The physical states K_L and K_S are the admixtures of K_1 and K_2,

$$K_S = \frac{K_1 + \overline{\varepsilon} K_2}{\sqrt{1+ \mid \overline{\varepsilon} \mid^2}}, \qquad K_L = \frac{K_2 + \overline{\varepsilon} K_1}{\sqrt{1+ \mid \overline{\varepsilon} \mid^2}}\,. \tag{3.10}$$

The parameter $\overline{\varepsilon}$ is very small. It is not a physical parameter as it depends on the the phase convention chosen for K^0 and $\overline{K}^0$.

Two pion final states are CP even state and three pion final states are CP odd state. As K_L and K_S both consist of K_1 and K_2, they decay to 3π via K_2 and 2π via K_1 component. The physical parameter ε_K is the measurement of the "indirect CP violation". It is defined as

$$\varepsilon_K = \frac{A(K_L \to (\pi\pi)_{I=0})}{A(K_S \to (\pi\pi)_{I=0})}, \tag{3.11}$$

It can also be written as,

$$\varepsilon_K = \frac{\exp(i\pi/4)}{\sqrt{2}\Delta M_K}\left(\mathrm{Im}M_{12} + 2\xi \mathrm{Re}M_{12}\right), \tag{3.12}$$

where

$$\xi = \frac{\mathrm{Im}A_0}{\mathrm{Re}A_0} \tag{3.13}$$

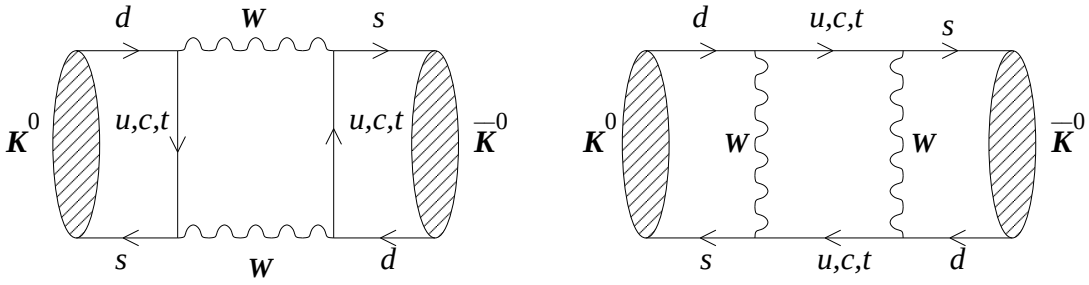

Figure 3.1: Box diagram of neutral kaon mixing.

with $A_0 \equiv A(K \to (\pi\pi)_{I=0})$ and ΔM_K denoting the $K_L - K_S$ mass difference. The off-diagonal element M_{12} in the neutral K-meson mass matrix represents $K^0(\bar{s}d) - \overline{K}^0(s\bar{d})$ mixing. It is given by

$$2m_K M_{12}^* = \langle \overline{K}^0 | \mathcal{H}_{\rm eff}(\Delta S = 2) | K^0 \rangle, \tag{3.14}$$

where $\mathcal{H}_{\rm eff}(\Delta S = 2)$ is the effective Hamiltonian for the $\Delta S = 2$ transitions and m_K is the K-meson mass.

To lowest order these transitions are induced through the box diagrams shown in Fig. (3.1). Including QCD corrections, the effective low energy Hamiltonian, to be derived from these diagrams, can be written as [50]:

$$\begin{aligned} \mathcal{H}_{\rm eff}^{\Delta S=2} &= \frac{G_{\rm F}^2}{16\pi^2} M_W^2 \left[\lambda_c^2 \eta_1 S_0(x_c) + \lambda_t^2 \eta_2 S_0(x_t) + 2\lambda_c \lambda_t \eta_3 S_0(x_c, x_t)\right] \times \\ &\quad \times \left[\alpha_s^{(3)}(\mu)\right]^{-2/9} \left[1 + \frac{\alpha_s^{(3)}(\mu)}{4\pi} J_3\right] Q(\Delta S = 2) + h.c. \end{aligned} \tag{3.15}$$

where $\lambda_i = V_{is}^* V_{id}$. Using unitarity relation $\lambda_u + \lambda_c + \lambda_t = 0$, λ_u is replaced in terms of λ_c and λ_t. Eq. (3.15) is valid for scales μ below the charm threshold $\mu_c = \mathcal{O}(m_c)$. In this case $\mathcal{H}_{\rm eff}^{\Delta S=2}$ consists of a single four-quark operator

$$Q(\Delta S = 2) = (\bar{s}d)_{V-A} (\bar{s}d)_{V-A}, \tag{3.16}$$

Functions like $S_0(x_i)$ where $i = u, c, t$ and $S_0(x_c, x_t)$ are the basic loop contributions from the box diagrams without QCD correction. The expressions

for these are as follows:

$$S_0(x_i) = \frac{4x_i - 11x_i^2 + x_i^3}{4(1-x_i)^2} - \frac{3x_i^3 \ln x_i}{2(1-x_i)^3}, \quad x_i = \frac{m_i^2}{M_W^2}, \tag{3.17}$$

$$S_0(x_c, x_t) = x_c \left[\ln \frac{x_t}{x_c} - \frac{3x_t}{4(1-x_t)} - \frac{3x_t^2 \ln x_t}{4(1-x_t)^2} \right], \tag{3.18}$$

Short-distance QCD effects are included in the correction factors η_1, η_2, η_3 and in the explicitly α_s-dependent terms in Eq. (3.15). The scale dependence and renormalization scheme dependence of $\alpha_s(\mu)$ and J_3 should cancel with the scale dependence and renormalization scheme dependence of the hadronic matrix element. In the NDR scheme $J_3 = 1.895$. The NLO values of the QCD factors η_1 , η_2 and η_3 are given as follows [51], [52]:

$$\eta_1 = 1.38 \pm 0.20, \qquad \eta_2 = 0.57 \pm 0.01, \qquad \eta_3 = 0.47 \pm 0.04. \tag{3.19}$$

The renormalization group invariant parameter B_K can be defined as

$$B_K = B_K(\mu) \left[\alpha_s^{(3)}(\mu)\right]^{-2/9} \left[1 + \frac{\alpha_s^{(3)}(\mu)}{4\pi} J_3\right] \tag{3.20}$$

$$\langle \overline{K}^0 | (\overline{s}d)_{V-A} (\overline{s}d)_{V-A} | K^0 \rangle \equiv \frac{8}{3} B_K(\mu) F_K^2 m_K^2 \tag{3.21}$$

We have used the value of $B_K = 0.86 \pm 0.14 \pm 0.06$ given in [15] in our calculation. Using Eq. (3.15) one finds

$$M_{12} = \frac{G_F^2}{12\pi^2} F_K^2 B_K m_K M_W^2 \left[\lambda_c^{*2} \eta_1 S_0(x_c) + \lambda_t^{*2} \eta_2 S_0(x_t) + 2\lambda_c^* \lambda_t^* \eta_3 S_0(x_c, x_t)\right], \tag{3.22}$$

where $F_K = 159.8 \pm 1.4 \pm 0.44$ [54] is the K-meson decay constant.

The last term in Eq. (3.12) can be neglected as compared to other uncertainties for example B_K, as it constitutes at most a 2 % correction to ε_K. Substituting Eq. (3.22) into Eq. (3.12), it can be written as

$$\varepsilon_K = C_\varepsilon B_K \mathrm{Im}\lambda_t \left\{ \mathrm{Re}\lambda_c \left[\eta_1 S_0(x_c) - \eta_3 S_0(x_c, x_t)\right] - \mathrm{Re}\lambda_t \eta_2 S_0(x_t) \right\} \exp(i\pi/4), \tag{3.23}$$

where the unitarity relation $\mathrm{Im}\lambda_c^* = \mathrm{Im}\lambda_t$ is used and $\mathrm{Re}\lambda_t/\mathrm{Re}\lambda_c = \mathcal{O}(\lambda^4)$ is

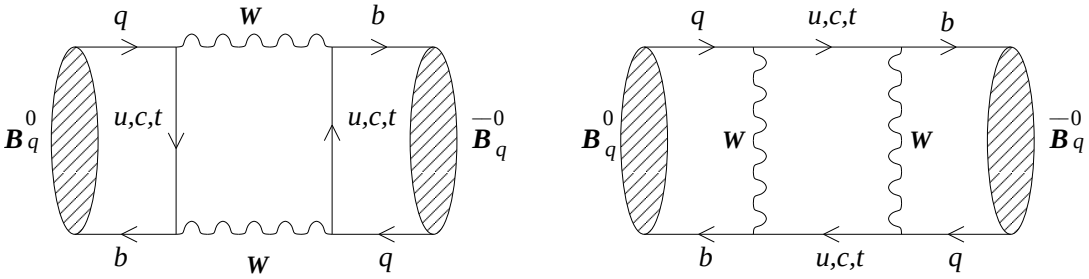

Figure 3.2: Box diagram of neutral B-meson mixing.

neglected in the evaluation of $\mathrm{Im}(\lambda_c^*\lambda_t^*)$. The numerical constant C_ε is given by

$$C_\varepsilon = \frac{G_{\mathrm{F}}^2 F_K^2 m_K M_W^2}{6\sqrt{2}\pi^2 \Delta M_K} = 3.78 \times 10^4\,. \tag{3.24}$$

The value of measured ΔM_K is $(5.31 \pm 0.01) \times 10^{-3}\mathrm{ps}^{-1}$ [54].

3.2.2 Mixing in Neutral B-meson

The strength of $B_q^0 - \overline{B}_q^0$ mixing, where $q = d, s$ is described by

$$\Delta M_q = 2|M_{12}^{(q)}|, \tag{3.25}$$

the mass difference between the mass eigenstates in the $B_d^0 - \overline{B}_d^0$ system and the $B_s^0 - \overline{B}_s^0$ system, respectively. In this case the off-diagonal term M_{12} of the neutral B-meson mass matrix is given by

$$2m_{B_q}|M_{12}^{(q)}| = |\langle \overline{B}_q^0 | \mathcal{H}_{\mathrm{eff}}(\Delta B = 2) | B_q^0 \rangle|. \tag{3.26}$$

These mixings are induced by the box diagrams shown in fig. (3.2). The effective Hamiltonian, valid for the scales $\mu_b = \mathcal{O}(m_b)$, can be written in the case of $B_d^0 - \overline{B}_d^0$ mixing as

$$\begin{aligned} \mathcal{H}_{\mathrm{eff}}^{\Delta B=2} &= \frac{G_{\mathrm{F}}^2}{16\pi^2} M_W^2 \left(V_{tb}^* V_{td}\right)^2 \eta_B S_0(x_t) \left[\alpha_s^{(5)}(\mu_b)\right]^{-6/23} \left[1 + \frac{\alpha_s^{(5)}(\mu_b)}{4\pi} J_5\right] \times \\ &\quad \times Q(\Delta B = 2) + h.c. \end{aligned} \tag{3.27}$$

Here

$$Q(\Delta B = 2) = (\bar{b}d)_{V-A}(\bar{b}d)_{V-A} \tag{3.28}$$

and $\eta_B = 0.55 \pm 0.01$ [52] is the short distance QCD correction factor. $J_5 = 1.627$ in the NDR scheme. In the case of $B_s^0 - \overline{B}_s^0$ mixing one should simply replace $d \to s$ in Eq. (3.27) and Eq. (3.28) with all other quantities unchanged. Due to CKM suppression, for neutral B-meson box diagrams, the charm quark and charm-top quark contribution terms are negligible compared to the top quark contribution. The B_{B_q} term is defined as,

$$B_{B_q} = B_{B_q}(\mu)\left[\alpha_s^{(5)}(\mu)\right]^{-6/23}\left[1 + \frac{\alpha_s^{(5)}(\mu)}{4\pi}J_5\right] \tag{3.29}$$

$$\langle \overline{B}_q^0|(\bar{b}q)_{V-A}(\bar{b}q)_{V-A}|B_q^0\rangle \equiv \frac{8}{3}B_{B_q}(\mu)F_{B_q}^2 m_{B_q}^2\,, \tag{3.30}$$

where F_{B_q} is the B_q-meson decay constant. Using Eq. (3.27) one finds

$$\Delta M_q = \frac{G_{\rm F}^2}{6\pi^2}\eta_B m_{B_q}(B_{B_q}F_{B_q}^2)M_W^2 S_0(x_t)|V_{tq}|^2, \tag{3.31}$$

which implies

$$\Delta M_d = 0.50/\text{ps} \times \left[\frac{\sqrt{B_{B_d}}F_{B_d}}{200\ \text{MeV}}\right]^2 \left[\frac{\overline{m_t}(m_t)}{170\ \text{GeV}}\right]^{1.52} \left[\frac{|V_{td}|}{8.8\times 10^{-3}}\right] \left[\frac{\eta_B}{0.55}\right] \tag{3.32}$$

and

$$\Delta M_s = 15.1/\text{ps} \times \left[\frac{\sqrt{B_{B_s}}F_{B_s}}{240\ \text{MeV}}\right]^2 \left[\frac{\overline{m_t}(m_t)}{170\ \text{GeV}}\right]^{1.52} \left[\frac{|V_{ts}|}{0.040}\right] \left[\frac{\eta_B}{0.55}\right]. \tag{3.33}$$

For our calculation, we have used [15], [53],

$$F_{B_d}\sqrt{B_{B_d}} = (0.228 \pm 0.033)\,\text{GeV}\,, \tag{3.34}$$

$$F_{B_s}\sqrt{B_{B_s}}|_{\rm JLQCD} = (0.245 \pm 0.021^{+0.003}_{-0.002})\,\text{GeV}\,. \tag{3.35}$$

3.3 Neutral Meson Mixing Correlated decay

Various leptonic and semileptonic decay couplings of neutral K and B mesons are related to the couplings of the $K^0 - \overline{K^0}, B_q^0 - \overline{B_q^0}$ mixing respectively. Bounds can be obtained for the same CKM matrix elements from both mixing and correlated decays. In this section we discuss about the SM scenario of those correlated leptonic and semileptonic decays.

3.3.1 Neutral Kaon decay

- $K_L \to l^+ l^-$

  The decay $K_L \to l^+ l^-$, where $l = e,\ \mu$, proceeds through loop diagrams. In the SM, the dominant contributions to this decay come from the W box and Z penguin diagrams. In addition, it receives long distance contributions from the two-photon intermediate states, which are difficult to calculate reliably. But the SM predicted terms are one order off from the NP terms. That is why we have neglected these terms in our calculation. At next-to-leading order, the effective Hamiltonian for $K_L \to l^+ l^-$ can be written as

  $$\mathcal{H}_{\text{eff}} = -\frac{G_F}{\sqrt{2}} \frac{\alpha}{2\pi \sin^2 \Theta_W} (V_{cs}^* V_{cd} Y_{NL} + V_{ts}^* V_{td} Y(x_t))(\bar{s}d)_{V-A} (\bar{l}l)_{V-A} + h.c. \tag{3.36}$$

  The function $Y(x_t)$ is given by $Y(x_t) \approx 1.03 Y_0(x)$, where

  $$Y_0(x) = \frac{x}{8} \left[\frac{x-4}{x-1} + \frac{3x}{(x-1)^2} \log(x) \right] \tag{3.37}$$

  The renormalized group (RG) expression Y_{NL} represents the charm contribution. It has two parts, one coming from the Z penguin and the other coming from the box diagrams. The detail expressions are given in [55].

- $K_L \to \pi^0 e^+ e^-$

  The effective Hamiltonian for $K_L \to \pi^0 e^+ e^-$ at scales $\mu < m_c$ is given

as follows:

$$\mathcal{H}_{\rm eff}(K_L \to \pi^0 e^+ e^-) = \frac{G_{\rm F}}{\sqrt{2}} V_{us}^* V_{ud} [\sum_{i=1}^{6,7V} [z_i(\mu) + \tau y_i(\mu)] \, Q_i + \tau y_{7A}(M_W) Q_{7A}] \,, \tag{3.38}$$

where the operators Q_i are given explicitly as follows:

Current–Current :

$$Q_1 = (\overline{s}_\alpha u_\beta)_{V-A} \, (\overline{u}_\beta d_\alpha)_{V-A}, \tag{3.39}$$
$$Q_2 = (\overline{s} u)_{V-A} \, (\overline{u} d)_{V-A}. \tag{3.40}$$

QCD–Penguins :

$$Q_3 = (\overline{s} d)_{V-A} \sum_{q=u,d,s} (\overline{q} q)_{V-A}, \tag{3.41}$$
$$Q_4 = (\overline{s}_\alpha d_\beta)_{V-A} \sum_{q=u,d,s} (\overline{q}_\beta q_\alpha)_{V-A}, \tag{3.42}$$
$$Q_5 = (\overline{s} d)_{V-A} \sum_{q=u,d,s} (\overline{q} q)_{V+A}, \tag{3.43}$$
$$Q_6 = (\overline{s}_\alpha d_\beta)_{V-A} \sum_{q=u,d,s} (\overline{q}_\beta q_\alpha)_{V+A}. \tag{3.44}$$

Electroweak–Penguins :

$$Q_7 = \frac{3}{2} \, (\overline{s} d)_{V-A} \sum_{q=u,d,s} e_q \, (\overline{q} q)_{V+A}, \tag{3.45}$$
$$Q_8 = \frac{3}{2} \, (\overline{s}_\alpha d_\beta)_{V-A} \sum_{q=u,d,s} e_q (\overline{q}_\beta q_\alpha)_{V+A}, \tag{3.46}$$
$$Q_9 = \frac{3}{2} \, (\overline{s} d)_{V-A} \sum_{q=u,d,s} e_q (\overline{q} q)_{V-A}, \tag{3.47}$$
$$Q_{10} = \frac{3}{2} \, (\overline{s}_\alpha d_\beta)_{V-A} \sum_{q=u,d,s} e_q \, (\overline{q}_\beta q_\alpha)_{V-A}. \tag{3.48}$$

and

$$Q_{7V} = (\overline{s}d)_{V-A}(\overline{e}e)_V, \tag{3.49}$$
$$Q_{7A} = (\overline{s}d)_{V-A}(\overline{e}e)_A. \tag{3.50}$$

Here, e_q denotes the electrical quark charges reflecting the electroweak origin of $Q_7, \ldots, Q_{10}$ and α, β are the colour indices. $V(A)$ stands for the Lorentz structure $\gamma^\mu(\gamma^\mu\gamma^5)$.

The Wilson coefficient (WC) functions $z_i(\mu)$ and $y_i(\mu)$ were calculated including the complete next-to-leading order (NLO) corrections in [56, 57, 58]. The details of these calculations can be found there and in the review [50]. These WCs describe the strength with which a given operator enters the Hamiltonian. The WCs are controlled by the renormalization group equations, and their values at a high energy scale (typically M_W) is supplied. They include all the perturbative corrections to the operators in question. The nonperturbative part comes in evaluating the matrix elements of the operators Q_i between initial and final states. The regularization scale μ is an arbitrary point (of the order m_c) that separates the high-energy perturbative corrections and the low-energy nonperturbative contributions. The final result, theoretically, should not depend on μ.

Three different type of contributions: CP conserving, indirectly CP violating and directly CP violating type can contribute in $K_L^0 \to \pi^0 l^+ l^-$. The estimation of the CP conserving part is very difficult as it can only be done outside the perturbative framework. The SM estimations give:

$$Br(K_{\rm L} \to \pi^0 e^+ e^-)_{\rm cons} \approx \begin{cases} (0.3 - 1.8) \times 10^{-12} & [59] \\ 4.0 \times 10^{-12} & [60] \\ (5 \pm 5) \times 10^{-12} & [61]. \end{cases} \tag{3.51}$$

The SM estimation of indirectly CP violating branching ratio [62], [63] is

$$Br(K_L \to \pi^0 e^+ e^-)_{\rm indir} \leq 1.6 \times 10^{-12}, \tag{3.52}$$

and the directly CP violating branching ratio [49] is

$$Br(K_L \to \pi^0 e^+ e^-)_{\rm dir} = \begin{cases} (4.5 \pm 2.6) \times 10^{-12} & \text{Scanning} \\ (4.2 \pm 1.4) \times 10^{-12} & \text{Gaussian,} \end{cases} \tag{3.53}$$

3.3.2 B_q^0 Meson decay

The B meson decay is controlled by an effective Hamiltonian of the form

$$\mathcal{H}_{eff} = \frac{G_F}{\sqrt{2}} \sum_i V_{CKM}^i C_i(\mu) O_i(\mu), \tag{3.54}$$

where O_i are the relevant local operators which govern the decays in question. V_{CKM}^i represents the CKM factors. Below we show six classes of operators which play the dominant role in the phenomenology of weak decays and mixing. We assume the charged current decay $b \to c$ of a $\overline{B}$ meson. The subscripts 1 and 8 denote whether the currents are in singlet-singlet or octet-octet combination of colour SU(3).

Current-Current:

$$O_1 = (\overline{c}b)_{8,V-A} \, (\overline{s}c)_{8,V-A}, \tag{3.55}$$

$$O_2 = (\overline{c}b)_{1,V-A} \, (\overline{s}c)_{1,V-A}. \tag{3.56}$$

Only a typical combination $\overline{s}c$ is shown; there may be other combinations.

QCD Penguins:

$$O_{3(4)} = (\overline{s}b)_{1(8),V-A} \sum_q (\overline{q}q)_{1(8),V-A}, \tag{3.57}$$

$$O_{5(6)} = (\overline{s}b)_{1(8),V-A} \sum_q (\overline{q}q)_{1(8),V+A}. \tag{3.58}$$

The sum runs over all the lighter flavours (u, d, s, c).

Electroweak Penguins:

$$O_{7(8)} = \frac{3}{2}\,(\bar{s}b)_{1(8),V-A}\sum_q e_q\,(\bar{q}q)_{1(8),V+A}, \tag{3.59}$$

$$O_{9(10)} = \frac{3}{2}\,(\bar{s}b)_{1(8),V-A}\sum_q e_q(\bar{q}q)_{1(8),V-A}. \tag{3.60}$$

Magnetic Penguins:

$$O_{7\gamma} = \frac{e}{8\pi^2}m_b\bar{s}\sigma^{\mu\nu}(1+\gamma_5)bF_{\mu\nu}, \tag{3.61}$$

$$O_{8G} = \frac{g}{8\pi^2}m_b\bar{s}_\alpha\sigma^{\mu\nu}(1+\gamma_5)T^a_{\alpha\beta}b_\beta G^a_{\mu\nu}. \tag{3.62}$$

Here α and β are colour indices and T^a are the SU(3) generators.

Semileptonic Operators:

$$O_{9V} = (\bar{d}b)_{1,V-A}(\bar{e}e)_V, \tag{3.63}$$

$$O_{10A} = (\bar{d}b)_{1,V-A}(\bar{e}e)_A \tag{3.64}$$

These operators also contribute to the leptonic decays. Again, this basis is for the SM only.

- **Leptonic decays $B_q^0 \to l^+l^-$**

  The decay $B_q \to l^+l^-$, where $q = d$ or s and $l = e$, μ or τ, proceeds through loop diagrams. In the SM, the dominant contribution to this decay comes from the W box and Z penguin diagrams. A significant contribution to this decay is made by the top quark in the loop. At low energies (of order m_b), the decay can be described by a local $(\bar{b}q)(\bar{l}l)$ coupling. These kind of couplings can appear through the effective Hamiltonian which is similar to the one given in Eq. (3.54). The branching fraction is given by

$$Br(B_q^0 \to l^+ l^-) = \frac{G_F^2}{8\pi} f_{B_q}^2 \tau_{B_q} m_{B_q}^3 \sqrt{(1-\frac{4m_l^2}{m_{B_q}^2})}[|C_P^{l\bar{l}} - \frac{2m_l}{m_{B_q}} C_A^{l\bar{l}}|^2 + \left(1-\frac{4m_l^2}{m_{B_q}^2}\right)|C_P^{\bar{l}l'}|^2] \quad (3.65)$$

In the SM $C_P^{\bar{l}l'}$ and $C_P^{l\bar{l}}$ arise from penguin diagram with physical and non-physical neutral scalar exchange, and are suppressed by a factor $(m_b/M_W)^2$. The decay rate is controlled by the coefficient

$$[C_A^{l\bar{l}}]_{SM} = \frac{\alpha V_{tb} V_{tq}^*}{\sqrt{8}\pi \sin^2\theta_w} Y(x_t) \quad (3.66)$$

where $\sin^2\theta_w$ is the weak mixing angle. the expression for $Y(x_t)$ is given in Eq. (3.37). For different lepton flavour the SM branching fractions are [64]

$$\begin{aligned} Br(B_d^0 \to e^+e^-) &\approx \mathcal{O}(10^{-14}), \\ Br(B_d^0 \to \mu^+\mu^-) &\approx \mathcal{O}(10^{-10}), \\ Br(B_d^0 \to \tau^+\tau^-) &\approx \mathcal{O}(10^{-8}). \\ Br(B_s^0 \to e^+e^-) &\approx \mathcal{O}(10^{-13}), \\ Br(B_s^0 \to \mu^+\mu^-) &\approx \mathcal{O}(10^{-9}), \\ Br(B_s^0 \to \tau^+\tau^-) &\approx \mathcal{O}(10^{-7}). \end{aligned} \quad (3.67)$$

These numbers show that purely leptonic decays are too rare to be observed unless they are significantly enhanced by new physics.

- **Semileptonic decays**

The semileptonic inclusive decays $B \to X_{s,d} l^+ l^-$, originating from the parton level process $b \to s(d) l^+ l^-$, can be calculated using the effective Hamiltonian formalism. The amplitude reads

$$\begin{aligned} A(B \to X_s l^+ l^-) &= \frac{\sqrt{2} G_F \alpha}{\pi} V_{tb} V_{ts}^* [C_9^{eff} \overline{s_L} \gamma^\mu b_L \bar{l} \gamma_\mu l + C_{10} \overline{s_L} \gamma^\mu b_L \bar{l} \gamma_\mu \gamma_5 l \\ &\quad -2 C_7^{eff} m_b \overline{s_L} i \sigma^{\mu\nu} \frac{q_\nu}{q^2} b_R \bar{l} \gamma_\mu l], \end{aligned} \tag{3.68}$$

where q^2 is the momentum transferred to the lepton pair. In addition to the RG evolutions of C_7 and C_9 at the weak scale, the WCs C_7^{eff} and C_9^{eff} contain, the mixing effects with operators O_{1-6} (for C_9) and O_2 and O_8 (for C_7); hence the superscript. There is also a sizeable long-distance contribution coming from $B \to K^{(*)}\psi$ and $\psi \to l^+ l^-$, where ψ is a generic vector $c\bar{c}$ state.

For the semileptonic decays, we use

$$\begin{aligned} \langle N(p_2)|\overline{s}\gamma^\mu b|M(p_1)\rangle &= P^\mu F_1(q^2) + q^\mu \frac{m_B^2 - m_K^2}{q^2} \left(F_0(q^2) - F_1(q^2)\right), \\ \langle \phi(p_2,\epsilon)|\ V_\mu \mp A_\mu\ |B_s(p_1)\rangle &= \frac{1}{m_{B_s} + m_\phi} [-iV(q^2) \varepsilon_{\mu\nu\alpha\beta} \epsilon^{*\nu} P^\alpha q^\beta \\ &\quad \pm A_0(q^2)(P\cdot q)\epsilon_\mu^* \pm A_+(q^2)(\epsilon^* \cdot p_1) P_\mu \\ &\quad \pm A_-(q^2)(\epsilon^* \cdot p_1) q_\mu] \end{aligned} \tag{3.69}$$

where M may be B_d or B_s and N may be π^0 or K^0. The m_{B_s} and m_ϕ are the meson masses, $p_1(p_2)$ is the momentum of the initial (final) meson, ϵ is the polarization vector of the vector meson ϕ, $P = p_1 + p_2$, $q = p_1 - p_2$, $V_\mu = \overline{q}_2 \gamma_\mu q_1$, $A_\mu = \overline{q}_2 \gamma_\mu \gamma_5 q_1$. V, $A_{0,\pm}$ and $F_{(1/0)}(q^2)$ are the form factors. The values of these form factors are taken from [65], [66].

Chapter 4

Constraining Scalar Leptoquarks from the K and B Sectors

4.1 Introduction

The $SU(3)_C \times SU(2)_L \times U(1)_Y$ standard model (SM) is the most elegant model which describes the phenomenology of the elementary particles in a very comprehensive way, but apparently in all probability, it is just an effective theory valid up to a scale which is much below the Planck scale. Though most of the data from the two B-factories BaBar and Belle have been well explained by the SM, bits and pieces of it still remain under shade and probably needs the attention of some new physics models to be fully understood. Hopefully these new physics (NP) models can be explored in the Large Hadron Collider (LHC) as they may be in the range of a few hundreds of GeV. Direct production of new particles will definitely signal NP; while it is an interesting problem to find out what type of NP is there (commonly known as the 'inverse problem'), it is also well-known that indirect data from low-energy experiments will help to pin down the exact structure of NP, including its flavour sector. The low-energy data, in particular the data coming from the B factories as well as from CDF, DØ, LHCb (and also from the general purpose ATLAS and CMS experiments) are going to play a crucial role in that.

In B system, from last few years experimental data indicate some subtle in-

consistency with the SM predicted values. Though the error bars are still large to draw any definite conclusion but we have reasons to be hopeful. There are already some interesting hints; just to name a few [32]: (i) the abnormally high branching ratios (BR) for the generic channels $B \to \eta' K, \eta K^*$; (ii) the direct CP-asymmetry in $B_d^0 \to \pi^+\pi^-$ as found by Belle; (iii) the discrepancy in the extracted value of $\sin(2\beta)$ from $B_d^0 \to J/\psi K_S$ and $B_d \to \phi K_S$; (iv) the anomalous direct CP-asymmetries in $B \to \pi K$ decays; (v) the large mixing phase in $B_s^0 - \overline{B_s^0}$ mixing; (vi) the fraction of longitudinally polarised final states in channels like $B \to \phi K^*$ and $B \to \rho K^*$; (vii) the larger branching fraction of $B^+ \to \tau^+\nu$ compared to the SM expectation; and (viii) the discrepancy in the extracted values of V_{ub} from inclusive and exclusive modes. However, one must not be over-enthusiastic since most of these channels are nonleptonic and QCD uncertainties are yet to be fully understood. But one may hope for more such anomalies from leptonic and hadronic B-factories. For the K system, the nonleptonic channels are extremely difficult for any systematic analysis of NP effects [67], but for the first time we are having precise data (or bound) on leptonic and semileptonic K decay channels from Brookhaven and DaΦne. It is always better to be ready for any unexpected result. A major motivation for this study is the B_s^0 physics that is going to be probed at LHC-b, and even at CMS or ATLAS during the low-luminosity run of the LHC. The leptonic and semileptonic decays are comparatively cleaner than their nonleptonic counterparts. If all, or most, of them survive the test of time and attain more significance, this will indicate a new physics whose flavour sector is definitely of the non-minimal flavour violating (NMFV) type.

One of the eligible NMFV NP candidate is the leptoquark (LQ) model. Classically, in the SM, quark and lepton fields are introduced as independent fields. But in the quantum theory, for each generation, the contribution to the hypercharge triangle anomaly coming from the quarks and the leptons are exactly equal in magnitude and opposite in sign, and they cancel each other. This inspires to have a possible SM extension, where quarks and leptons can directly interact with each other. These kinds of interactions can be mediated through leptoquarks, which can come from Grand Unified theory (GUT) inspired models. These lepto-quarks can come from Pati-Salam type $SU(4)$ [68], [69] or $SU(5)$ [70] based unified models. Some string theory inspired models [71], [72] based on E_6 group can also introduce leptoquarks. Extensive studies have been done on the technicolor based leptoquark models

[73], [74], [75], [76]. Composite models of quarks and leptons [77], [78], [79], [80], [81] can also form leptoquarks.

Leptoquarks are some hypothetical gauge particles which can be either scalar or vector. These particles allow to have a tree level transition from a quark to lepton or vice versa. These kinds of interactions are absent in the SM. Leptoquarks usually carry both baryon number and lepton number. They may or may not conserve these two numbers. Baryon and lepton number violating leptoquarks become very massive, of the $\mathcal{O}(10^{15}\text{GeV})$ to avoid proton decay or large Majorana neutrino masses, and these are of no interest to us. (There are exceptions; one can construct models where LQs violate both B and L and yet do not mediate proton decay. These LQs can be light. For example, see [82].) On the other hand we can have both baryon and lepton number conserving leptoquarks whose masses can be of the $\mathcal{O}(100\text{GeV})$. In this chapter we discuss the phenomenology of only those models that conserve both B and L; one can find extensive discussions on these models in [83, 84, 85]. Vector LQs, as well as some gauge-nonsinglet scalar ones, couple to neutrinos, and their couplings should be very tightly constrained from neutrino mass and mixing data.

Another phenomenological motivation for a LQ model is that this is one of the very few models (R-parity violating supersymmetry is another) where the neutral meson mixing diagram gets a new contribution to the absorptive part. Due to this, the width difference $\Delta\Gamma$ in the B_s system enhances[86], whereas in more popular NP models it can only decrease [87]. The NP also changes the CP-violating phase in $B_s \to J/\psi\phi$. This helps reducing the tension [88] of SM expectation and the Tevatron data on the CP-violating phase and width difference for B_s.

All flavour-changing observables constrain the product of at least two different LQ couplings, one linked with the parent flavour and another with the daughter flavour. The product couplings may be complex and it is generally impossible to absorb the phase just by a simple redefinition of the LQ field. We use the data from $K^0 - \overline{K^0}$, $B_s^0 - \overline{B_s^0}$ and $B_d^0 - \overline{B_d^0}$ mixing to constrain the relevant product couplings, generically denoted as $\lambda\lambda$. For the B system, we use the data on $\Delta M_{d,s}$ and the mixing phase $\sin(2\beta_{d,s})$, and for the K system, we use ΔM_K and ε_K. We do not discuss other CP violating parameters like

ε'/ε, since that has large theoretical uncertainties. We also discuss the correlated leptonic and semileptonic decays, i.e., the decays mediated by the same LQ couplings. While decays to most of the semileptonic channels have been observed, the clean leptonic channels only have an upper bound for almost all the cases, except the already observed leptonic decays $K_L \to e^+e^-, \mu^+\mu^-$. Note that the decay modes containing only leptons in the final states give more robust bounds compared to those which contains only hadrons in the final states.

A similar exercise have also been undertaken in [83, 71, 73, 89, 90]. We update these bounds with new data from the B factories and other collider experiments. In particular, in the subsequent sections, all the previous bounds that we quote have been taken from [83]. The $D^0 - \overline{D^0}$ system has not been considered due to the large theoretical uncertainties and dominance of long-distance contributions. Leptonic and semileptonic D and D_s decays have been used to put constraints on LQs that couple to the up-type quarks. In particular, LQ contribution might be interesting to explain the D_s leptonic decay anomaly [82, 91, 92]. The couplings that we constrain are generically of the type $\lambda_{ij}\lambda^*_{ik}$, where the k-th quark flavour changes to the j-th, but there is no flavour change in the lepton sector. One can, in principle, consider flavour changes in the lepton sector too; that kind of analysis is done in [93]. However, if one has a $\nu\overline{\nu}$ pair in the final state, as in $K_L \to \pi^0\nu\overline{\nu}$, there is a chance that lepton flavour is also violated.

The couplings, which are in general complex, may be constrained from a combined study of CP-conserving and CP-violating observables. For neutral mesons, these mean ΔM as well as ϵ_K and $\sin(2\beta_{d,s})$. However, for most of the cases, the leptonic and semileptonic decay channels provide the better bound. The analysis has been done keeping both the SM and LQ contributions, which keeps the possibility of a destructive intereference, and hence larger possible values of the LQ amplitudes, open.

4.2 Leptoquark

The leptoquark model by the Buchmuller, Ruckl and Wyler (BRW) [89] assumes that leptoquark interactions respect the $SU(3)_C \times SU(2)_L \times U(1)_Y$ symmetry of the Standard Model. The stability of the proton in nature

requires the leptoquarks to obey the conservation of the lepton and baryon numbers. Leptoquarks couple either to left-handed or to right-handed leptons and quarks (coupling to both type of electrons would mediate rare decays [90] which are not observed). We focus on the scalar LQ model, which conserves both B and L. The relevant part of the Lagrangian [83] can be written as

$$\begin{aligned}\mathcal{L}_S &= \{ (\lambda_{LS_0}\overline{q}_L^c i\sigma_2 l_L + \lambda_{RS_0}\overline{u}_R^c e_R)S_0^\dagger + \lambda_{R\tilde{S}_0}\overline{d}_R^c e_R \tilde{S}_0^\dagger + (\lambda_{LS_{\frac{1}{2}}}\overline{u}_R l_L + \\ &\quad \lambda_{RS_{\frac{1}{2}}}\overline{q}_L i\sigma_2 e_R)S_{\frac{1}{2}}^\dagger + \lambda_{L\tilde{S}_{\frac{1}{2}}}\overline{d}_R l_L \tilde{S}_{\frac{1}{2}}^\dagger + \lambda_{LS_1}\overline{q}_L^c i\sigma_2\sigma^a l_L \cdot S_1^{a\dagger} \} + h.c.\end{aligned} \tag{4.1}$$

where $(S_0, \tilde{S}_0)$, $(S_{\frac{1}{2}}, \tilde{S}_{\frac{1}{2}})$, and S_1^a $(a = 1, 2, 3)$ represent the $SU(2)$ singlet, doublet, and triplet LQs respectively. λ^{ij} is the coupling strength of a leptoquark to an i-th generation lepton and a j-th generation quark, which is in general complex. σ's are the Pauli spin matrices. Note that all the four terms that couple a neutrino with a LQ can have potential constraints on neutrino mass and mixing. For example, $\tilde{S}_{\frac{1}{2}}$ can generate the observed neutrino mixing pattern through a type-II seesaw mechanism [94, 95]. However, the constraints also depend on the vacuum expectation value of a higher-representation scalar field. That is why we show the non-neutrino constraints for these couplings too, keeping in mind that the neutrino constraints may be stronger.

In this work, we focus only on those processes that involve down-type quarks. Thus, there is no way to constrain λ_{RS_0} and $\lambda_{LS_{\frac{1}{2}}}$ from these processes. In fact, these two sets of coupling can be constrained from processes like D^0-$\overline{D}^0$ mixing and $\ell_i \to \ell_j + \gamma$. The latter can be constrained from neutrino mixing too, but as we have just mentioned, the limits would depend on other model parameters. We constrain only five types of scalar LQ couplings here: λ_{LS_0}, $\lambda_{R\tilde{S}_0}$, $\lambda_{RS_{\frac{1}{2}}}$, $\lambda_{L\tilde{S}_{\frac{1}{2}}}$ and λ_{LS_1}. The charges and isospin quantum numbers of different type of LQs are summarized in Table. (4.1), for scalar type LQ only. The possible couplings for each LQ with the leptons (e represents the charged leptons and ν represents the neutrinos) and quarks (u represents up-type of quarks and d represents down type of quarks) are shown in the fourth column of Table. (4.1).

While we have not explicitly shown the generation indices in eq. (4.1), it is assumed that the LQs can couple with fermions from two different genera-

	T_3	Q	Coupling
S_0	0	-1/3	$e_L u_L \quad e_R u_R \quad \nu_L d_L$
$\tilde{S}_0$	0	-4/3	$e_R d_R$
$S_{1/2}$	$-1/2$	$-5/3$	$e_R \overline{u}_L \quad e_L \overline{u}_R$
	$1/2$	$-2/3$	$e_R \overline{d}_L \quad \nu_L \overline{u}_R$
$\tilde{S}_{1/2}$	$-1/2$	$-2/3$	$e_L \overline{d}_R$
	$1/2$	$1/3$	$\nu_L \overline{d}_R$
S_1	-1	$-4/3$	$e_L d_L$
	0	$-1/3$	$e_L u_L \quad \nu_L d_L$
	1	$2/3$	$\nu_L u_L$

Table 4.1: Leptoquark classification according to the Buchmuller-Ruckl-Wyler model.

tions. There is another approach which we should mention here. If we start with the assumption that we have single non zero coupling, we can generate the other couplings following two other way:

- Lets start with a single non zero coupling at high scale and we can generate other non-zero couplings at low scale by RG running from high scale to low scale (more precisely writing Renormalizing Group (RG) equation for a coupling and following the perturbative unitarity condition, we can generate rest of the couplings). This is a standard practice followed in R-parity violating SUSY.

- There is another approach. Suppose we start with λ_{33}. If we assume that the quark states are not the physical states, but rather the weak eigenstates, one can rotate the weak basis and get some λ_{23} or λ_{13} type coupling. This will be the same λ, multiplied by some unknown number, less than 1. This multiplicative number is unknown because we do not know the matrix that rotates the down quark basis as this matrix need not be the CKM. This is the approach one has to follow if one assume that LQs couple to a single generation only, either 3rd or 1st or 2nd.

In SM, when we rotate u_L and d_L states from weak to mass basis by rotation matrices U_L and D_L respectively we get the CKM matrix as $V_{CKM} = {U_L}^\dagger D_L$. We know only this product. V_{CKM} is not a unit matrix tells us that these two bases are not parallel or aligned i.e. there is a misalignment and only that can be measured, not the individual rotation matrices. A charged current process has u_L on one side and d_L on the other, so it measures the CKM elements. This is just like the SM. For neutral currents, we have two down-type mass matrices. For CKM, the GIM mechanism operates. It may not be true for some new physics, but whatever it might be, it is not CKM. Since we take only one coupling at a time (one product to be precise), the unitarity check is not at all needed. The CKM matrix does not say anything about the rotation matrices of the right-chiral quark sector whereas our Lagrangian involves right-chiral quarks also.

- In our work, we have started with the Lagrangian which is defined in the mass basis itself. Of course, all couplings are arbitrary then, and this might appear to be pathological, but the SM with 12 Yukawa couplings is no less pathological. Now, if we define two couplings to start with, say λ_{33} and λ_{23}, then we can of course put a well-defined and meaningful limit on their product, say from $b \to s\tau^+\tau$. There is absolutely no ambiguity in this. Davidson et al. has also followed the same approach.

Thus, we will assume that whatever couplings are nonzero, are so in the physical basis of the quark fields, and the phase is arbitrary and not a function of the CKM parameters.

Leptoquarks appear naturally in many substructure models [96]. This is not surprising: if a constituent particle of a Standard Model fermion carries quark or lepton number, then a composite quark can turn into a composite lepton or vice-versa by exchanging the appropriate constituents. The bound state consisting of the exchanged constituents would be a leptoquark. This suggests that leptoquarks in composite models can naturally induce interactions where flavour or generation numbers are conserved overall, but separately violated in the quark and lepton sector.

The direct production limits depend on the LQ model, as well as the SM

fermions these LQs can couple to. The best limits are as follows [54]: $m_{LQ} > 256, 316, 229$ GeV for 1st, 2nd, and 3rd generation LQs respectively when they are pair produced, and $m_{LQ} > 298, 73$ GeV for 1st and 2nd generation LQs when there is single production. These are the absolute lower bounds at 95% CL, but the constraints are tighter if the LQ coupling to the SM fermions, denoted here by λ, is large. For example, if λ is of the order of the electromagnetic coupling, the first generation LQs were found to have a limit of 275-325 GeV by both the HERA experiments [97]. For even larger couplings ($\lambda = 0.2$-0.5 and above) the LEP experiments exclude a much wider mass range [98], but such strong couplings are already almost ruled out if LQ signals are to be observed at the LHC.

The present-day limits for pair-produced LQs are due to the Tevatron experiments [99]. The first generation LQs are searched in $2e+2j$ or $1e+2j$+MET channel; the second generation ones are in $2\mu+2j$ or $1\mu+2j$+MET channel; and the third generation ones are in $2\tau+2b$ or $2b$+MET channel. The details of these analysis are given in the original papers [100].

The production of LQ states, either single, associated with a lepton (from $qg \to LQ + \ell$), or in pair, from $q\overline{q}, gg \to LQ + \overline{LQ}$, has been studied in detail; for example, the reader may look at [95, 101, 102, 103]. At $\sqrt{s} = 14$ TeV, the cross-section of pair production of scalar leptoquarks is about 1 pb [103]. While this goes down significantly for the initial LHC run of $\sqrt{s} = 7$ TeV, one expects to see LQ signals upto $m_{LQ} = 500$ GeV even with 5 fb^{-1} of luminosity. The cross-section for single production depends on the value of λ. For $\lambda = \sqrt{4\pi\alpha}$, the electric charge, the cross-section for LQ plus charged lepton production is about 100 fb for $m_{LQ} = 500$ GeV. The cross-section is proportional to λ^2, so we expect events even with $\sqrt{s} = 7$ TeV and $\lambda \approx 0.05$. Obviously, for smaller values of λ, pair production will be more favoured, and we expect the preliminary run of LHC to establish a limit of the order of 500 GeV.

In this analysis, we will use a somewhat conservative reference mass value of 300 GeV for every LQ state, independent of the quantum numbers and generation. The bounds on the product couplings scale as m_{LQ}^2, so the bounds that we show should be multiplied by $(300/m_{LQ})^2$.

4.3 Relevant Expressions

4.3.1 Neutral meson mixing

In Chapter 3, we have already discussed the neutral meson mixing within the SM. In this chapter we discuss how NP affects the neutral meson mixing. We represent the neutral mesons in general by M^0 and $\overline{M^0}$, with the valence quark content $\overline{q}d$ and $q\overline{d}$ respectively. For $B_d^0 - \overline{B_d^0}$ and $K^0 - \overline{K^0}$ cases, q can be either b or s. For B_s system, q is replaced by b and d is by s. The off-diagonal element in the 2×2 effective Hamiltonian causes the $M^0 - \overline{M^0}$ mixing. The mass difference between the two mass eigenstates ΔM is given by (following the convention of [104])

$$\Delta m = 2|M_{12}|, \tag{4.2}$$

with the approximation $|M_{12}| \gg |\Gamma_{12}|$. However, this is true for the B system only. Let the SM amplitude be

$$|M_{12}^{SM}| \exp(-2i\theta_{SM}) \tag{4.3}$$

where $\theta_{SM} = \beta(\phi_1)$ for the $B_d^0 - \overline{B_d^0}$ system and approximately zero for the $K^0 - \overline{K^0}$ (and also for $B_s^0 - \overline{B_s^0}$) system.

If we have n number of NP amplitudes with weak phases θ_n, one can write

$$M_{12} = |M_{12}^{SM}| \exp(-2i\theta_{SM}) + \sum_{i=1}^{n} |M_{12}^{i}| \exp(-2i\theta_i). \tag{4.4}$$

This immediately gives the effective mixing phase θ_{eff} as

$$\theta_{eff} = \frac{1}{2} \arctan \frac{|M_{12}^{SM}| \sin(2\theta_{SM}) + \sum_i |M_{12}^{i}| \sin(2\theta_i)}{|M_{12}^{SM}| \cos(2\theta_{SM}) + \sum_i |M_{12}^{i}| \cos(2\theta_i)}, \tag{4.5}$$

and the mass difference between the mass eigenstates as

$$\begin{aligned}\Delta m &= 2[|M_{12}^{SM}|^2 + \sum_i |M_{12}^i|^2 \\ &+ 2|M_{12}^{SM}| \sum_i |M_{12}^i| \cos 2(\theta_{SM} - \theta_i) \\ &+ 2 \sum_i \sum_{j>i} |M_{12}^j||M_{12}^i| \cos 2(\theta_j - \theta_i)]^{1/2}. \end{aligned} \tag{4.6}$$

These are the necessary basic formulae. The main task is to find M_{12}^i and θ_i.

For the $K^0 - \overline{K^0}$ system [105], $|\Gamma_{12}|$ is non-negligible, and hence in this system

$$\begin{aligned}\Delta m &= 2\ Re \left[(M_{12} - \frac{i}{2}\Gamma_{12})(M_{12}^* - \frac{i}{2}\Gamma_{12}^*)\right]^{1/2}, \\ \Delta\Gamma &= -4\ Im \left[(M_{12} - \frac{i}{2}\Gamma_{12})(M_{12}^* - \frac{i}{2}\Gamma_{12}^*)\right]^{1/2}, \end{aligned} \tag{4.7}$$

so that $\Delta m = -(1/2)\Delta\Gamma$. Since the dominant decay is to the $I = 0$ final state, $Im\ \Gamma_{12}$ can be neglected and the expressions for

$$\Delta m = 2\ Re\ M_{12}, \quad \Delta\Gamma = 2\ Re\ \Gamma_{12}. \tag{4.8}$$

The CP-violating parameter ε_K is given by

$$|\varepsilon_K| = \frac{1}{2\sqrt{2}} \frac{Im\ M_{12}}{Re\ M_{12}}, \tag{4.9}$$

which can be written as

$$|\varepsilon_K| = \frac{1}{\sqrt{2}} \frac{Im\ M_{12}}{\Delta m_K}. \tag{4.10}$$

Note that $Re\ M_{12}$ has both short-distance (SD) and long-distance (LD) contributions. The LD contribution is not calculable; whereas the SD part can be estimated from box amplitude. This is the reason to choose the experimental value of Δm_K in the denominator of eq. (4.10).

For $K^0 - \overline{K^0}$ system, the short-distance SM amplitude is

$$\begin{aligned} M_{12}^{SM} &\equiv \frac{\langle \overline{K^0}|H_{eff}|K^0\rangle}{2m_K} \\ &\approx \frac{G_F^2}{6\pi^2}(V_{cd}V_{cs}^*)^2\eta_K m_K f_K^2 B_K m_W^2 S_0(x_c), \end{aligned} \tag{4.11}$$

where generically $x_j = m_j^2/m_W^2$, f_K is the K meson decay constant. η_K (also called η_{cc} in the literature) and B_K parametrize the short- and the long-distance QCD corrections respectively. The tiny top-quark loop dependent part responsible for CP violation has been neglected. The function S_0 is given by

$$S_0(x) = \frac{4x - 11x^2 + x^3}{4(1-x)^2} - \frac{3x^3 \ln x}{2(1-x)^3}. \tag{4.12}$$

For the $B_q^0 - \overline{B_q^0}$ system ($q = d$ for $B_d^0 - \overline{B_d^0}$ and $q = s$ for $B_s^0 - \overline{B_s^0}$), we have an analogous equation, dominated by the top quark loop:

$$\begin{aligned} M_{12}^{SM} &\equiv \frac{\langle \overline{B_q^0}|H_{eff}|B_q^0\rangle}{2m_{B_q}} \\ &= \frac{G_F^2}{6\pi^2}(V_{tq}V_{tb}^*)^2\eta_{B_q} m_{B_q} f_{B_q}^2 B_{B_q} m_W^2 S_0(x_t). \end{aligned} \tag{4.13}$$

In the presence of NP, the general $\Delta F = 2$ effective Hamiltonian can be written as

$$\mathcal{H}_{eff}^{\Delta F=2} = \sum_{i=1}^{5} c_i(\mu) O_i(\mu) + \sum_{i=1}^{3} \tilde{c}_i(\mu)\tilde{O}_i(\mu) + H.c. \tag{4.14}$$

where μ is the regularization scale, and

$$\begin{aligned} O_1 &= (\overline{q}\gamma^\mu P_L d)_1(\overline{q}\gamma_\mu P_L d)_1, \\ O_2 &= (\overline{q}P_R d)_1(\overline{q}P_R d)_1, \\ O_3 &= (\overline{q}P_R d)_8(\overline{q}P_R d)_8, \\ O_4 &= (\overline{q}P_L d)_1(\overline{q}P_R d)_1, \\ O_5 &= (\overline{q}P_L d)_8(\overline{q}P_R d)_8, \end{aligned} \tag{4.15}$$

where q is either b or s for $B_d^0 - \overline{B_d^0}$ and $K^0 - \overline{K^0}$, where as for $B_s^0 - \overline{B_s^0}$, q is replaced by b and d is by s and $P_{R(L)} = (1 + (-)\gamma_5)/2$. The subscripts 1 and 8 indicate whether the currents are in color-singlet or in color-octet combination. The $\tilde{O}_i$s are obtained from corresponding O_is by replacing $L \leftrightarrow R$. The Wilson coefficients c_i at $q^2 = m_W^2$ include NP effects, coming from the couplings and the internal propagators. However, for most of the NP models, and certainly for the case we are discussing here, the NP particles are heavier than m_W and hence the running of the coefficients between m_W and $\mu = \mathcal{O}(m_b)$ are controlled by the SM Hamiltonian alone. In other words, NP determines only the boundary conditions of the renormalization group (RG) equations. For the evolution of these coefficients down to the low-energy scale, we follow Ref.[106], which uses, for $B_q^0 - \overline{B_q^0}$ mixing, $\mu = m_b = 4.6$ GeV and for $K^0 - \overline{K^0}$ mixing $\mu = 2.0$ GeV. The expectation values of these operators between $\overline{M^0}$ and M^0 at the scale μ are analogous to those as given in [107].

4.3.2 Leptonic and Semileptonic Decays

For almost all the cases, the SM leptonic decay widths for neutral mesons are way too small to be taken into account, and we can safely saturate the present bound with the NP amplitude alone, except for the K_L sector. For example, the branching ratio of $B_s \to \mu^+\mu^-$ is about 3.4×10^{-9} and that of $B_d \to \mu^+\mu^-$ is about 1.0×10^{-10} in the SM, while the experimental limits are at the ballpark of 4-6$\times 10^{-8}$. Another exception is the $B^- \to l^-\overline{\nu}$ decay, which proceeds through the annihilation channel in the SM:

$$\mathrm{Br}(B^- \to l^-\overline{\nu}) = \frac{1}{8\pi} G_F^2 m_B m_l^2 f_B^2 |V_{ub}|^2 \tau_B \left(1 - \frac{m_l^2}{m_B^2}\right)^2 , \tag{4.16}$$

where τ_B is the lifetime of the B meson.

For the semileptonic decays, we use the following standard convention [108], given for the $B \to K^{(*)}\ell^+\ell^-$ transition:

$$
\begin{aligned}
\langle K(p_2)|\bar{b}\gamma_\mu s|B(p_1)\rangle &= P_\mu F_1(q^2) + q_\mu \frac{m_B^2 - m_K^2}{q^2}\left(F_0(q^2) - F_1(q^2)\right), \\
\langle K^*(p_2,\epsilon)|\bar{b}\gamma_\mu(1\mp\gamma_5)s\ |B(p_1)\rangle &= \mp i q_\mu \frac{2m_{K^*}}{q^2}\epsilon^*.q\left[A_3(q^2) - A_0(q^2)\right] \\
&\quad \pm i\epsilon_\mu^*(m_B + m_{K^*})A_1(q^2) \\
&\quad \mp \frac{i}{m_B + m_{K^*}} P_\mu(\epsilon^*.q)A_2(q^2) \\
&\quad -\varepsilon_{\mu\nu\alpha\beta}\epsilon^{*\nu}p_2^\alpha q^\beta \frac{2V(q^2)}{m_B + m_{K^*}}, \qquad (4.17)
\end{aligned}
$$

where $P = p_1 + p_2$, and $q = p_1 - p_2$. The pole dominance ensures that $A_3(0) = A_0(0)$, and $A_3(q^2)$ can be expressed in terms of A_1 and A_2.

4.4 Constraints on the leptoquark couplings

4.4.1 From neutral meson mixing

Consider the neutral meson $M^0 \equiv q_j\overline{q_k}$. The oscillation can have a new LQ mediated amplitude, with i-type leptons and some scalar LQs in the box, as shown in Fig. (4.1). The amplitude is proportional to $(\lambda_{ik}^*\lambda_{ij})^2$. We consider, as in the standard practice, a hierarchical coupling scheme, so that we may consider only two LQ couplings to be nonzero at the most. Also, we consider any one type of LQ to be present at the same time. This keeps the discussion simple and the numerical results easily tractable; however, this may not be the case where we have some high-energy texture of the couplings and there can be a number of nonzero couplings at the weak scale.

For the LQ box, one must consider the same type of lepton flowing inside the box if we wish to restrict the number of LQ couplings to 2. The effective Hamiltonian contains the operator $\tilde{O}_1$, defined as

$$
\tilde{O}_1 = \left[\bar{b}\gamma^\mu P_R d\right]_1 \left[\bar{b}\gamma_\mu P_R d\right]_1 , \qquad (4.18)
$$

(where the subscript 1 indicates the $SU(3)_c$ singlet nature of the current),

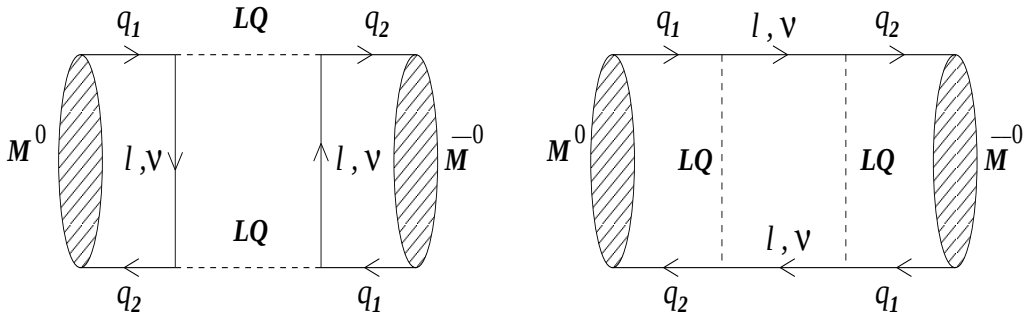

Figure 4.1: Leptoquark contributions to $M^0 - \overline{M^0}$ mixing.

and is given by

$$\mathcal{H}_{LQ} = \frac{(\lambda^*_{ik}\lambda_{iq})^2}{128\pi^2}\left[\frac{c_1}{m^2_{LQ}}\left\{I\left(\frac{{m_l}^2}{m^2_{LQ}}\right)\right\} + \frac{c_2}{m^2_{LQ}}\right]\tilde{O}_1\,, \tag{4.19}$$

where $c_1 = 1$, $c_2 = 0$ for $S_0, \tilde{S}_0$ and $S_{\frac{1}{2}}$, $c_1 = c_2 = 1$ for $\tilde{S}_{\frac{1}{2}}$, and $c_1 = 4$, $c_2 = 1$ for S_1. Therefore, if we are allowed to neglect the SM, the limits on the product couplings for $(\lambda_{LS_0}, \lambda_{R\tilde{S}_0}, \lambda_{RS_{1/2}})$, $\lambda_{L\tilde{S}_{1/2}}$, and λ_{LS_1} should be at the ratio of $1 : \frac{1}{\sqrt{2}} : \frac{1}{\sqrt{5}}$. The operator $\tilde{O}_1$ is multiplicatively renormalized and the LQ couplings are those obtained at the weak scale. The function $I(x)$, defined as

$$I(x) = \frac{1 - x^2 + 2x\log x}{(1-x)^3}\,, \tag{4.20}$$

is always very close to $I(0) = 1$; note that we have taken all LQs to be degenerate at 300 GeV.

4.4.2 From Leptonic and Semileptonic Decays

The LQ couplings which may contribute to $K^0 - \overline{K^0}$, $B^0_d - \overline{B^0_d}$ and $B^0_s - \overline{B^0_s}$ mixing should also affect various LQ-mediated semileptonic ($b \to d(s)l^+l^-$, $s \to dl^+l^-$) and purely leptonic ($B^0_{d(s)} \to l^+l^-$, $K^0 \to l^+l^-$) decays. The estimated BRs of leptonic flavour conserving $\Delta B(S) = 1$ processes within

Interaction	4-fermion vertex	Fierz-transformed vertex
$(\lambda_{LS_0}\overline{q}_L^c i\sigma_2 l_L + \lambda_{RS_0}\overline{u}_R^c e_R)S_0^\dagger$	$G(\overline{d}_L^c\nu_L)(\overline{\nu}_L d_L^c)$	$\frac{1}{2}G(\overline{d}_L^c\gamma^\mu d_L^c)(\overline{\nu}_L\gamma_\mu\nu_L)$
$\lambda_{R\tilde{S}_o}\overline{d}_R^c e_R\tilde{S}_0^\dagger$	$G(\overline{d}_R^c e_R)(\overline{e}_R d_R^c)$	$\frac{1}{2}G(\overline{d}_R^c\gamma^\mu d_R^c)(\overline{e}_R\gamma_\mu e_R)$
$(\lambda_{LS_{1/2}}\overline{u}_R l_L + \lambda_{RS_{1/2}}\overline{q}_L i\sigma_2 e_R)S_{1/2}^\dagger$	$G(\overline{d}_L e_R)(\overline{e}_R d_L)$	$\frac{1}{2}G(\overline{d}_L\gamma_\mu d_L)(\overline{e}_R\gamma_\mu e_R)$
$\lambda_{L\tilde{S}_{1/2}}\overline{d}_R l_L\tilde{S}_{1/2}^\dagger$	$G(\overline{d}_R\nu_L)(\overline{\nu}_L d_R)$	$\frac{1}{2}G(\overline{d}_R\gamma^\mu d_R)(\overline{\nu}_L\gamma_\mu\nu_L)$
	$G(\overline{d}_R e_L)(\overline{e}_L d_R)$	$\frac{1}{2}G(\overline{d}_R\gamma^\mu d_R)(\overline{e}_L\gamma_\mu e_L)$
$\lambda_{LS_1}\overline{q}_L^c i\sigma_2\vec{\sigma} l_L\cdot\vec{S}_1^\dagger$	$G(\overline{\nu}_L d_L^c)$	$\frac{1}{2}G(\overline{d}_L^c\gamma^\mu d_L^c)(\overline{\nu}_L\gamma_\mu\nu_L)$
	$2G(\overline{d}_L^c e_L)(\overline{e}_L d_L^c)$	$G(\overline{d}_L^c\gamma^\mu d_L^c)(\overline{e}_L\gamma_\mu e_L)$

Table 4.2: Effective four-fermion operators for scalar leptoquarks. G generically stands for λ^2/m_{LQ}^2.

SM are very small compared to their experimental numbers or upper bounds, except for $K_L \to e^+e^-, \mu^+\mu^-$. Therefore it is quite reasonable to ignore the SM effects for these channels while constraining the LQ couplings. For these mixing correlated decays, the final state leptons must be of the same flavour. The leptonic decay modes are theoretically clean and free from any hadronic uncertainties. The semileptonic modes have the usual form-factor uncertainties, and the SM contribution cannot be neglected here.

To construct four-fermion operators from λ type couplings which mediate leptonic and semileptonic B and K decays, one needs to integrate out the LQ field. The effective 4-fermi Hamiltonians and vertices which are related to the mixing is given in Table 4.2. The vertices show that the limits coming from leptonic or semileptonic decays will be highly correlated. For charged leptons in the final state, one can constrain $R\tilde{S}_0$, $RS_{\frac{1}{2}}$, $L\tilde{S}_{\frac{1}{2}}$, or LS_1 type LQs. The bounds for the first three will be the same, which is just twice that of LS_1. Similarly, if we have neutrinos in the final state, LS_0, $L\tilde{S}_{\frac{1}{2}}$, or LS_1 type LQ couplings are bounded, all limits being the same.

The product LQ coupling may in general be complex. If we neglect the SM, there is no scope of CP violation and the data constrains only the magnitude of the product, so if we wish, we can take the product to be real. In fact, if we assume CP invariance, K_S decay channels to $\ell_i^+\ell_i^-$ constrain only the

real part of the product couplings, and K_L constrains the imaginary part. For the processes where the SM contribution cannot be neglected, we have saturated the difference between the highest experimental prediction and the lowest SM expectation with an incoherently summed LQ amplitude. For a quick reference, the data on the leptonic and semileptonic channels is shown in Tables 4.3 and 4.4. Note that these bounds are almost free from QCD uncertainties except for the decay constants of the mesons, and hence are quite robust. There are other semileptonic channels which we do not show here, e.g., $B \to K^* \nu\overline{\nu}$, because they yield less severe bounds.

Mode	Branching ratio	Mode	Branching ratio
$K_S \to e^+e^-$	$< 9 \times 10^{-9}$	$K_S \to \mu^+\mu^-$	$< 3.2 \times 10^{-7}$
$K_L \to e^+e^-$	$9^{+6}_{-4} \times 10^{-12}$	$K_L \to \mu^+\mu^-$	$(6.84 \pm 0.11) \times 10^{-9}$
$B_d \to \mu^+\mu^-$	$< 1.0 \times 10^{-8}$	$B_d \to \mu^+\mu^-$	$< 1.0 \times 10^{-8}$
$B_d \to \tau^+\tau^-$	$< 4.1 \times 10^{-3}$	$B_s \to e^+e^-$	$< 5.4 \times 10^{-5}$
$B_s \to \mu^+\mu^-$	$< 3.3 \times 10^{-8}$		

Table 4.3: Branching ratios for some leptonic decays of K and B mesons [54]. The limits are at 90% confidence level. The SM expectation is negligible.

From the decay width of $B_{d(s)}(K^0) \to l^-l^+$

- $B_q^0 \to l^+l^-$

We get the following constraints from $B_q^0 \to l^+l^-$ decay:

$$\begin{aligned} |\lambda^{lq}_{RS_o}\lambda^{l3*}_{RS_o}| &< 2\sqrt{F_{B_q^0}}\tilde{m}_o^2, \\ |\lambda^{lq}_{RS_{1/2}}\lambda^{l3*}_{RS_{1/2}}| &< 2\sqrt{F_{B_q^0}}m_{1/2}^2, \end{aligned} \tag{4.21}$$

Mode	Branching ratio	SM expectation
$K_S \to \pi^0 e^+ e^-$	$3.0^{+1.5}_{-1.2} \times 10^{-9}$	2.1×10^{-10}
$K_S \to \pi^0 \mu^+ \mu^-$	$2.9^{+1.5}_{-1.2} \times 10^{-9}$	4.8×10^{-10}
$K_L \to \pi^0 e^+ e^-$	$< 2.8 \times 10^{-10}$	2.4×10^{-11}
$K_L \to \pi^0 \mu^+ \mu^-$	$< 3.8 \times 10^{-10}$	4.4×10^{-12}
$K_L \to \pi^0 \nu\overline{\nu}$	$< 6.7 \times 10^{-8}$	$(2.8 \pm 0.6) \times 10^{-11}$
$K^+ \to \pi^+ \nu\overline{\nu}$	$(17.3^{+11.5}_{-10.5}) \times 10^{-11}$	$(8.5 \pm 0.7) \times 10^{-11}$
$K^+ \to \pi^+ e^+ e^-$	$(2.88 \pm 0.13) \times 10^{-7}$	$(2.74 \pm 0.23) \times 10^{-7}$
$K^+ \to \pi^+ \mu^+ \mu^-$	$(8.1 \pm 1.4) \times 10^{-8}$	$(6.8 \pm 0.6) \times 10^{-8}$
$B_d \to \pi^0 e^+ e^-$	$< 1.4 \times 10^{-7}$	3.3×10^{-8}
$B_d \to \pi^0 \mu^+ \mu^-$	$< 1.8 \times 10^{-7}$	3.3×10^{-8}
$B_d \to K^0 e^+ e^-$	$(1.3^{+1.6}_{-1.1}) \times 10^{-7}$	2.6×10^{-7}
$B_d \to K^0 \mu^+ \mu^-$	$(5.7^{+2.2}_{-1.8}) \times 10^{-7}$	$(3.3 \pm 0.7) \times 10^{-7}$
$B_d \to K^* \mu^+ \mu^-$	$(1.06 \pm 0.17) \times 10^{-6}$	$(1.0 \pm 0.4) \times 10^{-6}$
$B_d \to K^* e^+ e^-$	1.39×10^{-6}	$(1.3 \pm 0.4) \times 10^{-6}$
$B_d \to \pi^0 \nu\overline{\nu}$	$< 2.2 \times 10^{-4}$	$(8.5 \pm 3.5) \times 10^{-8}$
$B_d \to K^0 \nu\overline{\nu}$	$< 1.6 \times 10^{-4}$	$(1.35 \pm 0.35) \times 10^{-5}$
$B_d \to K^{*0} \nu\overline{\nu}$	$< 1.2 \times 10^{-4}$	3.8×10^{-6}
$B^+ \to \pi^+ e^+ e^-$	$< 8.0 \times 10^{-6}$	$(2.03 \pm 0.23) \times 10^{-8}$
$B^+ \to \pi^+ \mu^+ \mu^-$	$< 6.9 \times 10^{-6}$	$(2.03 \pm 0.23) \times 10^{-8}$
$B^+ \to \pi^+ \nu\overline{\nu}$	$< 100 \times 10^{-6}$	$(9.7 \pm 2.1) \times 10^{-6}$
$B^+ \to K^+ e^+ e^-$	$< 1.25 \times 10^{-5}$	6.0×10^{-7}
$B^+ \to K^+ \mu^+ \mu^-$	$< 8.3 \times 10^{-6}$	6.0×10^{-7}
$B^+ \to K^{+*} \nu\overline{\nu}$	$< 8.0 \times 10^{-5}$	$(12.0 \pm 4.4) \times 10^{-6}$
$B^+ \to K^+ \nu\overline{\nu}$	$< 14 \times 10^{-6}$	$(4.5 \pm 0.7) \times 10^{-6}$
$B_s \to \phi \mu^+ \mu^-$	$(1.44 \pm 0.57) \times 10^{-6}$	1.6×10^{-6}
$B_s \to \phi \nu\overline{\nu}$	$< 5.4 \times 10^{-3}$	$(13.9 \pm 5.0) \times 10^{-6}$

Table 4.4: Branching ratios for some semileptonic K and B decays [54, 109, 110, 111, 112]. The limits are at 90% confidence level. Also shown are the central values for the SM. For the SM expectations shown with an error margin, we have taken the lowest possible values, so that the LQ bounds are most conservative. The systematic and statistical errors have been added in quadrature.

$$
\begin{aligned}
|\lambda^{lq}_{L\tilde{S}_{1/2}}\lambda^{l3^*}_{L\tilde{S}_{1/2}}| &< 2\sqrt{F_{B^0_q}}m^2_{\tilde{1}/2}, \\
|\lambda^{lq}_{LS_1}\lambda^{l3^*}_{LS_1}| &< \sqrt{F_{B^0_q}}m^2_1,
\end{aligned}
\tag{4.22}
$$

where,

$$
\begin{aligned}
F_{B^0_q} &= \frac{1}{F'_{B^0_q}}\mathcal{B}r\left(B^0_q \to l^+l^-\right), \\
F'_{B^0_q} &= \frac{1}{32\pi}f_{B^0_q}\tau_{B^0_q}M^3_{B^0_q}m_l\sqrt{1-4\frac{m^2_l}{M^2_{B^0_q}}}.
\end{aligned}
\tag{4.23}
$$

q is d for B^0_d and s for B^0_s. $f_{B^0_q}, \tau_{B^0_q}$ and $M_{B^0_q}$ are the decay constant, lifetime and the mass of B^0_q respectively. m_l represents the mass of the lepton.

- $K^0_{S(L)} \to l^+l^-$

We get the following constraints from $K^0_{S(L)} \to l^+l^-$ decay:

$$
\begin{aligned}
\mathcal{R}\text{eal}(\mathcal{I}\text{mg})|\lambda^{l2}_{R\tilde{S}_o}\lambda^{l1^*}_{R\tilde{S}_o}| &< 2\sqrt{F_{K^0_{S(L)}}}\tilde{m}^2_o, \\
\mathcal{R}\text{eal}(\mathcal{I}\text{mg})|\lambda^{l2}_{RS_{1/2}}\lambda^{l1^*}_{RS_{1/2}}| &< 2\sqrt{F_{K^0_{S(L)}}}m^2_{1/2}, \\
\mathcal{R}\text{eal}(\mathcal{I}\text{mg})|\lambda^{l2}_{L\tilde{S}_{1/2}}\lambda^{l1^*}_{L\tilde{S}_{1/2}}| &< 2\sqrt{F_{K^0_{S(L)}}}m^2_{\tilde{1}/2}, \\
\mathcal{R}\text{eal}(\mathcal{I}\text{mg})|\lambda^{l2}_{LS_1}\lambda^{l1^*}_{LS_1}| &< \sqrt{F_{K^0_{S(L)}}}m^2_1,
\end{aligned}
\tag{4.24}
$$

where,

$$
\begin{aligned}
F_{K^0_{S(L)}} &= \frac{1}{F'_{K^0_{S(L)}}}\mathcal{B}r\left(K^0_{S(L)} \to l^+l^-\right), \\
F'_{K^0_{S(L)}} &= \frac{1}{16\pi}f_{K^0}\tau_{K^0_{S(L)}}M^3_{K^0_{S(L)}}m_l\sqrt{1-4\frac{m^2_l}{M^2_{K^0}}}.
\end{aligned}
\tag{4.25}
$$

f_{K^0} and $\tau_{K^0_{S(L)}}$ are the decay constant and lifetime of $K^0_{S(L)}$ respectively. M_{K^0} is the mass of K^0. Note that K_L has a lifetime two orders of

magnitude larger than that of K_S and hence the bounds coming from K_L decays are going to be tighter by that amount.

4.5 Numerical Inputs

The numerical inputs have been taken from various sources and listed in Table 4.5. We use the BSW form factors [108] with a simple pole dominance, and the relevant form factors at zero momentum transfer $q^2 = 0$ are taken as follows [113]:

$$F_0^{B\to K}(0) = F_1^{B\to K}(0) = 0.38\,, \quad F_0^{B\to\pi}(0) = F_1^{B\to\pi}(0) = 0.33\,,$$
$$B \to K^* : V(0) = 0.37\,, A_1(0) = A_2(0) = 0.33\,, A_0(0) = 0.32\,, \quad (4.26)$$

while we take $F_0^{K\to\pi}(0) = 0.992$. This is not incompatible with the lattice QCD result of 0.9560(84) [114]. The theoretical uncertainty comes mostly from the form factors, but is never more than 10% for the LQ coupling bounds. The bounds are not a sensitive function of the exact values of the form factors, and remain more or less the same even when one uses the light-cone form factors.

The mass differences ΔM are all pretty well-measured; for consistency, we use the UTfit values [16]. We use $\sin(2\beta_d)$ as measured in the charmonium channel [32]. The SM prediction is taken from the measurement of the UT sides only since that is least likely to be affected by new physics. (However, this need not be true always. For example, if there is a new physics contributing in the $B_d^0 - \overline{B_d^0}$ mixing amplitude, the extracted value of V_{td} may not be equal to its SM value.) For β_s, which is defined as $\arg(-V_{ts}V_{tb}^*/V_{cs}V_{cb}^*)$, the errors are asymmetric:

$$\beta_s = \left(0.47^{+0.13}_{-0.21}\right) \cup \left(1.09^{+0.21}_{-0.13}\right)\,, \quad (4.27)$$

which we show in a symmetrized manner. The decay constants $f_{B_{d,s}}$ are taken from [15] as a lattice average of various groups. The same holds for $f_B\sqrt{B_B}$ and ξ, defined as $\xi = f_{B_s}\sqrt{B_{B_s}}/f_{B_d}\sqrt{B_{B_d}}$, whose value we take to be $1.258 \pm 0.020 \pm 0.043$.

Observable	Value	Observable	Value
Δm_K	5.301×10^{-3} ps^{-1}	$\lvert\varepsilon_K\rvert$	$(2.228 \pm 0.011) \times 10^{-3}$
Δm_{B_d}	(0.507 ± 0.005) ps^{-1}	B_K	0.75 ± 0.07
Δm_{B_s}	(17.77 ± 0.12) ps^{-1}	η_{B_K}	1.38 ± 0.53
$\eta_{B_{B_d}(B_{B_s})}$	0.55 ± 0.01	f_K	160 MeV
$\sin(2\beta_d)_{exp}$	0.668 ± 0.028	f_{B_s}	(228 ± 17) MeV
$\sin(2\beta_d)_{SM}$	0.731 ± 0.038	f_{B_s}/f_{B_d}	$(1.199 \pm 0.008 \pm 0.023)$
$(\beta_s)_{exp}$	$(0.43 \pm 0.17) \cup (1.13 \pm 0.17)$	$f_{B_s}\sqrt{B_{B_s}}$	$(257 \pm 6 \pm 21)$ MeV

Table 4.5: Input parameters. For the form factors, see text.

4.6 Analysis

4.6.1 Neutral Meson Mixing

While our bounds are shown in Table 4.6 following the procedure outlined in Section 4.4.1, let us try to understand the origin of these bounds.

Take Figure 4.2 (a) as an example, which shows the bounds on the real and imaginary parts of $\lambda_{i1}\lambda^*_{i2}$. This is shown for the triplet LQ S_1; all LQs produce a similar diagram, with the limits properly scaled. To get an idea of the scaling, one may again look at Table 4.6, and scale accordingly.

For the K system, we use ΔM_K and $|\varepsilon_K|$ as the constraints. The SM part is assumed to be dominated by the short-distance contributions only. Note the spoke-like structure; this is because $|\varepsilon_K|$ gives a very tight constraint on $\mathrm{Im}(M_{12})$ and only those points are chosen for which $(\lambda\lambda^*)^2$ is almost real. However, as we will see later, all the bounds except those for the LS_0 type LQs will be superseded by those coming from leptonic and semileptonic K decays; however, $i = 3$ bounds will stand.

A similar analysis is shown for the $B^0_d - \overline{B^0_d}$ system in Figure 4.2 (b) and Table 4.6. Note that the bounds on the real and the imaginary parts of any product coupling are almost the same. This is, of course, no numerical acci-

dent. To understand this, let us analyse the origin of these bounds. There are two main constraints for the B_d system: ΔM_d and $\sin(2\beta_d)$. There will be a region, centred around the origin of $Re(\lambda\lambda) - Im(\lambda\lambda)$ plane (since ΔM_d can be explained by the SM alone), where $|\lambda\lambda|$ is small and the phase can be arbitrary. At the 1σ level, this region appears to be small, because the measured value of $\sin(2\beta_d)$ from the charmonium channels is just barely compatible with that obtained from a measurement of the sides of the unitarity triangles. The region expands if we take the error bars to be larger. This is the SM-dominated region, where LQ creeps in to whatever place is left available. Any analysis, taking both SM and LQ but assuming incoherent sum of amplitudes, should generate this region only.

However, there is always scope for fully constructive or destructive interference between SM and any NP. Consider a situation where the LQ contribution is large, so large that even after a destructive interference with the SM amplitude, enough is left to saturate ΔM_d. This LQ-dominated region (this is true for all NP models in general) gives us the bounds, and in the limit where the SM can be neglected, the bounds on $Re(\lambda\lambda)$ are almost the same as on $Im(\lambda\lambda)$. The alignment of the fourfold symmetric structure is different from Figure 4.2 (b) because of the sizable value of $\sin(2\beta_d)$.

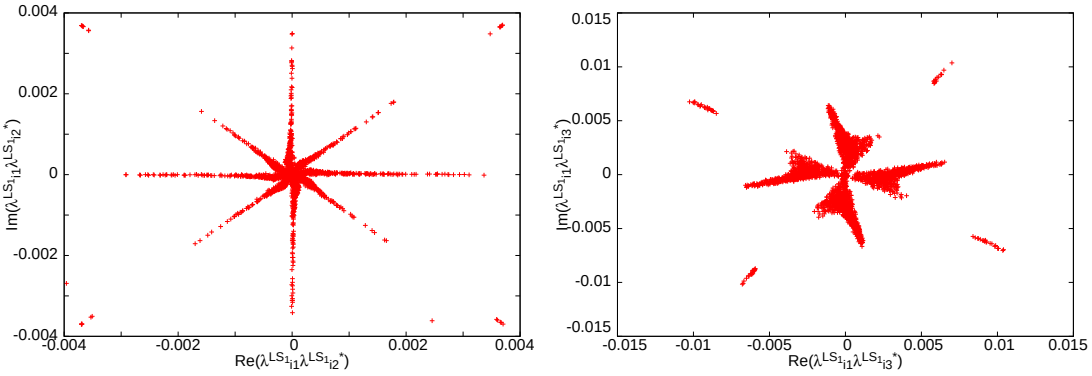

(a) (b)

Figure 4.2: (a) Allowed parameter space for $\lambda_{i1}\lambda^*_{i2}$ for λ_{LS_1} type couplings. (b) The same for $\lambda_{i1}\lambda^*_{i3}$.

Process & indices	LQ Type	Real Only	Real part of Complex	Img part of Complex	$\lvert\lambda\lambda^*\rvert$
$K^0 - \overline{K^0}$	LS_0, $R\tilde{S}_0$, $RS_{\frac{1}{2}}$	0.008	0.008	0.008	0.008
$(i1)(i2)^*$	$L\tilde{S}_{\frac{1}{2}}$	0.0055	0.0055	0.0055	0.0055
	LS_1	0.0036	0.0036	0.0036	0.0036
$B_d^0 - \overline{B_d^0}$	LS_0, $R\tilde{S}_0$, $RS_{\frac{1}{2}}$	0.009	0.022	0.022	0.027
$(i1)(i3)^*$	$L\tilde{S}_{\frac{1}{2}}$	0.0063	0.016	0.016	0.019
	LS_1	0.004	0.010	0.010	0.012
$B_s^0 - \overline{B_s^0}$	LS_0, $R\tilde{S}_0$, $RS_{\frac{1}{2}}$	0.05	0.13	0.13	0.18
$(i2)(i3)^*$	$L\tilde{S}_{\frac{1}{2}}$	0.034	0.09	0.09	0.13
	LS_1	0.02	0.06	0.06	0.08

Table 4.6: Bounds from the neutral meson mixing. The third column shows the bounds when the couplings are assumed to be real. The last three columns are for complex couplings.

The limits for the B_s system are shown in Figure 4.3. Note that the origin is excluded at the 1σ level; this is due to the large observed values of β_s: $\beta_s = (25 \pm 10)^\circ \cup (65 \pm 10)^\circ$ in the first quadrant and a mirror image in the second quadrant.

The magnitude of the product is bounded to be less than 0.08 at the 1σ level for the triplet LQ, and scaled according to Table 4.6. For $i = 2$, the relevant coupling mediates the leptonic decay $B_s \to \mu^+\mu^-$ and semileptonic $B_d \to K^{(*)}\mu^+\mu^-$ decays. We will see in the next part, just like the K system, that the constraints coming from such decays are much stronger. The same observation is true for $i = 1$. Again, only for λ_{LS_0} type couplings, there is no leptonic or semileptonic contributions (the down-type quark current couples with the neutrino current only), and the bounds coming from the mixing stand. Thus, for $i = 1, 2$ and any other LQ except S_0, it is extremely improbable that the LQ contribution explains the large mixing phase.

What happens for $i = 3$? This will mediate the decays $B_s \to \tau^+\tau^-$ and $B \to X_s\tau^+\tau^-$. While there is no data on these channels yet, we may have a consistency check with the lifetime of B_s. This tells us that couplings as large as 0.05 are allowed, but the decay $B_s \to \tau^+\tau^-$ should be close to the discovery limit. This will be an interesting channel to explore at the LHC. There is an exception: if we consider λ_{LS_0} type couplings, neutrinos flow inside the box, and then we have final-state neutrinos, and not τ leptons.

Note that the box diagram with leptoquarks and leptons has a nonzero absorptive part, which is responsible for the corresponding correlated decays. This affects the width differences $\Delta\Gamma_{d,s}$. As has been shown in [86], NP that contributes to $\Delta\Gamma$ may enhance the mixing phase in the $B_s^0 - \overline{B_s^0}$ box, contrary to the Grossman theorem [87], which tells that the mixing phase in the B_s system must decrease due to NP if there is no absorptive amplitude in the box diagram. The effect on $\Delta\Gamma_d/\Gamma_d$ is negligible; with the bounds that we get here, it is never more than 1%, or even less (note that [86] uses a LQ mass of 100 GeV and we need to scale their results). For B_s, $\Delta\Gamma_s/\Gamma_s$ may go up to 30% without significantly enhancing the leptonic branching ratios like $B_s \to \tau^+\tau^-$, and one can also get a significant nonzero phase in the $B_s^0 - \overline{B_s^0}$ mixing that is indicated by the present experiments [88].

$K_{L(S)}$ Decay	Coupling	$\lvert\lambda\lambda^*\rvert$	$B_{d(s)}$ Decay	Coupling	$\lvert\lambda\lambda^*\rvert$
$K_S \to e^+e^-$	$(12)(11)^*$	1.8×10^{-1}	$B_d \to \mu^+\mu^-$	$(21)(23)^*$	2.8×10^{-3}
$K_S \to \mu^+\mu^-$	$(22)(21)^*$	5.5×10^{-3}	$B_d \to \tau^+\tau^-$	$(31)(33)^*$	1.2×10^{-1}
$K_L \to e^+e^-$	$(12)(11)^*$	2.4×10^{-4}	$B_s \to \mu^+\mu^-$	$(22)(23)^*$	4.3×10^{-3}
$K_L \to \mu^+\mu^-$	$(22)(21)^*$	6.4×10^{-6}			

Table 4.7: Bounds from the correlated leptonic $K_{L(S)}$ and $B_{d(s)}$ decays. The LQs are either of $R\tilde{S}_0$, $RS_{\frac{1}{2}}$, or $L\tilde{S}_{\frac{1}{2}}$ type. For LS_1 type LQ, the bounds are half of that shown here.

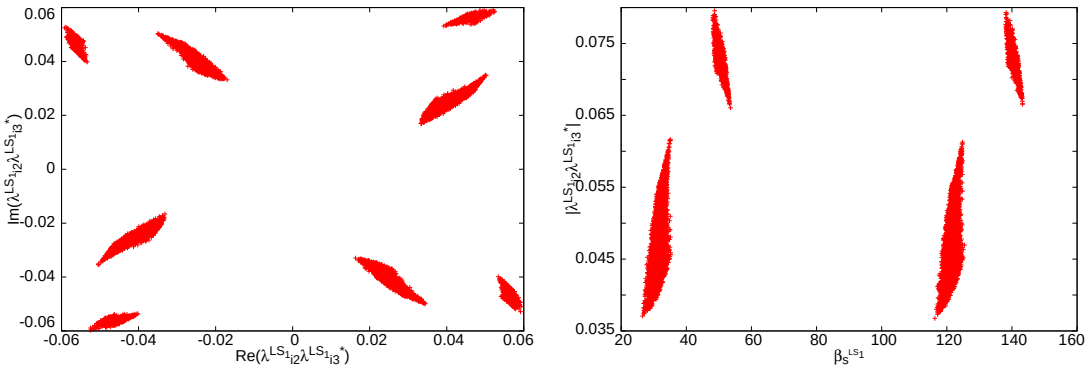

(a) (b)

Figure 4.3: (a) Allowed parameter space for $\lambda_{i2}\lambda^*_{i3}$ (b) The reach for the angle β_s. For more details, see text.

4.6.2 Leptonic and Semileptonic Decays

We have assumed only two LQ couplings to be present simultaneously, with identical lepton indices. Thus we will be interested only in lepton flavour conserving processes. A similar analysis was done in [115] for vector LQs. Our bounds are shown in Table 4.7 and Table 4.8.

Decay channel	Coupling	$\lvert\lambda\lambda^*\rvert$	Decay channel	Coupling	$\lvert\lambda\lambda^*\rvert$
$K_S \to \pi^0 e^+ e^-$	$(11)(12)^*$	2.8×10^{-3}	$K_L \to \pi^0 e^+ e^-$	$(11)(12)^*$	2.8×10^{-5}
$K_S \to \pi^0 \mu^+ \mu^-$	$(21)(22)^*$	4.6×10^{-3}	$K_L \to \pi^0 \mu^+ \mu^-$	$(21)(22)^*$	5.9×10^{-5}
$K^+ \to \pi^+ e^+ e^-$	$(11)(12)^*$	1.2×10^{-3}	$K^+ \to \pi^+ \mu^+ \mu^-$	$(21)(22)^*$	9.5×10^{-4}
$K_L \to \pi^0 \nu\overline{\nu}$	$(i1)(i2)^*$	4.6×10^{-4}			
$B_d \to \pi^0 e^+ e^-$	$(11)(13)^*$	1.1×10^{-3}	$B^+ \to \pi^+ e^+ e^-$	$(11)(13)^*$	5.0×10^{-4}
$B_d \to \pi^0 \mu^+ \mu^-$	$(21)(23)^*$	1.2×10^{-3}	$B^+ \to \pi^+ \mu^+ \mu^-$	$(21)(23)^*$	4.6×10^{-4}
$B_d \to K^0 e^+ e^-$	$(12)(13)^*$	3.6×10^{-4}	$B^+ \to K^+ e^+ e^-$	$(12)(13)^*$	7.0×10^{-3}
$B_d \to K^* e^+ e^-$	$(12)(13)^*$	9.7×10^{-4}	$B_d \to K^* \mu^+ \mu^-$	$(22)(23)^*$	1.1×10^{-3}
$B_d \to K^0 \mu^+ \mu^-$	$(22)(23)^*$	1.5×10^{-3}	$B^+ \to K^+ \mu^+ \mu^-$	$(22)(23)^*$	5.6×10^{-3}
$B_d \to \pi^0 \nu\overline{\nu}$	$(i1)(i3)^*$	4.4×10^{-2}	$B^+ \to \pi^+ \nu\overline{\nu}$	$(i1)(i3)^*$	2.0×10^{-2}
$B_d \to K^0 \nu\overline{\nu}$	$(i2)(i3)^*$	2.6×10^{-2}	$B^+ \to K^+ \nu\overline{\nu}$	$(i2)(i3)^*$	6.5×10^{-3}
$B_d \to K^{0*} \nu\overline{\nu}$	$(i2)(i3)^*$	1.5×10^{-2}	$B^+ \to K^{+*} \nu\overline{\nu}$	$(i2)(i3)^*$	1.2×10^{-2}
$B_s \to \phi \mu^+ \mu^-$	$(22)(23)^*$	7.9×10^{-4}	$B_s \to \phi \nu\overline{\nu}$	$(i2)(i3)^*$	9.1×10^{-2}

Table 4.8: Bounds from the correlated semileptonic B and K decays. The LQs are either of $R\tilde{S}_0$, $RS_{\frac{1}{2}}$, or $L\tilde{S}_{\frac{1}{2}}$ type. For LS_1 type LQ, the bounds are half of that shown here. For the final state neutrino channels, the LQ can be LS_0, $L\tilde{S}_{\frac{1}{2}}$, or LS_1 type, all giving the same bound.

Apart from the leptonic K_L decays, the SM amplitudes can be neglected as a first approximation. Thus, one may saturate the experimental bounds with the LQ amplitude alone. This generates most of the numbers in Table 4.7. For K_L decays, we consider the SM part too, and add the amplitudes incoherently. Note that K_L decays only constrain the imaginary part of the LQ coupling. This can be understood as follows. Consider the decay $K_L \to \mu^+\mu^-$. While in the limit of CP invariance, one can write $K_L = (K^0 - \overline{K}^0)/\sqrt{2}$, it is $\lambda_{21}\lambda_{22}^*$ that mediates K^0 decay and $\lambda_{21}^*\lambda_{22}$ that mediates $\overline{K}^0$ decay. Taking the combination, the imaginary part of the coupling is responsible for K_L decays, and the real part is responsible for K_S decays. As mentioned earlier, $B_s \to \tau^+\tau^-$ does not have a limit yet, but the SM expectation is about $\mathcal{O}(10^{-6})$, and if $|\lambda_{32}\lambda_{33}| \sim 10^{-2}$, one expects the BR to be of the order of 4×10^{-5}.

For the channel $K^+ \to \pi^+\nu\overline{\nu}$, the outgoing neutrino can have any flavour, and so the bound is valid for $i = 1, 2, 3$. However, these bounds are valid when one can have a neutrino in the final state, i.e., for LQs of the L category, which couple with lepton doublets.

Semileptonic decays give the best bounds, but they are the least robust one, considering the uncertainty in the form factors. While we take the BSW form factors [108], the lattice QCD or light-cone sum rules based form factors may change the final results by at most 10%. To be conservative, we saturate the difference between the SM prediction and the maximum of the data by LQ contributions.

Let us just say a few words about $B^- \to \tau^-\overline{\nu}$. In the SM, the branching ratio can be worked out from Eq. (4.16) and is $(9.3^{+3.4}_{-2.3}) \times 10^{-5}$, where the major sources of uncertainty are $|V_{ub}|$ and f_B. The observed number, $(14.3 \pm 3.7) \times 10^{-5}$ [32] is a bit above the SM prediction. The tension can be alleviated with LS_0 or LS_1 type leptoquarks; the necessary combination is $\lambda_{31}\lambda_{33}^*$, and the bounds that we have obtained on this particular combination in Table 4.10 can easily jack up the branching ratio to the observed level. A similar exercise has been done for the leptonic D_s decays in [91].

We have summarized our bounds in Tables 4.9, 4.10, and 4.11. These tables

LQ type	indices	Previous Bound	This analysis			
			From Mixing		From Decay	
			Real part	Imag. part	Channel	Bound
LS_0	$(i1)(i2)^*$	1.8×10^{-4}	8×10^{-3}	8×10^{-3}	$K_L \to \pi^0 \nu\overline{\nu}$	4.6×10^{-4}
$R\tilde{S_0}$,	$(11)(12)^*$	2.7×10^{-3}	8×10^{-3}	8×10^{-3}	$K^+ \to \pi^+ e^+ e^-$	1.2×10^{-3}
					$K_L \to \pi^0 e^+ e^-$	(2.8×10^{-5})
$RS_{1/2}$	$(21)(22)^*$	5.4×10^{-5}	8×10^{-3}	8×10^{-3}	$K^+ \to \pi^+ \mu^+ \mu^-$	9.5×10^{-4}
					$K_L \to \mu^+ \mu^-$	6.4×10^{-6}
	$(31)(32)^*$	0.018	8×10^{-3}	8×10^{-3}	—	—
$L\tilde{S}_{1/2}$	$(11)(12)^*$	1.8×10^{-4}	5.6×10^{-3}	5.6×10^{-3}	$K^+ \to \pi^+ e^+ e^-$	1.2×10^{-3}
					$K_L \to \pi^0 e^+ e^-$	(2.8×10^{-5})
	$(21)(22)^*$	1.8×10^{-4}	5.6×10^{-3}	5.6×10^{-3}	$K^+ \to \pi^+ \mu^+ \mu^-$	9.5×10^{-4}
					$K_L \to \mu^+ \mu^-$	(6.4×10^{-6})
	$(31)(32)^*$	5.4×10^{-5}	5.6×10^{-3}	5.6×10^{-3}	$K_L \to \pi^0 \nu\overline{\nu}$	4.6×10^{-4}
LS_1	$(11)(12)^*$	1.8×10^{-4}	3.6×10^{-3}	3.6×10^{-3}	$K^+ \to \pi^+ e^+ e^-$	6.0×10^{-4}
					$K_L \to \pi^0 e^+ e^-$	(1.4×10^{-5})
	$(21)(22)^*$	2.7×10^{-5}	3.6×10^{-3}	3.6×10^{-3}	$K^+ \to \pi^+ \mu^+ \mu^-$	4.8×10^{-4}
					$K_L \to \mu^+ \mu^-$	(3.2×10^{-6})
	$(31)(32)^*$	1.8×10^{-4}	3.6×10^{-3}	3.6×10^{-3}	$K_L \to \pi^0 \nu\overline{\nu}$	4.6×10^{-4}

Table 4.9: Bounds coming from $K^0 - \overline{K^0}$ mixing and correlated decays. The better bounds have been emphasized. Note that K_S decays constrain Re $(\lambda_{i1}\lambda^*_{i2})$ while K^+ decays constrain only the magnitudes; however, in view of a tight constraint on the imaginary part, the bound from K^+ decay can be taken to be on the real part of the product coupling. Here and in the next two tables, all numbers in the "Previous bound" column are taken from [83], with scaling the LQ mass to 300 GeV.

LQ type	indices	Previous Bound	This analysis			
			From Mixing		From Decay	
			Real part	Imag. part	Channel	Bound
LS_0	$(i1)(i3)^*$	0.036	0.022	0.022	$B^+ \to \pi^+ \nu\overline{\nu}$	2.0×10^{-2}
$R\tilde{S}_0$, $RS_{1/2}$	$(11)(13)^*$	0.054	0.022	0.022	$B^+ \to \pi^+ e^+ e^-$	5.0×10^{-4}
	$(21)(23)^*$	7.2×10^{-3}	0.022	0.022	$B^+ \to \pi^+ \mu^+ \mu^-$	4.6×10^{-4}
	$(31)(33)^*$	0.054	*0.022*	*0.022*	$B_d \to \tau^+ \tau^-$	1.2×10^{-1}
$L\tilde{S}_{1/2}$	$(11)(13)^*$	0.054	0.016	0.016	$B^+ \to \pi^+ e^+ e^-$	5.0×10^{-4}
	$(21)(23)^*$	7.2×10^{-3}	0.016	0.016	$B^+ \to \pi^+ \mu^+ \mu^-$	4.6×10^{-4}
	$(31)(33)^*$	0.054	*0.016*	*0.016*	$B^+ \to \pi^+ \nu\overline{\nu}$	2.0×10^{-2}
LS_1	$(11)(13)^*$	0.036	0.010	0.010	$B^+ \to \pi^+ e^+ e^-$	2.5×10^{-4}
	$(21)(23)^*$	3.6×10^{-3}	0.010	0.010	$B^+ \to \pi^+ \mu^+ \mu^-$	2.3×10^{-4}
	$(31)(33)^*$	0.027	0.010	0.010	$B_d \to \tau^+ \tau^-$	6.2×10^{-2}

Table 4.10: Bounds coming from $B_d^0 - \overline{B_d^0}$ mixing and correlated decays. The better bounds have been emphasized.

LQ type	indices	Previous Bound	This analysis			
			From Mixing		From Decay	
			Real part	Imag. part	Channel	Bound
LS_0	$(i2)(i3)^*$	0.36	0.13	0.13	$B^+ \to K^+\nu\overline{\nu}$	6.5×10^{-3}
$R\tilde{S}_0$,	$(12)(13)^*$	5.4×10^{-3}	0.13	0.13	$B_d \to K^0 e^+ e^-$	3.6×10^{-4}
$RS_{1/2}$	$(22)(23)^*$	7.2×10^{-3}	0.13	0.13	$B_d \to K^* \mu^+ \mu^-$	1.1×10^{-3}
	$(32)(33)^*$	.09	*0.13*	*0.13*	—	—
$L\tilde{S}_{1/2}$	$(12)(13)^*$	5.4×10^{-3}	0.09	0.09	$B_d \to K^0 e^+ e^-$	3.6×10^{-4}
	$(22)(23)^*$	7.2×10^{-3}	0.09	0.09	$B_d \to K^* \mu^+ \mu^-$	1.1×10^{-3}
	$(32)(33)^*$	0.054	0.09	0.09	$B^+ \to K^+\nu\overline{\nu}$	9.3×10^{-3}
LS_1	$(12)(13)^*$	2.7×10^{-3}	0.06	0.06	$B_d \to K^0 e^+ e^-$	1.8×10^{-4}
	$(22)(23)^*$	3.6×10^{-3}	0.06	0.06	$B_d \to K^* \mu^+ \mu^-$	5.5×10^{-4}
	$(32)(33)^*$	0.045	0.06	0.06	$B^+ \to K^+\nu\overline{\nu}$	6.5×10^{-3}

Table 4.11: Bounds coming from $B_s^0 - \overline{B_s^0}$ mixing and correlated decays. The better bounds have been emphasized.

contain no new information, but just shows the best bound for a given LQ type and a given set of indices. They further show that
(i) Except for R-type LQs with indices (31)(33), semileptonic, and in a few cases leptonic, decays give the best constraints. In most of the cases they are one or more orders of magnitude stronger than those coming from the mixing, so with those LQs, one should not expect much discernible effects from CP asymmetries.
(ii) While the bounds coming from decays are only on the magnitude of the product couplings, information on the complex weak phases of these couplings must come from mixing data, unless one makes a careful study of semileptonic CP asymmetries.

4.7 Summary and Conclusions

In this work we have computed the bounds on several scalar leptoquark coupling combinations coming from $M^0 - \overline{M^0}$ mixing as well as leptonic and semileptonic decays. Though such an analysis is not new, we have implemented several features in this analysis which were not been taken into account in earlier studies. Apart from the improved data on the B system, we have also used the data on CP violating phases, and obtained nontrivial constraints on the real and imaginary parts of the couplings. We note that for the gauge-singlet LQ S_0 with λ_{LS_0} type couplings, it is possible to alleviate the mild tension between the measured and predicted values of $\sin(2\beta_d)$, as well as to explain the large mixing phase in the B_s system. For this type of LQs, there are no modifications in leptonic or semileptonic channels, unless we consider final-state neutrinos.

For all other type of LQs, leptonic and semileptonic decays provide the better constraints (the exceptions are final-state τ channels). We do not expect any effects on nonleptonic final states like those coming from, say, R-parity violating supersymmetry with λ' type couplings. While the bounds coming from the leptonic channels are quite robust (apart from the mild uncertainty in the meson decay constants), those coming from semileptonic decays have an inherent uncertainty of the order of 10-15%, whose origin is the imprecise nature of the form factors.

Chapter 5

Summary

5.1 Conclusion

This thesis is based on some phenomenological aspects of B-physics. In this chapter we summarize the thesis and point out the main results of our work. In Chapter 1, we discuss how CP violation in the quark sector is introduced in the SM through the CKM mechanism; which processes should be examined to acquire information about the CKM matrix elements; how CKM matrix can be parametrized. We discuss two popular parametrizations of CKM matrix: (i) Standard parametrization and (ii) Wolfenstein Parametrization. This is followed by a detailed discussion of the unitarity triangle and its parameters. We discuss how experiments and global fits are indicating that the CKM matrix is the dominant source of CP violation in the SM. We conclude this chapter indicating some of the reasons to suspect that SM is insufficient to explain nature completely and we probably need some new physics to understand it better.

In Chapter 2, we present one of the most exciting puzzles of B physics in a model independent way: The variation of the measured $B_d^0 - \overline{B_d^0}$ mixing phase β/ϕ_1 in $b \to c\bar{c}s$ and $b \to s\bar{q}q$ (where $q = u, d, s$) modes is regarded as a possible probe of New Physics. Within the Standard Model, the amplitude for modes involving $\overline{b} \to \overline{s}$ transitions receive contributions from two amplitudes with different weak phases. Unless one of the amplitudes is negligible, some deviation is in fact expected. Estimates of this discrepancy using hadronic assumptions, however, are unable to produce the observed effect; indeed, the sign of the discrepancy within SM is opposite to the observed

value. Convincing arguments regarding the true nature of this discrepancy are lacking. In light of this, the relevant question is "Under what conditions can this discrepancy be regarded as an unambiguous signal of NP?" In this thesis we address this question using a model independent approach.

We demonstrate that the deviation in the measured β/ϕ_1, within the SM, due to pollution from another amplitude, is not only always less than the weak phase of the polluting amplitude, but also has always the same sign as the weak phase of the polluting amplitude. The only exception is to have large destructive interference between the two amplitudes. Without making any hadronic model-based assumptions, we examine the conditions under which such a destructive interference is possible within the SM. We find that a deviation larger than a few degrees is possible only if the observed decay rates result from fine-tuned cancellations between amplitudes whose squares are at least an order of magnitude larger than the decay rates themselves. This can be tested at near-future Super-B factories.

In Chapter 3, we discuss various phenomenological aspects of K and B mesons within SM. This forms the basis for the calculation in Chapter 4. We address the neutral $K^0 - \overline{K^0}$, $B_d^0 - \overline{B_d^0}$ and $B_s^0 - \overline{B_s^0}$ mixing in this chapter. The SM scenario of neutral K and B mesons mixing correlated leptonic and semileptonic decays are presented after that.

In Chapter 4, we discuss the Lepto-Quark Model which is one of the promising candidates for a NP model. Our model is based on the scalar type of leptoquarks with baryon and lepton number conserving renormalizable couplings, consistent with the symmetries of the SM. At low energies, leptoquarks could induce two-lepton two-quark interactions, like those mediated by the electroweak four-fermion vertices. This suggests that the leptoquark Yukawa coupling-squared ($\equiv \lambda^2$), divided by the mass-squared ($\equiv m_{lq}^2$) is at least as small as the weak coupling G_F.

In this work we compute the bounds on the product couplings of the type $\lambda\lambda$ coming from $K^0 - \overline{K^0}$, $B_d^0 - \overline{B_d^0}$ and $B_s^0 - \overline{B_s^0}$ mixing. Though such an analysis is not new, we implement several features in this analysis which were not taken care in earlier studies. Previously there was a lower limit only on Δm_{B_s}. Here we use the current bound on it and $\sin 2\beta_s$ limit also. We consider the

exact expression for the box amplitude taking all possible processes, including the one from the SM. The possibility that the LQ product couplings may be complex is also considered. The analysis is done assuming all leptoquarks are degenerate at 300 GeV. The interference between charge (-1/3) LQ and charge (-4/3) LQ for S_1 and charge (1/3) LQ and charge (-2/3) LQ for $\tilde{S}_{1/2}$ are considered here. Similar assumption is taken for the same type of couplings. We consider that only one LQ is present at a time. The constraints obtained for the leptonic and semi leptonic decay modes are much tighter than the bounds obtained from mixing. We find that a number of them have better bounds from their previous bounds. We present the bounds on the real and imaginary parts of $\lambda\lambda$ which carry the information of the phase of new physics. This is a new observation which was not taken into account earlier.

Bibliography

[1] J. H. Christenson, J. W. Cronin, V. L. Fitch, and R. Turlay, Phys. Rev. Lett. 13, 138-140 (1964).

[2] V. Fanti et al. [NA48 Collaboration], Phys. Lett. B465, 335 (1999).

[3] A. Alavi-Harati et al. [KTeV Collaboration], Phys. Rev. Lett. 83, 22 (1999).

[4] Danilo Zavrtanik et al. [CPLEAR Collaboration], Nuclear Instruments and Methods in Physics Research A 446, 132-137 (2000).

[5] B. Aubert et al. [BaBar Collaboration], Phys. Rev. Lett. 87, 091801 (2001).

[6] K. Abe et al. [Belle Collaboration], Phys. Rev. Lett. 87, 091802 (2001).

[7] B. Aubert et al. [BaBar Collaboration], Phys. Rev. Lett. 93, 131801 (2004); Y. Chao et al. [Belle Collaboration], Phys. Rev. Lett. 93, 191802 (2004).

[8] N. Cabibbo, Phys. Rev. Lett. 10, 531-532 (1963).

[9] M. Kobayashi and T. Maskawa, Prog. Theor. Phys. 49, 652-657 (1973).

[10] Y. Nir, [arXiv:hep-ph/0510413] (2005).

[11] R. Fleischer, [arXiv:hep-ph/0608010] (2006).

[12] G. C. Branco, L. Lavoura and J. P. Silva, CP violation, Oxford University Press.

[13] C. Jarlskog, Phys. Rev. Lett. 55, 1039 (1985).

[14] A. Ceccucci, Z. Ligeti, and Y. Sakai, Particle data group, (2008).

[15] J. Charles et al. [CKMfitter Group], Eur. Phys. J. C41, 1-131 (2005), updated results and plots available at: http://ckmfitter.in2p3.fr

[16] M. Bona et al. [UTfit Collaboration], JHEP 507, 28 (2005), and updates at http://www.utfit.org/.

[17] M. Bona et al. [UTfit Collaboration], JHEP 0803, 049 (2008).

[18] C. Jarlskog, CP violation, edited by C. Jarlskog, World Scientific Publication, Singapore, (1989).

[19] L. Chau and W. Keung, Phys. Rev. Lett. 53, 1802 (1984).

[20] L. Wolfenstein, Phys. Rev. Lett. 51, 1945 (1983).

[21] A. J. Buras, M. E. Lautenbacher, and G. Ostermaier, Phys. Rev. D 50, 3433 (1994).

[22] R. Aleksan, B. Kayser and D. London, Phys. Rev. Lett. 73, 18 (1994).

[23] C. Jarlskog and R. Stora, Phys. Lett. B208, 268 (1988).

[24] C. Dib, I. Dunietz, F. J. Gilman and Y. Nir, Phys. Rev. D 41, 1522 (1990).

[25] Manuel Drees, Rohini M. Godbole and Probir Roy, Theory and Phenomenology of Sparticles, World Scientific (2004).

[26] B. Lee, C. Quigg and H. Thacker, Phys. Rev. D 16, 1519 (1977); D. A. Dicus and V. S. Mathur, Phys. Rev. D 7, 3111 (1973).

[27] Y. Grossman and M.P. Worah, Phys. Lett. B 395, 241 (1997); R. Fleischer, Int. J. Mod. Phys. A 12, 2459 (1997).

[28] A. R.Williamson and J. Zupan, Phys. Rev. D 74, 014003 (2006).

[29] M. Beneke, Phys. Lett. B 620, 143 (2005).

[30] H.Y. Cheng, C.K. Chua and A. Soni, Phys. Rev. D 72, 014006 (2005); G. Buchalla, G. Hiller, Y. Nir and G. Raz, JHEP 0509, 074 (2005).

[31] Rahul Sinha, Basudha Misra and Wei-shu Hou, Phys. Rev. Lett. 97, 131802 (2006).

[32] Heavy Flavor Averaging Group [HFAG], online update at http://www.slac.stanford.edu/xorg/hfag.

[33] I.I. Bigi and A.I. Sanda, Nucl. Phys. B193, 85 (1981); A.B. Carter and A.I. Sanda, Phys. Rev. D 23, 1567 (1981).

[34] J. Zupan [arXiv:hep-ph/0707.1323].

[35] M. Beneke and D. Yang, Nucl. Phys. B 736, 34 (2006).

[36] H. n. Li and S. Mishima, Phys. Rev. D 74, 094020 (2006).

[37] M. Beneke and M. Neubert, Nucl. Phys. B 675, 333 (2003).

[38] H. n. Li, S. Mishima and A. I. Sanda, Phys. Rev. D 72, 114005 (2005).

[39] H. n. Li and S. Mishima, Phys. Rev. D 74, 094020 (2006).

[40] M. Gronau, J. L. Rosner and J. Zupan, Phys. Rev. D 74, 093003 (2006).

[41] Y. Grossman, Z. Ligeti, Y. Nir and H. Quinn, Phys. Rev. D 68, 015004 (2003).

[42] G. Engelhard and G. Raz, Phys. Rev. D 72, 114017 (2005).

[43] G. Engelhard, Y. Nir and G. Raz, Phys. Rev. D 72, 075013 (2005).

[44] R. Fleischer, S. Recksiegel and F. Schwab, Eur. Phys. J. C 51, 55 (2007).

[45] M. Gell-Mann, A. Pais, Phys. Rev. D 97, 1387 (1955).

[46] C. Albajar et al. [UA1 Collaboration], Phys. Lett. B 186, 247 (1987); H. Albrecht et al. [ARGUS Collaboration], Phys. Lett. B 192, 245 (1987).

[47] A. Abulencia et al. [CDF Collaboration], Phys. Rev. Lett. 97, 242003 (2006).

[48] B. Aubert, et al. [BaBar Collaboration], Phys. Rev. Lett. 98, 211802 (2007); K. Abe et al. [BELLE Collaboration], Phys. Rev. Lett. 99, 131803 (2007).

[49] Andrzej J. Buras, Robert Fleischer, Adv. Ser. Direct. HighEnergyPhys. 15, 65 (1998), arXiv:hep- ph/9704376].

[50] G. Buchalla, A. J. Buras and M. Lautenbacher, Rev. Mod. Phys. 68, 1125 (1996).

[51] S. Herrlich and U. Nierste, Nucl. Phys. B 419, 292 (1994); Phys. Rev. D 52, 6505 (1995); Nucl. Phys. B 476, 27 (1996).

[52] A. J. Buras, M. Jamin and P. H. Weisz, Nucl. Phys. B 347, 491 (1990).

[53] S. Aoki et al. [JLQCD coll.], Phys. Rev. Lett. 91, 212001 (2003).

[54] C. Amsler et al. [Particle Data Group], Physics Letters B 667, 1 (2008).

[55] G. Buchalla, A. J. Buras and M. E. Lautenbacher [arXiv:hep-ph/9512380].

[56] A. J. Buras, M. Jamin, M. E. Lautenbacher and P. H. Weisz, Nucl. Phys. B 370, 69 (1992); Nucl. Phys. B 400, 37 (1993).

[57] A. J. Buras, M. Jamin, M. E. Lautenbacher, Nucl. Phys. B 400, 75 (1993); Nucl. Phys. B 408, 209 (1993).

[58] M. Ciuchini, E. Franco, G. Martinelli and L. Reina, Phys. Lett. B 301, 163 (1994); Nucl. Phys. B 415, 403 (1994).

[59] A. G. Cohen, G. Ecker and A. Pich, Phys. Lett. B 304, 347 (1993).

[60] P. Heiliger and L. Seghal, Phys. Rev. D 47, 4920 (1993).

[61] J. F. Donoghue and F. Gabbiani, Phys. Rev. D 51, 2187 (1995).

[62] G. Ecker, A. Pich and E. De Rafael, Nucl. Phys. B 291, 692 (1987); Nucl. Phys. B 303, 665 (1988); C. Bruno and J. Prades, Z. Phys. C 57, 585 (1993).

[63] A. Pitch, [arXiv: hep-ph/9610243].

[64] A. J. Buras et al. Phys. Lett. B 566, 115 (2003); Nucl. Phys. B 404, 3 (1993).

[65] C.Q.Geng and C.C.Liu, J. Phys. G 29, 1103 (2003).

[66] A. Ali, G. Kramer and C.-D. Lü, Phys. Rev. D 58, 094009 (1998).

[67] A. Masiero and H. Murayama, Phys. Rev. Lett. 83, 907 (1999).

[68] J.C. Pati and A. Salam, Phys. Rev. D 10, 275 (1974).

[69] J.C. Pati, A. Salam, Phys. Rev. D 8, 1240 (1973); Phys.Rev. Lett. 31, 661 (1973); H. Georgi and S.L. Glashow, Phys. Rev. Lett. **32**, 438 (1974).

[70] H. Georgi and S.L. Glashow, Phys. Rev. Lett. 32, 438 (1974).

[71] B.A. Campbell, J. Ellis, K. Enqvist, M.K. Gaillard, and D.V. Nanopoulos, Int. J. Mod. Phys. A 2, 831 (1987).

[72] J. Hewett, T. Rizzo, Phys. Rep. 183, 193 (1989).

[73] S. Dimopoulos, J. Ellis, Nucl. Phys B 182, 505 (1981).

[74] O. Shenkar, Nucl. Phys. B 206, 253 (1982).

[75] O. Shenkar, Nucl. Phys. B 204, 375 (1982).

[76] For a review, see: E. Farhi and L. Susskind, Phys. Reports 74, 277 (1981); K. Lane and M. Ramana, Phys. Rev. D 44, 2678 (1991).

[77] For a review, see: I. Bars, Proc. of the 1984 Summer Study on the SSC, editors R.Donaldson, J. Morphin APF New York, 38 (1985); W. Buchmuller, Acta Phys. Austr. Suppl. XXVII 517 (1985); B. Schremp and F. Schremp, Phys. Lett. B 153, 101 (1985); R. Peccei, in Proceedings of the 2nd Lake Louise Winter Institute, J.M. Cameron et al., eds., World Scientific, Singapore (1987).

[78] L.F. Abbott, E. Farhi, Phys. Lett.B 101, 69 (1981); Nucl. Phys. B 189, 547 (1981).

[79] W. Bardeen, V. Visnjic, Nucl. Phys. B 194, 151 (1982); W. Buchmuller, R. Peccei, T. Yanagida, Phys. Lett. B 124, 67 (1983); R. Barbieri, A. Masiero, G. Veneziano, Phys. Lett. B 128, 179 (1983).

[80] B. Schrempp, F. Schrempp, Nucl. Phys. B 231, 109 (1984).

[81] J.C. Pati, Phys. Lett. B 228, 228 (1989).

[82] I. Dorsner, S. Fajfer, J.F. Kamenik and N. Kosnik, Phys. Lett. **B682**, 67 (2009).

[83] S. Davidson, D. Bailey, B.A. Campbell, Z. Phys. C 61, 613 (1994).

[84] M. Leurer, Phys. Rev. **D49**, 333 (1994).

[85] M. Leurer, Phys. Rev. **D50**, 536 (1994).

[86] A. Dighe, A. Kundu, and S. Nandi, Phys. Rev. **D76**, 054005 (2007).

[87] Y. Grossman, Phys. Lett. **B380**, 99 (1996).

[88] T. Aaltonen *et al.* [CDF Collaboration], Phys. Rev. Lett. **100**, 161802 (2008); V.M. Abazov *et al.* [DØ Collaboration], Phys. Rev. Lett. **101**, 241801 (2008).

[89] W. Buchmuller, R. Ruckl and D. Wyler, Phys. Lett. **B191**, 442 (1987) [Erratum-ibid. B **448**, 320 (1999)]; W. Buchmuller and D. Wyler, Phys. Lett. **B177**, 377 (1986); Nucl. Phys. **B268**, 621 (1986).

[90] M. Leurer, Phys. Rev. **D46**, 3757 (1992); R. Mohapatra, G. Segre, and L. Wolfenstein, Phys. Lett. **B145**, 433 (1984); I. Bigi, G. Knopp, and P.M. Zerwas, Phys. Lett. **B166**, 238 (1986); A.J. Davies and X. He, Phys. Rev. **D43**, 225 (1991).

[91] B.A. Dobrescu and A.S. Kronfeld, Phys. Rev. Lett. **100**, 241802 (2008).

[92] S. Fajfer and N. Kosnik, Phys. Rev. **D79**, 017502 (2009).

[93] A.D. Smirnov, Mod. Phys. Lett. **A22**, 2353 (2007).

[94] I. Dorsner and P. Fileviez Perez, Nucl. Phys. **B723**, 53 (2005).

[95] P. Fileviez Perez, T. Han, T. Li, and M.J. Ramsey-Musolf, Nucl. Phys. **B819**, 139 (2009).

[96] W. Buchmuller, Phys. Lett B 145, 151 (1984); B. Schrempp, F. Schrempp, Phys. Lett B 153, 101 (1985).

[97] A. Aktas *et al.* [H1 Collaboration], Phys. Lett. **B629**, 9 (2005); S. Chekanov *et al.* [Zeus Collaboration], Phys. Rev. **D68**, 052004 (2003).

[98] G. Abbiendi *et al.* [OPAL Collaboration], Eur. Phys. J. C **31**, 281 (2003).

[99] T. Nunnemann, arXiv:0909.2507[hep-ex];

[100] V.M. Abazov *et al.* [DØ Collaboration], Phys. Lett. **B671**, 224 (2009); Phys. Lett. **B668**, 357 (2008); Phys. Rev. Lett. **101**, 241802 (2008); Phys. Lett. **B647**, 74 (2007); Phys. Rev. Lett. **99**, 061801 (2007); T. Aaltonen *et al.* [CDF Collaboration], Phys. Rev. **D77**, 091105 (2008).

[101] J. Blumlein, E. Boos and A. Kryukov, Zeit. Phys. C **76**, 137 (1997).

[102] V.A. Mitsou, N.C. Benekos, I. Panagoulias and T.D. Papadopoulou, Czech.J.Phys. **55**, B659 (2005); M. Kramer, T. Plehn, M. Spira and P.M. Zerwas, Phys. Rev. **D71**, 057503 (2005); B. Dion, L. Marleau, G. Simon and M. de Montigny, Eur. Phys. J. C **2**, 497 (1998).

[103] A. Belyaev, C. Leroy, R. Mehdiyev and A. Pukhov, JHEP(0509,005,2005).

[104] A.J. Buras and R. Fleischer, [arXiv:hep-ph/9704376], (1997); Heavy Flavours II, World Scientific, Singapore, ed. A.J. Buras and M. Lindner, (1997).

[105] E.A. Paschos and U. Türke, Phys. Rep. 178, 145 (1989).

[106] D. Bećirević et al. Nucl. Phys. B 634, 105 (2002).

[107] J.P. Saha and A. Kundu, Phys. Rev. D 70, 096002 (2004).

[108] M. Wirbel, B. Stech and M. Bauer, Z-Physics C 29, 637 (1985).

[109] A. Ishikawa *et al.* [Belle Collaboration], Phys. Rev. Lett. **96**, 251801 (2006); J.T. Wei *et al.* [Belle Collboration], Phys. Rev. Lett. **103**, 171801 (2009).

[110] B. Aubert *et al.* [Babar Collaboration], Phys. Rev. **D73**, 092001 (2006); Phys. Rev. **D79**, 031102 (2009).

[111] F. Ambrosino *et al.* [KLOE Collaboration], Phys. Lett. **B672**, 203 (2009).

[112] H. Miyake, arXiv:1003.0164[hep-ex].

[113] A. Ali, G. Kramer and C.-D. Lü, Phys. Rev. **D58**, 094009 (1998).

[114] V. Lubicz *et al.*, Phys. Rev. **D80**, 111502 (2009).

[115] M. Herz, arXiv:hep-ph/0301079.